

Charmless Hadronic Two-body Decays of B_u and B_d Mesons

Yaw-Hwang Chen

Department of Physics, National Cheng-Kung University
Tainan, Taiwan 700, Republic of China

Hai-Yang Cheng, B. Tseng, Kwei-Chou Yang

Institute of Physics, Academia Sinica
Taipei, Taiwan 115, Republic of China

Abstract

Two-body charmless nonleptonic decays of B_u and B_d mesons are studied within the framework of generalized factorization in which the effective Wilson coefficients c_i^{eff} are renormalization-scale and -scheme independent while factorization is applied to the tree-level hadronic matrix elements. Contrary to previous studies, our c_i^{eff} do not suffer from gauge and infrared problems. Nonfactorizable effects are parametrized in terms of $N_c^{\text{eff}}(LL)$ and $N_c^{\text{eff}}(LR)$, the effective numbers of colors arising from $(V - A)(V - A)$ and $(V - A)(V + A)$ four-quark operators, respectively. Tree and penguin transitions are classified into six different classes. The data of $B^- \rightarrow \rho^0 \pi^-$ and $B^- \rightarrow \phi K^-$ clearly indicate that $N_c^{\text{eff}}(LR) \neq N_c^{\text{eff}}(LL)$: The first measurement of the $b \rightarrow u$ mode $B^- \rightarrow \rho^0 \pi^-$ and the experimental information on the tree-dominated mode $B^- \rightarrow \omega \pi^-$ all imply that $N_c^{\text{eff}}(LL)$ is less than 3, whereas the CLEO measurement of $B^- \rightarrow \phi K^-$ shows $N_c^{\text{eff}}(LR) > 3$. For given input parameters, the prediction of $\mathcal{B}(B \rightarrow \eta' K)$ is largely improved by setting $N_c^{\text{eff}}(LL) \sim 2$ and $N_c^{\text{eff}}(LR) > N_c^{\text{eff}}(LL)$; in particular, the charm content of the η' contributes in the right direction. The decay rate of $B \rightarrow \phi K^*$ is very sensitive to the form-factor ratio A_2/A_1 ; the absence of $B \rightarrow \phi K$ events does not necessarily invalidate the factorization approach. If the branching ratio of $B^- \rightarrow \omega K^-$ is experimentally found to be significantly larger than that of $B^- \rightarrow \rho^0 K^-$, we argue that inelastic final-state rescattering may account for the disparity between ωK^- and $\rho^0 K^-$. By contrast, if $\mathcal{B}(B^- \rightarrow \rho^0 K^-) \sim \mathcal{B}(B^- \rightarrow \omega K^-)$ is observed, then W -annihilation and/or spacelike penguins could play a prominent role. The decay modes $\overline{B}_d^0 \rightarrow \phi \pi^0, \phi \eta, \phi \eta', \phi \rho^0, \phi \omega, B^- \rightarrow \phi \pi^-, \phi \rho^-$ involving a vector meson ϕ are dominated by electroweak penguins. We show that a unitarity angle γ larger than 90° is helpful for explaining the $\pi^+ \pi^-, \pi K$ and $\eta' K$ data. The relative magnitudes of tree, QCD penguin and electroweak penguin amplitudes are tabulated for all charmless $B \rightarrow PP, VP, VV$ decays. Our favored predictions for branching ratios are those for $N_c^{\text{eff}}(LL) \approx 2$ and $N_c^{\text{eff}}(LR) \sim 5$.

I. INTRODUCTION

The study of exclusive nonleptonic weak decays of B mesons is of great interest for several reasons: many of rare hadronic B decay modes are dominated by the gluonic penguin mechanism and large direct CP asymmetries are expected in many charged B decays. Hence the analysis and measurement of charmless hadronic B decays will enable us to understand the QCD and electroweak penguin effects in the Standard Model (SM) and provide a powerful tool of seeing physics beyond the SM. The sizable direct CP violation expected in exclusive rare decay modes of B mesons will allow the determination of the Cabibbo-Kobayashi-Maskawa (CKM) unitarity angles.

In past years we have witnessed remarkable progress in the study of exclusive charmless B decays. Experimentally, CLEO [1] has discovered many new two-body decay modes

$$B \rightarrow \eta' K^\pm, \eta' K^0, \pi^\pm K^0, \pi^\pm K^\mp, \pi^0 K^\pm, \rho^0 \pi^\pm, \omega K^\pm, \quad (1.1)$$

and found a possible evidence for $B \rightarrow \phi K^*$. Moreover, CLEO has provided new improved upper limits for many other decay modes. While all the channels that have been measured so far are penguin dominated, the most recently observed $\rho^0 \pi^-$ mode is dominated by the tree diagram. In the meantime, updates and new results of many $B \rightarrow PV$ decays with $P = \eta, \eta', \pi, K$ and $V = \omega, \phi, \rho, K^*$ as well as $B \rightarrow PP$ decays will be available soon. With the B factories Babar and Belle starting to collect data, many exciting and harvest years in the arena of B physics and CP violation are expected to come.

Some of the CLEO data are surprising from the theoretical point of view: The measured branching ratios for $B^\pm \rightarrow \eta' K^\pm$ and $B^\pm \rightarrow \omega K^\pm$ are about several times larger than the naive theoretical estimate. Since then the theoretical interest in hadronic charmless B decays is surged and recent literature is rife with all kinds of interesting interpretations of data, both within and beyond the SM.

An earlier systematic study of exclusive nonleptonic two-body decays of B mesons was made in [2]. Two different approaches were employed in this reference: the effective Hamiltonian approach in conjunction with the factorization hypothesis for hadronic matrix elements and a model-independent analysis based on the quark-diagram approach developed by Chau and one of us (H.Y.C.) [3]. Many significant improvements and developments have been achieved over past years. For example, a next-to-leading order effective Hamiltonian for current-current operators and QCD as well as electroweak penguin operators becomes available. The renormalization scheme and scale problems with the factorization approach for matrix elements can be circumvented by employing scale- and scheme-independent effective Wilson coefficients. Heavy-to-light form factors have been computed using QCD sum rules, lattice QCD and potential models. A great interest in the flavor-SU(3) quark diagram approach was also revived in recent years. In particular, this method has been widely utilized as a model-independent extraction of the CKM unitary triangle.

We will present in this paper an updated and vigorous analysis of hadronic two-body charmless decays of B_u and B_d mesons (for B_s mesons, see [4]). We will pay special attention to two important issues: the gauge and infrared problems with the effective Wilson

coefficients, and the nonfactorized effect characterized by the parameter N_c^{eff} , the effective number of colors.

One of the principal difficulties with naive factorization is that the hadronic matrix element under the factorization approximation is renormalization scale μ independent as the vector or axial-vector current is partially conserved. Consequently, the amplitude $c_i(\mu)\langle O \rangle_{\text{fact}}$ is not physical as the scale dependence of Wilson coefficients does not get compensation from the matrix elements. A plausible solution to the problem is to extract the μ dependence from the matrix element $\langle O(\mu) \rangle$, and then combine it with the μ -dependent Wilson coefficients to form scale- and scheme-independent effective coefficients c_i^{eff} . The factorization approximation is applied afterwards to the hadronic matrix element of the operator O at the tree level. However, it was pointed out recently in [5] that c_i^{eff} suffer from gauge and infrared ambiguities since an off-shell external quark momentum, which is usually chosen to regulate the infrared divergence occurred in the radiative corrections to the local 4-quark operators, will introduce a gauge dependence.

A closely related problem is connected to the generalized factorization approach in which the nonfactorized contribution to the matrix element in $B \rightarrow PP, VP$ decays is lumped into the effective number of colors N_c^{eff} , called $1/\xi$ in [6]. The deviation of $1/N_c^{\text{eff}}$ from $1/N_c$ measures the nonfactorizable effect. The unknown parameter N_c^{eff} is usually assumed to be universal (i.e., channel independent) within the framework of generalized factorization and it can be extracted from experiment. However, as stressed by Buras and Silvestrini [5], if c_i^{eff} are gauge and infrared regulator dependent, then the values of N_c^{eff} extracted from the data on two-body hadronic decays are also gauge dependent and therefore they cannot have any physical meaning. Recently, this controversy on gauge dependence and infrared singularity connected with the effective Wilson coefficients is resolved by Li and two of us (H.Y.C. and K.C.Y.) [7]: Gauge invariance of the decay amplitude is maintained under radiative corrections by assuming on-shell external quarks. The infrared pole emerged in a physical on-shell scheme signifies the nonperturbative dynamics involved in a decay process and has to be absorbed into a universal hadron wave function. As a consequence, it is possible to construct the effective Wilson coefficients which are not only renormalization scale- and scheme-independent but also gauge invariant and infrared finite.

For penguin-dominated rare B decays, there is another subtle issue for the effective parameter N_c^{eff} . As shown in [8], nonfactorizable effects in the matrix elements of $(V-A)(V+A)$ operators are *a priori* different from that of $(V-A)(V-A)$ operators, i.e. $N_c^{\text{eff}}(LR) \neq N_c^{\text{eff}}(LL)$. We will demonstrate in the present work that the most recently measured $B^- \rightarrow \rho^0 \pi^-$ decay together with the experimental information on the tree-dominated modes $B^- \rightarrow \omega \pi^-$ clearly imply $N_c^{\text{eff}}(LL) < 3$, while the CLEO measurement of $B^- \rightarrow \phi K^-$ indicates $N_c^{\text{eff}}(LR) > 3$. Contrary to the previous studies, we show that the experimental data of $\rho^0 \pi^\pm$ and ϕK^\pm cannot be accommodated simultaneously by treating $N_c^{\text{eff}}(LL) = N_c^{\text{eff}}(LR)$. This observation is very crucial for improving the discrepancy between theory and experiment for $B \rightarrow \eta' K$ decays.

This paper is organized as follows. In Sec. II we discuss the gauge and infrared problems connected with the effective Wilson coefficients and their solution. Input parameters necessary for calculations such as quark mixing matrix elements, running quark masses,

decay constants, heavy-to-light form factors are summarized in Sec. III. In Sec. IV we classify the factorized decay amplitudes into six different classes. Results for branching ratios and their implications are discussed in details in Sec. V with special attention paid to $B \rightarrow \rho\pi, \omega\pi, \phi K, \phi K^*, \eta' K, K\pi$ modes; in particular, all possible sources of theoretical uncertainties are summarized in Sec. V.G. The role of final-state interactions played in charmless B decays is elaborated on in Sec. VI. For reader's convenience, we compare our results with the literature in Sec. VII. Sec. VIII is for the conclusion. Factorized amplitudes for all charmless $B \rightarrow PP, VP, VV$ decays are tabulated in the Appendix.

II. FRAMEWORK

The effective Hamiltonian is the standard starting point for describing the nonleptonic weak decays of hadrons. The relevant effective $\Delta B = 1$ weak Hamiltonian for hadronic charmless B decays is

$$\mathcal{H}_{\text{eff}}(\Delta B = 1) = \frac{G_F}{\sqrt{2}} \left\{ V_{ub}V_{uq}^* [c_1(\mu)O_1^u(\mu) + c_2(\mu)O_2^u(\mu)] + V_{cb}V_{cq}^* [c_1(\mu)O_1^c(\mu) + c_2(\mu)O_2^c(\mu)] - V_{tb}V_{tq}^* \sum_{i=3}^{10} c_i(\mu)O_i(\mu) \right\} + \text{h.c.}, \quad (2.1)$$

where $q = d, s$, and

$$\begin{aligned} O_1^u &= (\bar{u}b)_{V-A}(\bar{q}u)_{V-A}, & O_2^u &= (\bar{u}_\alpha b_\beta)_{V-A}(\bar{q}_\beta u_\alpha)_{V-A}, \\ O_1^c &= (\bar{c}b)_{V-A}(\bar{q}c)_{V-A}, & O_2^c &= (\bar{c}_\alpha b_\beta)_{V-A}(\bar{q}_\beta c_\alpha)_{V-A}, \\ O_{3(5)} &= (\bar{q}b)_{V-A} \sum_{q'} (\bar{q}'q')_{V-A(V+A)}, & O_{4(6)} &= (\bar{q}_\alpha b_\beta)_{V-A} \sum_{q'} (\bar{q}'_\beta q'_\alpha)_{V-A(V+A)}, \\ O_{7(9)} &= \frac{3}{2}(\bar{q}b)_{V-A} \sum_{q'} e_{q'}(\bar{q}'q')_{V+A(V-A)}, & O_{8(10)} &= \frac{3}{2}(\bar{q}_\alpha b_\beta)_{V-A} \sum_{q'} e_{q'}(\bar{q}'_\beta q'_\alpha)_{V+A(V-A)}, \end{aligned} \quad (2.2)$$

with O_3 – O_6 being the QCD penguin operators, O_7 – O_{10} the electroweak penguin operators and $(\bar{q}_1 q_2)_{V\pm A} \equiv \bar{q}_1 \gamma_\mu (1 \pm \gamma_5) q_2$. In order to ensure the renormalization-scale and -scheme independence for the physical amplitude, the matrix elements of 4-quark operators have to be evaluated in the same renormalization scheme as that for Wilson coefficients and renormalized at the same scale μ .

Although the hadronic matrix element $\langle O(\mu) \rangle$ can be directly calculated in the lattice framework, it is conventionally evaluated under the factorization hypothesis so that $\langle O(\mu) \rangle$ is factorized into the product of two matrix elements of single currents, governed by decay constants and form factors. In spite of its tremendous simplicity, the naive factorization approach encounters two major difficulties. One of them is that the hadronic matrix element under factorization is renormalization scale μ independent as the vector or axial-vector current is partially conserved. Consequently, the amplitude $c_i(\mu)\langle O \rangle_{\text{fact}}$ is not truly physical as the scale dependence of Wilson coefficients does not get compensation from the matrix elements.

A plausible solution to the aforementioned scale problem is to extract the μ dependence from the matrix element $\langle O(\mu) \rangle$, and combine it with the μ -dependent Wilson coefficient functions to form μ -independent effective coefficients. Schematically, we may write

$$c(\mu)\langle O(\mu) \rangle = c(\mu)g(\mu)\langle O \rangle_{\text{tree}} \equiv c^{\text{eff}}\langle O \rangle_{\text{tree}}. \quad (2.3)$$

The factorization approximation is applied afterwards to the hadronic matrix element of the operator O at the tree level. Since the tree-level matrix element $\langle O \rangle_{\text{tree}}$ is renormalization scheme and scale independent, so are the effective Wilson coefficients c_i^{eff} . However, the problem is that we do not know how to carry out first-principles calculations of $\langle O(\mu) \rangle$ and hence $g(\mu)$. It is natural to ask the question: Can $g(\mu)$ be evaluated at the quark level in the same way as the Wilson coefficient $c(\mu)$? One of the salient features of the operator product expansion (OPE) is that the determination of the short-distance $c(\mu)$ is independent of the choice of external states. Consequently, we can choose quarks as external states in order to extract $c(\mu)$. For simplicity, we consider a single multiplicatively renormalizable 4-quark operator O (say, O_+ or O_-) and assume massless quarks. The QCD-corrected weak amplitude induced by O in full theory is

$$A_{\text{full}} = \left[1 + \frac{\alpha_s}{4\pi} \left(-\frac{\gamma}{2} \ln \frac{M_W^2}{-p^2} + a \right) \right] \langle O \rangle_q, \quad (2.4)$$

where γ is an anomalous dimension, p is an off-shell momentum of the external quark lines, which is introduced as an infrared cutoff, and the non-logarithmic constant term a in general depends on the gauge chosen for the gluon propagator. The subscript q in (2.4) emphasizes the fact that the matrix element is evaluated between external quark states. In effective theory, the renormalized $\langle O(\mu) \rangle_q$ is related to $\langle O \rangle_q$ in full theory via

$$\begin{aligned} \langle O(\mu) \rangle_q &= \left[1 + \frac{\alpha_s}{4\pi} \left(-\frac{\gamma}{2} \ln \frac{\mu^2}{-p^2} + r \right) \right] \langle O \rangle_q \\ &\equiv g'(\mu, -p^2, \lambda) \langle O \rangle_q, \end{aligned} \quad (2.5)$$

where g' indicates the perturbative corrections to the 4-quark operator renormalized at the scale μ . The constant term r is in general renormalization scheme and gauge dependent, and it has the general expression [5]:

$$r = r^{\text{NDR,HV}} + \lambda r^\lambda, \quad (2.6)$$

where NDR and HV stand for the naive dimension regularization and 't Hooft-Veltman renormalization schemes, respectively, and λ is a gauge parameter with $\lambda = 0$ corresponding to Landau gauge. Matching the effective theory with full theory, $A_{\text{full}} = A_{\text{eff}} = c(\mu)\langle O(\mu) \rangle_q$, leads to

$$c(\mu) = 1 + \frac{\alpha_s}{4\pi} \left(-\frac{\gamma}{2} \ln \frac{M_W^2}{\mu^2} + d \right), \quad (2.7)$$

where $d = a - r$. Evidently, the Wilson coefficient is independent of the infrared cutoff and it is gauge invariant as the gauge dependence is compensated between a and r . Of course, $c(\mu)$ is still renormalization scheme and scale dependent.

Since A_{eff} in full theory [Eq. (2.4)] is μ and scheme independent, it is obvious that

$$c'^{\text{eff}} = c(\mu)g'(\mu, -p^2, \lambda) \quad (2.8)$$

is also independent of the choice of the renormalization scheme and scale. Unfortunately, c'^{eff} is subject to the ambiguities of the infrared cutoff and gauge dependence. As stressed in [5], the gauge and infrared dependence always appears as long as the matrix elements of operators are calculated between quark states. By contrast, the effective coefficient $c^{\text{eff}} = c(\mu)g(\mu)$ should not suffer from these problems.

It was recently shown in [7] that the above-mentioned problems on gauge dependence and infrared singularity connected with the effective Wilson coefficients can be resolved by perturbative QCD (PQCD) factorization theorem. In this formalism, partons, *i.e.*, external quarks, are assumed to be on shell, and both ultraviolet and infrared divergences in radiative corrections are isolated using the dimensional regularization. Because external quarks are on shell, gauge invariance of the decay amplitude is maintained under radiative corrections to all orders. This statement is confirmed by an explicit one-loop calculation in [7]. The obtained ultraviolet poles are subtracted in a renormalization scheme, while the infrared poles are absorbed into universal nonperturbative bound-state wave functions. The remaining finite piece is grouped into a hard decay subamplitude. The decay rate is then factorized into the convolution of the hard subamplitude with the bound-state wave functions, both of which are well-defined and gauge invariant. Explicitly, the effective Wilson coefficient has the expression

$$c^{\text{eff}} = c(\mu)g_1(\mu)g_2(\mu_f) , \quad (2.9)$$

where $g_1(\mu)g_2(\mu_f)$ is identified as the factor $g(\mu)$ defined in Eq. (2.3). In above equation $g_1(\mu)$ is an evolution factor from the scale μ to m_b , whose anomalous dimension is the same as that of $c(\mu)$, and $g_2(\mu_f)$ describes the evolution from m_b to μ_f (μ_f being a factorization scale arising from the dimensional regularization of infrared divergences), whose anomalous dimension differs from that of $c(\mu)$ because of the inclusion of the dynamics associated with spectator quarks. The infrared pole emerged in the physical on-shell scheme signifies the nonperturbative dynamics involved in a decay process and it has to be absorbed into the universal meson wave functions.* Hence, in the PQCD formalism the effective Wilson coefficients are gauge invariant, infrared finite, scheme and scale independent.

In the above framework, $\langle O \rangle_{\text{tree}}$ is related to the meson wave function $\phi(\mu_f)$ (see [7] for detail). For our purposes of applying factorization, we will set $\mu_f = m_b$ to compute

*For inclusive processes, the infrared divergence due to radiative corrections is compensated by gluon bremsstrahlung, leading to a well-defined and finite correction. However, for exclusive hadronic decay processes the loop-induced infrared divergence is not canceled by gluon bremsstrahlung in the quark \rightarrow three quarks decay process. In fact, the bremsstrahlung contribution is irrelevant to the hadronic matrix elements for exclusive decays. In the present framework of perturbative QCD factorization theorem, the infrared pole is absorbed by bound-state wave functions rather than canceled by the bremsstrahlung process.

c^{eff} and then evaluate the tree level hadronic matrix element $\langle O \rangle_{\text{tree}}$ using the factorization approximation. It is straightforward to calculate $g_1(\mu)$ from the vertex correction diagrams (see Fig. 1) and penguin-type diagrams for the 4-quark operators O_i ($i = 1, \dots, 10$). In general,

$$\langle O_i(\mu) \rangle = \left[\mathbb{1} + \frac{\alpha_s(\mu)}{4\pi} \hat{m}_s(\mu) + \frac{\alpha}{4\pi} \hat{m}_e(\mu) \right]_{ij} \langle O_j \rangle_{\text{tree}}, \quad (2.10)$$

where the one-loop QCD and electroweak corrections to matrix elements are parametrized by the matrices \hat{m}_s and \hat{m}_e , respectively. Hence,

$$c_i^{\text{eff}} = \left[\mathbb{1} + \frac{\alpha_s(\mu)}{4\pi} \hat{m}_s^T(\mu) + \frac{\alpha}{4\pi} \hat{m}_e^T(\mu) \right]_{ij} c_j(\mu), \quad (2.11)$$

where the superscript T denotes a transpose of the matrix. Following the notation of [9,10], we obtain[†]

$$\begin{aligned} c_1^{\text{eff}} \Big|_{\mu_f=m_b} &= c_1(\mu) + \frac{\alpha_s}{4\pi} \left(\gamma^{(0)T} \ln \frac{m_b}{\mu} + \hat{r}^T \right)_{1i} c_i(\mu), \\ c_2^{\text{eff}} \Big|_{\mu_f=m_b} &= c_2(\mu) + \frac{\alpha_s}{4\pi} \left(\gamma^{(0)T} \ln \frac{m_b}{\mu} + \hat{r}^T \right)_{2i} c_i(\mu), \\ c_3^{\text{eff}} \Big|_{\mu_f=m_b} &= c_3(\mu) + \frac{\alpha_s}{4\pi} \left(\gamma^{(0)T} \ln \frac{m_b}{\mu} + \hat{r}^T \right)_{3i} c_i(\mu) - \frac{\alpha_s}{24\pi} (C_t + C_p + C_g), \\ c_4^{\text{eff}} \Big|_{\mu_f=m_b} &= c_4(\mu) + \frac{\alpha_s}{4\pi} \left(\gamma^{(0)T} \ln \frac{m_b}{\mu} + \hat{r}^T \right)_{4i} c_i(\mu) + \frac{\alpha_s}{8\pi} (C_t + C_p + C_g), \\ c_5^{\text{eff}} \Big|_{\mu_f=m_b} &= c_5(\mu) + \frac{\alpha_s}{4\pi} \left(\gamma^{(0)T} \ln \frac{m_b}{\mu} + \hat{r}^T \right)_{5i} c_i(\mu) - \frac{\alpha_s}{24\pi} (C_t + C_p + C_g), \\ c_6^{\text{eff}} \Big|_{\mu_f=m_b} &= c_6(\mu) + \frac{\alpha_s}{4\pi} \left(\gamma^{(0)T} \ln \frac{m_b}{\mu} + \hat{r}^T \right)_{6i} c_i(\mu) + \frac{\alpha_s}{8\pi} (C_t + C_p + C_g), \\ c_7^{\text{eff}} \Big|_{\mu_f=m_b} &= c_7(\mu) + \frac{\alpha_s}{4\pi} \left(\gamma^{(0)T} \ln \frac{m_b}{\mu} + \hat{r}^T \right)_{7i} c_i(\mu) + \frac{\alpha}{8\pi} C_e, \\ c_8^{\text{eff}} \Big|_{\mu_f=m_b} &= c_8(\mu) + \frac{\alpha_s}{4\pi} \left(\gamma^{(0)T} \ln \frac{m_b}{\mu} + \hat{r}^T \right)_{8i} c_i(\mu), \\ c_9^{\text{eff}} \Big|_{\mu_f=m_b} &= c_9(\mu) + \frac{\alpha_s}{4\pi} \left(\gamma^{(0)T} \ln \frac{m_b}{\mu} + \hat{r}^T \right)_{9i} c_i(\mu) + \frac{\alpha}{8\pi} C_e, \\ c_{10}^{\text{eff}} \Big|_{\mu_f=m_b} &= c_{10}(\mu) + \frac{\alpha_s}{4\pi} \left(\gamma^{(0)T} \ln \frac{m_b}{\mu} + \hat{r}^T \right)_{10i} c_i(\mu), \end{aligned} \quad (2.12)$$

[†]Unlike [9,10], we have included vertex corrections to the electroweak coefficients $c_7 - c_{10}$. It also seems to us that a constant term $\frac{2}{3}$ is missed in [9,10] in the coefficient $\tilde{G}(m_i)$ in front of $(c_4 + c_6)$ in C_p [see Eq. (2.13)].

where the matrices $\gamma^{(0)}$ as well as \hat{r} arise from the vertex corrections to the operators $O_1 - O_{10}$ (see Fig. 1), C_t , C_p , C_e and C_g from the QCD penguin-type diagrams of the operators $O_{1,2}$, the QCD penguin-type diagrams of the operators $O_3 - O_6$, the electroweak penguin-type diagram of $O_{1,2}$, and tree-level diagram of the dipole operator O_g , respectively:

$$\begin{aligned}
C_t &= - \left(\frac{\lambda_u}{\lambda_t} \tilde{G}(m_u) + \frac{\lambda_c}{\lambda_t} \tilde{G}(m_c) \right) c_1, \\
C_p &= [\tilde{G}(m_q) + \tilde{G}(m_b)] c_3 + \sum_{i=u,d,s,c,b} \tilde{G}(m_i) (c_4 + c_6), \\
C_g &= - \frac{2m_b}{\sqrt{\langle k^2 \rangle}} c_g^{\text{eff}}, \\
C_e &= - \frac{8}{9} \left(\frac{\lambda_u}{\lambda_t} \tilde{G}(m_u) + \frac{\lambda_c}{\lambda_t} \tilde{G}(m_c) \right) (c_1 + 3c_2), \\
\tilde{G}(m_q) &= \frac{2}{3} \kappa - G(m_q, k, \mu),
\end{aligned} \tag{2.13}$$

with $\lambda_{q'} \equiv V_{q'b} V_{q'q}^*$, and κ being a parameter characterizing the γ_5 scheme dependence in dimensional regularization, for example,

$$\kappa = \begin{cases} 1 & \text{NDR,} \\ 0 & \text{HV.} \end{cases} \tag{2.14}$$

The function $G(m, k, \mu)$ in Eq. (2.13) is given by

$$G(m, k, \mu) = -4 \int_0^1 dx x(1-x) \ln \left(\frac{m^2 - k^2 x(1-x)}{\mu^2} \right), \tag{2.15}$$

where k^2 is the momentum squared carried by the virtual gluon. For $k^2 > 4m^2$, its analytic expression is given by

$$\begin{aligned}
\text{Re } G &= \frac{2}{3} \left(-\ln \frac{m^2}{\mu^2} + \frac{5}{3} + 4 \frac{m^2}{k^2} - \left(1 + 2 \frac{m^2}{k^2} \right) \sqrt{1 - 4 \frac{m^2}{k^2}} \ln \frac{1 + \sqrt{1 - 4 \frac{m^2}{k^2}}}{1 - \sqrt{1 - 4 \frac{m^2}{k^2}}} \right), \\
\text{Im } G &= \frac{2}{3} \pi \left(1 + 2 \frac{m^2}{k^2} \right) \sqrt{1 - 4 \frac{m^2}{k^2}}.
\end{aligned} \tag{2.16}$$

It should be remarked that although the penguin coefficients $c_3 - c_{10}$ are governed by the penguin diagrams with t quark exchange, the effective Wilson coefficients do incorporate the perturbative effects of the penguin diagrams with internal u and c quarks induced by the current-current operator O_1 .

The matrix \hat{r} in (2.12) gives momentum-independent constant terms which depend on the treatment of γ_5 in dimensional regularization. To compute the anomalous dimension $\gamma^{(0)}$ and the matrix \hat{r} , we work in the on-shell (massless) fermion scheme and assume zero momentum transfer squared between color-singlet currents, i.e. $(p_1 - p_3)^2 = 0$ for O_{odd} operators and $(p_1 - p_4)^2 = 0$ for O_{even} operators as required by the light final bound state, for which the transferred energy squared is equal to the mass squared of the bound state and

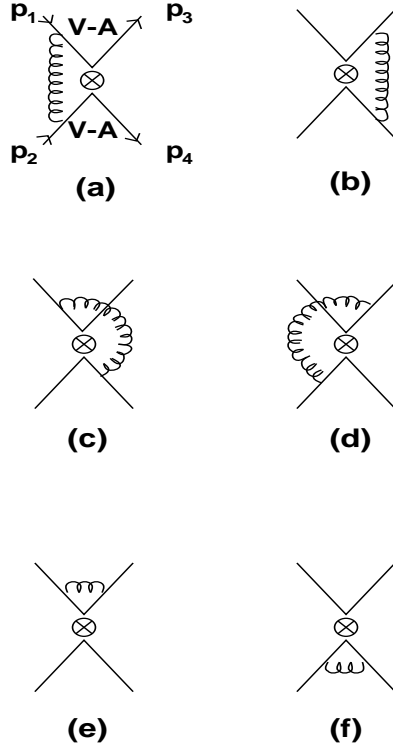


FIG. 1. Vertex corrections to the 4-quark operators $O_1 - O_{10}$.

hence is negligible. Then energy conservation implies that $(p_1 + p_2)^2 = -(-p_2 + p_3)^2$ for the case of massless external fermions if $(p_1 - p_3)^2 = 0$. However, the b quark mass cannot be ignored in the b decay processes. Therefore, we should have $(p_1 + p_2)^2 + (-p_2 + p_3)^2 = m_b^2$ for charmless B decays. Considering the possible spectator quark effects, the reasonable kinematic range for $(p_1 + p_2)^2$ and $(-p_2 + p_3)^2$ lies in the region between $m_b^2/2$ and m_b^2 . Here we choose $(p_1 + p_2)^2 \approx (-p_2 + p_3)^2 \approx m_b^2$ for O_{odd} operators and $(p_1 - p_4)^2 = 0$, $(p_1 + p_2)^2 \approx (-p_2 + p_4)^2 \approx m_b^2$ for O_{even} operators (see Fig. 1 for notation). The results are insensitive to the kinematics of the Mandelstam variables.

We obtain the logarithmic term $\ln(m_b/\mu)$ in Eq. (2.12) with the anomalous dimension [9,11]

$$\gamma^{(0)} = \begin{pmatrix} -2 & 6 & 0 & 0 & 0 & 0 & 0 & 0 & 0 & 0 \\ 6 & -2 & 0 & 0 & 0 & 0 & 0 & 0 & 0 & 0 \\ 0 & 0 & -2 & 6 & 0 & 0 & 0 & 0 & 0 & 0 \\ 0 & 0 & 6 & -2 & 0 & 0 & 0 & 0 & 0 & 0 \\ 0 & 0 & 0 & 0 & 2 & -6 & 0 & 0 & 0 & 0 \\ 0 & 0 & 0 & 0 & 0 & -16 & 0 & 0 & 0 & 0 \\ 0 & 0 & 0 & 0 & 0 & 0 & 2 & -6 & 0 & 0 \\ 0 & 0 & 0 & 0 & 0 & 0 & 0 & -16 & 0 & 0 \\ 0 & 0 & 0 & 0 & 0 & 0 & 0 & 0 & -2 & 6 \\ 0 & 0 & 0 & 0 & 0 & 0 & 0 & 0 & 6 & -2 \end{pmatrix}, \quad (2.17)$$

and the matrix \hat{r}

$$\hat{r}_{\text{NDR}} = \begin{pmatrix} 3 & -9 & 0 & 0 & 0 & 0 & 0 & 0 & 0 & 0 \\ -9 & 3 & 0 & 0 & 0 & 0 & 0 & 0 & 0 & 0 \\ 0 & 0 & 3 & -9 & 0 & 0 & 0 & 0 & 0 & 0 \\ 0 & 0 & -9 & 3 & 0 & 0 & 0 & 0 & 0 & 0 \\ 0 & 0 & 0 & 0 & -1 & 3 & 0 & 0 & 0 & 0 \\ 0 & 0 & 0 & 0 & -3 & 1 & 0 & 0 & 0 & 0 \\ 0 & 0 & 0 & 0 & 0 & 0 & -1 & 3 & 0 & 0 \\ 0 & 0 & 0 & 0 & 0 & 0 & -3 & 1 & 0 & 0 \\ 0 & 0 & 0 & 0 & 0 & 0 & 0 & 0 & 3 & -9 \\ 0 & 0 & 0 & 0 & 0 & 0 & 0 & 0 & -9 & 3 \end{pmatrix} \quad (2.18)$$

in the NDR scheme, and

$$\hat{r}_{\text{HV}} = \begin{pmatrix} \frac{7}{3} & -7 & 0 & 0 & 0 & 0 & 0 & 0 & 0 & 0 \\ -7 & \frac{7}{3} & 0 & 0 & 0 & 0 & 0 & 0 & 0 & 0 \\ 0 & 0 & \frac{7}{3} & -7 & 0 & 0 & 0 & 0 & 0 & 0 \\ 0 & 0 & -7 & \frac{7}{3} & 0 & 0 & 0 & 0 & 0 & 0 \\ 0 & 0 & 0 & 0 & -3 & 9 & 0 & 0 & 0 & 0 \\ 0 & 0 & 0 & 0 & 1 & -\frac{1}{3} & 0 & 0 & 0 & 0 \\ 0 & 0 & 0 & 0 & 0 & 0 & -3 & 9 & 0 & 0 \\ 0 & 0 & 0 & 0 & 0 & 0 & 1 & -\frac{1}{3} & 0 & 0 \\ 0 & 0 & 0 & 0 & 0 & 0 & 0 & 0 & \frac{7}{3} & -7 \\ 0 & 0 & 0 & 0 & 0 & 0 & 0 & 0 & -7 & \frac{7}{3} \end{pmatrix} \quad (2.19)$$

in the HV scheme. It is interesting to note that the $(V - A)(V - A)$ operators $O_1 - O_4$, O_9 , O_{10} have the same $\gamma^{(0)}$ and \hat{r} matrix elements and likewise for $(V - A)(V + A)$ operators $O_5 - O_8$.

From Eq. (2.12) it is clear that the effective Wilson coefficients depend on CKM matrix elements and the gluon's momentum k^2 . Using the next-to-leading order (NLO) $\Delta B = 1$ Wilson coefficients obtained in the HV and NDR schemes at $\mu = m_b(m_b)$, $\Lambda_{\overline{\text{MS}}}^{(5)} = 225$ MeV and $m_t = 170$ GeV in Table 22 of [11], we obtain the numerical values of effective renormalization-scheme and -scale independent, gauge invariant Wilson coefficients c_i^{eff} for $b \rightarrow s$, $b \rightarrow d$ and $\bar{b} \rightarrow \bar{d}$ transitions (see Table I), where uses have been made of the Wolfenstein parameters $\rho = 0.175$ and $\eta = 0.370$ (see Sec. III.A) and the quark masses given in Eq. (3.4). Note that effective Wilson coefficients for $\bar{b} \rightarrow \bar{s}$ transition are the same as that for $b \rightarrow s$ to the accuracy considered in Table I. We see that $c_2^{\text{eff}} = -0.365$ is quite different from the NLO Wilson coefficients: $c_2^{\text{NDR}}(m_b) = -0.185$ and $c_2^{\text{HV}}(m_b) = -0.228$ [11], but close to the lowest order value $c_2^{\text{L.O.}}(m_b) = -0.308$ [11].

Several remarks are in order. (i) There exist infrared double poles, i.e., $1/\epsilon_{\text{IR}}^2$, in some of the amplitudes in Fig. 1, but they are canceled out when summing over all the amplitudes. (ii) Care must be taken when applying the projection method to reduce the tensor products of Dirac matrices to the form $\Gamma \otimes \Gamma$ with $\Gamma = \gamma_\mu(1 - \gamma_5)$. As shown in [7], sometimes it is erroneous to apply the projection method without taking into account the effect of evanescent operators. (iii) When quarks are on their mass shell, it is straightforward to

TABLE I. Numerical values of the effective Wilson coefficients c_i^{eff} for $b \rightarrow s$, $b \rightarrow d$ and $\bar{b} \rightarrow \bar{d}$ transitions evaluated at $\mu_f = m_b$ and $k^2 = m_b^2/2$, where use of the Wolfenstein parameters $\rho = 0.175$ and $\eta = 0.370$ has been made.

	$b \rightarrow s, \bar{b} \rightarrow \bar{s}$	$b \rightarrow d$	$\bar{b} \rightarrow \bar{d}$
c_1^{eff}	1.168	1.168	1.168
c_2^{eff}	-0.365	-0.365	-0.365
c_3^{eff}	$0.0225 + i0.0045$	$0.0224 + i0.0038$	$0.0227 + i0.0052$
c_4^{eff}	$-0.0458 - i0.0136$	$-0.0454 - i0.0115$	$-0.0464 - i0.0155$
c_5^{eff}	$0.0133 + i0.0045$	$0.0131 + i0.0038$	$0.0135 + i0.0052$
c_6^{eff}	$-0.0480 - i0.0136$	$-0.0475 - i0.0115$	$-0.0485 - i0.0155$
c_7^{eff}/α	$-0.0303 - i0.0369$	$-0.0294 - i0.0329$	$-0.0314 - i0.0406$
c_8^{eff}/α	0.055	0.055	0.055
c_9^{eff}/α	$-1.427 - i0.0369$	$-1.426 - i0.0329$	$-1.428 - i0.0406$
$c_{10}^{\text{eff}}/\alpha$	0.48	0.48	0.48

show that the gauge dependent contributions to Figs. 1(a) and 1(b) are compensated by that of Figs. 1(c) and 1(d), while the gauge dependent part of Figs. 1(e) and 1(f) is canceled by that of the quark wave function renormalization [7]. (iv) For comparison with (2.18), the matrix \hat{r} obtained in the NDR γ_5 scheme using off-shell regularization and Landau gauge is given by[‡]

$$\hat{r}_{\text{NDR}}^{\lambda=0} = \begin{pmatrix} \frac{7}{3} & -7 & 0 & 0 & 0 & 0 & 0 & 0 & 0 & 0 \\ -7 & \frac{7}{3} & 0 & 0 & 0 & 0 & 0 & 0 & 0 & 0 \\ 0 & 0 & \frac{7}{3} & -7 & 0 & 0 & 0 & 0 & 0 & 0 \\ 0 & 0 & -7 & \frac{7}{3} & 0 & 0 & 0 & 0 & 0 & 0 \\ 0 & 0 & 0 & 0 & -\frac{2}{3} & 2 & 0 & 0 & 0 & 0 \\ 0 & 0 & 0 & 0 & -2 & \frac{34}{3} & 0 & 0 & 0 & 0 \\ 0 & 0 & 0 & 0 & 0 & 0 & -\frac{2}{3} & 2 & 0 & 0 \\ 0 & 0 & 0 & 0 & 0 & 0 & -2 & \frac{34}{3} & 0 & 0 \\ 0 & 0 & 0 & 0 & 0 & 0 & 0 & 0 & \frac{7}{3} & -7 \\ 0 & 0 & 0 & 0 & 0 & 0 & 0 & 0 & -7 & \frac{7}{3} \end{pmatrix}. \quad (2.20)$$

The numerical results of c_i^{eff} obtained using (2.20) are similar to that listed in Table I except for $c_{2,6,10}^{\text{eff}}$: $c_2^{\text{eff}} = -0.325$, $c_6^{\text{eff}} = -0.0560 - i0.0136$ and $c_{10}^{\text{eff}} = 0.263\alpha$. We see from Table I that, contrary to the commonly used value (but not gauge invariant) $\text{Re } c_6^{\text{eff}} \approx -0.060 \sim -0.063$ in the literature, the *gauge-invariant* effective penguin coefficient $\text{Re } c_6^{\text{eff}} \approx -0.048$ does not get much enhancement, recalling that $c_6(m_b) = -0.041$ to NLO [11]. (v) To check the scheme

[‡]Our expression for $\hat{r}_{\text{NDR}}^{\lambda=0}$ is slightly different from that given in [9] for the matrix elements \hat{r}_{55} to \hat{r}_{88} .

and scale independence of effective Wilson coefficients, say $c_{1,2}^{\text{eff}}$, it is convenient to work in the diagonal basis in which the operators $O_{\pm} = \frac{1}{2}(O_1 \pm O_2)$ do not mix under renormalization. The Wilson coefficients in general have the expressions [11]:

$$c_{\pm}(\mu) = \left[1 + \frac{\alpha_s(\mu)}{4\pi} J_{\pm} \right] \left[\frac{\alpha_s(m_W)}{\alpha_s(\mu)} \right]^{\gamma_{\pm}^{(0)}/(2\beta_0)} \left[1 + \frac{\alpha_s(m_W)}{4\pi} (B_{\pm} - J_{\pm}) \right], \quad (2.21)$$

where $c_{\pm} = c_1 \pm c_2$, $\beta_0 = 11 - \frac{2}{3}n_f$ with n_f being the number of flavors between m_W and μ scales, B_{\pm} specifies the initial condition of $c(m_W)$: $c(m_W) = 1 + \frac{\alpha_s(m_W)}{4\pi} B_{\pm}$ and it is γ_5 -scheme dependent, and $J_{\pm} = \gamma_{\pm}^{(0)}\beta_1/(2\beta_0^2) - \tilde{\gamma}_{\pm}^{(1)}/(2\beta_0)$ with $\beta_1 = 102 - 38n_f/3$. The anomalous dimensions $\tilde{\gamma}_{\pm}^{(1)} = \gamma_{\pm}^{(1)} - 2\gamma_J$ are γ_5 -scheme dependent, where $\gamma_{\pm}^{(1)}$ are the two-loop anomalous dimensions of O_{\pm} and γ_J is the anomalous dimension of the weak current in full theory. (The complete expression for $\gamma_{\pm}^{(1)}$ and γ_J in different schemes can be found in [11], for example.) As stressed in [12], $c(\mu)$ do not depend on the external states; any external state can be used for their extraction, the only requirement being that the infrared and mass singularities are properly regularized. This means that the short-distance Wilson coefficients calculated from Eq. (2.21) are independent of the fermion state, on-shell or off-shell. Since $B_{\pm} - J_{\pm}$ is scheme independent [11,12], the scheme dependence of $c_{\pm}(\mu)$ is solely governed by J_{\pm} . Using the fact that $\tilde{\gamma}_{\pm}^{(1)}$ are also free of the external-state dependence, we have shown explicitly in [7] the renormalization scheme independence of $\hat{r}_{\pm}^T + J_{\pm}$ and hence c_{\pm}^{eff} . It is also straightforward to show that, to the leading logarithmic approximation, the scale dependence of $c_{\pm}(\mu)$ arising from the $\alpha_s(m_W)/\alpha_s(\mu)$ term in Eq. (2.21) is compensated by the $\gamma^{(0)T} \ln(m_b/\mu)$ term in Eq. (2.12).

III. INPUT PARAMETERS

A. Quark mixing matrix

It is convenient to parametrize the quark mixing matrix in terms of the Wolfenstein parameters: A , λ , ρ and η [13],

$$V = \begin{pmatrix} 1 - \frac{1}{2}\lambda^2 & \lambda & A\lambda^3(\rho - i\eta) \\ -\lambda & 1 - \frac{1}{2}\lambda^2 & A\lambda^2 \\ A\lambda^3(1 - \rho - i\eta) & -A\lambda^2 & 1 \end{pmatrix} + \mathcal{O}(\lambda^4), \quad (3.1)$$

where $\lambda = 0.2205$ is equivalent to $\sin\theta_C$ with θ_C being the Cabibbo angle. Note that this parametrization is an approximation of the exact Chau-Keung parametrization [14] of the quark mixing matrix. For the parameter A , we fix it to $A = 0.815$ corresponding to $|V_{cb}| = 0.0396$. As for the parameters ρ and η , two different updated analyses [15,16] have been performed using the combination of the precise measurement of ΔM_d , the mass difference in the B_d system, the updated limit on ΔM_s , the mass difference in the B_s system, and the determination of $|V_{ub}|$ from charmless semileptonic B decays. The results

$$\rho(1 - \frac{\lambda^2}{2}) = 0.189 \pm 0.074, \quad \eta(1 - \frac{\lambda^2}{2}) = 0.354 \pm 0.045, \quad (3.2)$$

and

$$\rho = 0.160_{-0.070}^{+0.094}, \quad \eta = 0.381_{-0.058}^{+0.061} \quad (3.3)$$

are cited in [15] and [16], respectively; they are obtained by a simultaneous fit to all the available data. In either fit, it is clear that $\sqrt{\rho^2 + \eta^2} = 0.41$ is slightly larger than the previous analysis. For our purposes in the present paper we will employ the values $\rho = 0.175$ and $\eta = 0.370$; they correspond to the unitarity angles: $\alpha = 91^\circ$, $\beta = 24^\circ$ and $\gamma = 65^\circ$. We shall see in Sec. V that some of hadronic rare B decay data will be much more easily accounted for if $\gamma > 90^\circ$ or $\rho < 0$. Therefore, we shall use $\gamma = 65^\circ$ as a benchmarked value and then discuss the impact of a negative ρ whenever necessary.

B. Running quark masses

We shall see later that running quark masses appear in the matrix elements of $(S - P)(S + P)$ penguin operators through the use of equations of motion. The running quark mass should be applied at the scale $\mu \sim m_b$ because the energy released in the energetic two-body charmless decays of the B meson is of order m_b . Explicitly, we use [17]

$$\begin{aligned} m_u(m_b) &= 3.2 \text{ MeV}, & m_d(m_b) &= 6.4 \text{ MeV}, & m_s(m_b) &= 90 \text{ MeV}, \\ m_c(m_b) &= 0.95 \text{ GeV}, & m_b(m_b) &= 4.34 \text{ GeV}, \end{aligned} \quad (3.4)$$

in ensuing calculation, where $m_s(m_b) = 90 \text{ MeV}$ corresponds to $m_s = 140 \text{ MeV}$ at $\mu = 1 \text{ GeV}$.

C. Decay constants

For the decay constants we use $f_\pi = 132 \text{ MeV}$, $f_K = 160 \text{ MeV}$, $f_\rho = 216 \text{ MeV}$, $f_{K^*} = 221 \text{ MeV}$, $f_\omega = 195 \text{ MeV}$ and $f_\phi = 237 \text{ MeV}$. To determine the decay constants of the η and η' mesons, defined by $\langle 0 | \bar{q} \gamma_\mu \gamma_5 q | \eta^{(\prime)} \rangle = i f_{\eta^{(\prime)}}^q p_\mu$, we need to know the wave functions of the physical η' and η states which are related to that of the SU(3) singlet state η_0 and octet state η_8 by

$$\eta' = \eta_8 \sin \theta + \eta_0 \cos \theta, \quad \eta = \eta_8 \cos \theta - \eta_0 \sin \theta. \quad (3.5)$$

When the $\eta - \eta'$ mixing angle is -19.5° , the expressions of the η' and η wave functions become very simple [2]:

$$|\eta'\rangle = \frac{1}{\sqrt{6}} |\bar{u}u + \bar{d}d + 2\bar{s}s\rangle, \quad |\eta\rangle = \frac{1}{\sqrt{3}} |\bar{u}u + \bar{d}d - \bar{s}s\rangle, \quad (3.6)$$

recalling that

$$|\eta_0\rangle = \frac{1}{\sqrt{3}} |\bar{u}u + \bar{d}d + \bar{s}s\rangle, \quad |\eta_8\rangle = \frac{1}{\sqrt{6}} |\bar{u}u + \bar{d}d - 2\bar{s}s\rangle. \quad (3.7)$$

At this specific mixing angle, $f_{\eta'}^u = \frac{1}{2}f_{\eta'}^s$ in the SU(3) limit. Introducing the decay constants f_8 and f_0 by

$$\langle 0|A_\mu^0|\eta_0\rangle = if_0p_\mu, \quad \langle 0|A_\mu^8|\eta_8\rangle = if_8p_\mu, \quad (3.8)$$

and noting that due to SU(3) breaking the matrix elements $\langle 0|A_\mu^{0(8)}|\eta_{8(0)}\rangle$ do not vanish in general and they will induce a two-angle mixing among the decay constants:

$$f_{\eta'}^u = \frac{f_8}{\sqrt{6}}\sin\theta_8 + \frac{f_0}{\sqrt{3}}\cos\theta_0, \quad f_{\eta'}^s = -2\frac{f_8}{\sqrt{6}}\sin\theta_8 + \frac{f_0}{\sqrt{3}}\cos\theta_0. \quad (3.9)$$

Likewise, for the η meson

$$f_\eta^u = \frac{f_8}{\sqrt{6}}\cos\theta_8 - \frac{f_0}{\sqrt{3}}\sin\theta_0, \quad f_\eta^s = -2\frac{f_8}{\sqrt{6}}\cos\theta_8 - \frac{f_0}{\sqrt{3}}\sin\theta_0. \quad (3.10)$$

It must be accentuated that the two-mixing angle formalism proposed in [18,19] applies to the decay constants of the η' and η rather than to their wave functions. Based on the ansatz that the decay constants in the quark flavor basis follow the pattern of particle state mixing, relations between θ_8 , θ_0 and θ are derived in [19]. It is found in [19] that phenomenologically

$$\theta_8 = -21.2^\circ, \quad \theta_0 = -9.2^\circ, \quad \theta = -15.4^\circ, \quad (3.11)$$

and

$$f_8/f_\pi = 1.26, \quad f_0/f_\pi = 1.17. \quad (3.12)$$

Numerically, we obtain

$$f_{\eta'}^u = 78 \text{ MeV}, \quad f_{\eta'}^s = -112 \text{ MeV}, \quad f_\eta^u = 63 \text{ MeV}, \quad f_\eta^s = 137 \text{ MeV}. \quad (3.13)$$

The decay constant $f_{\eta'}^c$, defined by $\langle 0|\bar{c}\gamma_\mu\gamma_5c|\eta'\rangle = if_{\eta'}^c q_\mu$, has been determined from theoretical calculations [20–23] and from the phenomenological analysis of the data of $J/\psi \rightarrow \eta_c\gamma$, $J/\psi \rightarrow \eta'\gamma$ and of the $\eta\gamma$ and $\eta'\gamma$ transition form factors [9,19,24–27]; it lies in the range $-2.0 \text{ MeV} \leq f_{\eta'}^c \leq -18.4 \text{ MeV}$. In this paper we use the values

$$f_{\eta'}^c = -(6.3 \pm 0.6) \text{ MeV}, \quad f_\eta^c = -(2.4 \pm 0.2) \text{ MeV}, \quad (3.14)$$

as obtained from a phenomenological analysis performed in [19].

D. Form factors

As for form factors, we follow [28] to use the following parametrization:

$$\begin{aligned} \langle 0|A_\mu|P(q)\rangle &= if_P q_\mu, & \langle 0|V_\mu|V(p, \varepsilon)\rangle &= f_V m_V \varepsilon_\mu, \\ \langle P'(p')|V_\mu|P(p)\rangle &= \left(p_\mu + p'_\mu - \frac{m_P^2 - m_{P'}^2}{q^2} q_\mu\right) F_1(q^2) + F_0(q^2) \frac{m_P^2 - m_{P'}^2}{q^2} q_\mu, \\ \langle V(p', \varepsilon)|V_\mu|P(p)\rangle &= \frac{2}{m_P + m_V} \epsilon_{\mu\nu\alpha\beta} \varepsilon^{*\nu} p^\alpha p'^\beta V(q^2), \\ \langle V(p', \varepsilon)|A_\mu|P(p)\rangle &= i\left[(m_P + m_V)\varepsilon_\mu^* A_1(q^2) - \frac{\varepsilon^* \cdot p}{m_P + m_V} (p + p')_\mu A_2(q^2) \right. \\ &\quad \left. - 2m_V \frac{\varepsilon^* \cdot p}{q^2} q_\mu [A_3(q^2) - A_0(q^2)]\right], \end{aligned} \quad (3.15)$$

where $q = p - p'$, $F_1(0) = F_0(0)$, $A_3(0) = A_0(0)$, and

$$A_3(q^2) = \frac{m_P + m_V}{2m_V} A_1(q^2) - \frac{m_P - m_V}{2m_V} A_2(q^2). \quad (3.16)$$

We consider two different form-factor models for heavy-to-light form factors: the Bauer-Stech-Wirbel (BSW) model [28] and the light-cone sum rule (LCSR) model [29]. The relevant form factors at zero momentum transfer are listed in Table II.

Table II. Form factors at zero momentum transfer for $B \rightarrow P$ and $B \rightarrow V$ transitions evaluated in the BSW model [28,6]. The values given in the square brackets are obtained in the light-cone sum rule (LCSR) analysis [29]. We have assumed SU(3) symmetry for the $B \rightarrow \omega$ form factors in the LCSR approach. In realistic calculations we use Eq. (3.19) for $B \rightarrow \eta^{(\prime)}$ form factors.

Decay	$F_1 = F_0$	V	A_1	A_2	$A_3 = A_0$
$B \rightarrow \pi^\pm$	0.333 [0.305]				
$B \rightarrow K$	0.379 [0.341]				
$B \rightarrow \eta$	0.168 [—]				
$B \rightarrow \eta'$	0.114 [—]				
$B \rightarrow \rho^\pm$		0.329 [0.338]	0.283 [0.261]	0.283 [0.223]	0.281 [0.372]
$B \rightarrow \omega$		0.232 [0.239]	0.199 [0.185]	0.199 [0.158]	0.198 [0.263]
$B \rightarrow K^*$		0.369 [0.458]	0.328 [0.337]	0.331 [0.203]	0.321 [0.470]

It should be stressed that the form factors for $B \rightarrow \eta^{(\prime)}$ transition calculated by BSW [28] did not include the wave function normalization and mixing angles. In the relativistic quark model calculation of $B \rightarrow \eta^{(\prime)}$ transition, BSW put in the $u\bar{u}$ constituent quark mass only. That is, the form factors considered by BSW are actually $F_0^{B\eta_{u\bar{u}}}$ and $F_0^{B\eta'_{u\bar{u}}}$. To compute the physical form factors, one has to take into account the wave function normalizations of the η and η' :

$$F_{0,1}^{B\eta} = \left(\frac{1}{\sqrt{6}} \cos \theta - \frac{1}{\sqrt{3}} \sin \theta \right) F_{0,1}^{B\eta_{u\bar{u}}}, \quad F_{0,1}^{B\eta'} = \left(\frac{1}{\sqrt{6}} \sin \theta + \frac{1}{\sqrt{3}} \cos \theta \right) F_{0,1}^{B\eta'_{u\bar{u}}}. \quad (3.17)$$

Using $F_0^{B\eta_{u\bar{u}}}(0) = 0.307$ and $F_0^{B\eta'_{u\bar{u}}}(0) = 0.254$ from BSW [6], we find $F_0^{B\eta}(0) = 0.168$ and $F_0^{B\eta'}(0) = 0.114$ as shown in Table II. However, as we shall see in Sec. V.D, the form factor $F_0^{B\eta'}$ is preferred to be a bit larger in order to accommodate the data of $B \rightarrow \eta' K$. Hence, we shall assume the nonet symmetry relation $\sqrt{3}F_0^{B\eta_0}(0) = \sqrt{6}F_0^{B\eta_8}(0) = F_0^{B\pi^\pm}(0)$ to obtain $F_0^{B\eta_0}$, $F_0^{B\eta_8}$ and then relate them to the physical form factors via

$$F_0^{B\eta} = \cos \theta F_0^{B\eta_8} - \sin \theta F_0^{B\eta_0}, \quad F_0^{B\eta'} = \sin \theta F_0^{B\eta_8} + \cos \theta F_0^{B\eta_0}. \quad (3.18)$$

Numerically, we obtain

$$F_0^{B\eta}(0) = 0.181, \quad F_0^{B\eta'}(0) = 0.148, \quad (3.19)$$

for $F_0^{B\pi^\pm}(0) = 0.33$.

For the q^2 dependence of form factors in the region where q^2 is not too large, we shall use the pole dominance ansatz, namely,

$$f(q^2) = \frac{f(0)}{(1 - q^2/m_*^2)^n}, \quad (3.20)$$

where m_* is the pole mass given in [6]. A direct calculation of $B \rightarrow P$ and $B \rightarrow V$ form factors at timelike momentum transfer is available in the relativistic light-front quark model [30] with the results that the q^2 dependence of the form factors A_0 , A_2 , V , F_1 is a dipole behavior (i.e. $n = 2$), while A_1 , F_0 exhibit a monopole dependence ($n = 1$). Note that the original BSW model assumes a monopole behavior for all the form factors. This is not consistent with heavy quark symmetry for heavy-to-heavy transition. Therefore, in the present paper we will employ the BSW model for the heavy-to-light form factors at zero momentum transfer but take a different ansatz for their q^2 dependence, namely a dipole dependence for F_1 , A_0 , A_2 and V . In the light-cone sum rule analysis of [29], the form-factor q^2 dependence is evaluated using the parametrization

$$f(q^2) = \frac{f(0)}{1 - a(q^2/m_B^2) + b(q^2/m_B^2)^2}, \quad (3.21)$$

where the values of a and b are given in [29]. The hadronic charmless B decays are in general insensitive to the expressions of form-factor q^2 dependence because q^2 is small. Nevertheless, we find that the decay rates of $B \rightarrow VV$ show a moderate dependence on the q^2 behavior of form factors.

IV. FACTORIZED AMPLITUDES

A. Effective parameters and nonfactorizable effects

It is known that the effective Wilson coefficients appear in the factorizable decay amplitudes in the combinations $a_{2i} = c_{2i}^{\text{eff}} + \frac{1}{N_c} c_{2i-1}^{\text{eff}}$ and $a_{2i-1} = c_{2i-1}^{\text{eff}} + \frac{1}{N_c} c_{2i}^{\text{eff}}$ ($i = 1, \dots, 5$). Phenomenologically, the number of colors N_c is often treated as a free parameter to model the nonfactorizable contribution to hadronic matrix elements and its value can be extracted from the data of two-body nonleptonic decays. As shown in [31–33], nonfactorizable effects in the decay amplitudes of $B \rightarrow PP$, VP can be absorbed into the parameters a_i^{eff} . This amounts to replacing N_c in a_i^{eff} by $(N_c^{\text{eff}})_i$. Explicitly,

$$a_{2i}^{\text{eff}} = c_{2i}^{\text{eff}} + \frac{1}{(N_c^{\text{eff}})_{2i}} c_{2i-1}^{\text{eff}}, \quad a_{2i-1}^{\text{eff}} = c_{2i-1}^{\text{eff}} + \frac{1}{(N_c^{\text{eff}})_{2i-1}} c_{2i}^{\text{eff}}, \quad (i = 1, \dots, 5), \quad (4.1)$$

where

$$(1/N_c^{\text{eff}})_i \equiv (1/N_c) + \chi_i, \quad (4.2)$$

with χ_i being the nonfactorizable terms which receive main contributions from color-octet current operators [34]. In the absence of final-state interactions, we shall assume that χ_i

and hence $(N_c^{\text{eff}})_i$ are real. If χ_i are universal (i.e. process independent) in charm or bottom decays, then we have a generalized factorization scheme in which the decay amplitude is expressed in terms of factorizable contributions multiplied by the universal effective parameters a_i^{eff} . For $B \rightarrow VV$ decays, this new factorization implies that nonfactorizable terms contribute in equal weight to all partial wave amplitudes so that a_i^{eff} can be defined. Phenomenological analyses of the two-body decay data of D and B mesons indicate that while the generalized factorization hypothesis in general works reasonably well, the effective parameters $a_{1,2}^{\text{eff}}$ do show some variation from channel to channel, especially for the weak decays of charmed mesons (see e.g. [31]). A recent updated analysis of $B \rightarrow D\pi$ data gives [35]

$$N_c^{\text{eff}}(B \rightarrow D\pi) \sim (1.8 - 2.1), \quad \chi_2(B \rightarrow D\pi) \sim (0.15 - 0.24). \quad (4.3)$$

It is customary to assume in the literature that $(N_c^{\text{eff}})_1 \approx (N_c^{\text{eff}})_2 \cdots \approx (N_c^{\text{eff}})_{10}$ so that the subscript i can be dropped; that is, the nonfactorizable term is often postulated to behave in the same way in penguin and tree decay amplitudes. A closer investigation shows that this is not the case. We have argued in [8] that nonfactorizable effects in the matrix elements of $(V - A)(V + A)$ operators are *a priori* different from that of $(V - A)(V - A)$ operators. One primary reason is that the Fierz transformation of the $(V - A)(V + A)$ operators $O_{5,6,7,8}$ is quite different from that of $(V - A)(V - A)$ operators $O_{1,2,3,4}$ and $O_{9,10}$. As a result, contrary to the common assertion, $N_c^{\text{eff}}(LR)$ induced by the $(V - A)(V + A)$ operators are theoretically different from $N_c^{\text{eff}}(LL)$ generated by the $(V - A)(V - A)$ operators [8]. Therefore, we shall assume that

$$\begin{aligned} N_c^{\text{eff}}(LL) &\equiv (N_c^{\text{eff}})_1 \approx (N_c^{\text{eff}})_2 \approx (N_c^{\text{eff}})_3 \approx (N_c^{\text{eff}})_4 \approx (N_c^{\text{eff}})_9 \approx (N_c^{\text{eff}})_{10}, \\ N_c^{\text{eff}}(LR) &\equiv (N_c^{\text{eff}})_5 \approx (N_c^{\text{eff}})_6 \approx (N_c^{\text{eff}})_7 \approx (N_c^{\text{eff}})_8, \end{aligned} \quad (4.4)$$

and $N_c^{\text{eff}}(LR) \neq N_c^{\text{eff}}(LL)$ in general. In principle, N_c^{eff} can vary from channel to channel, as in the case of charm decay. However, in the energetic two-body B decays, N_c^{eff} is expected to be process insensitive as supported by the data [34]. From the data analysis in Sec. V, we shall see that $N_c^{\text{eff}}(LL) < 3$ and $N_c^{\text{eff}}(LR) > 3$.

The N_c^{eff} -dependence of the effective parameters a_i^{eff} is shown in Table III for several representative values of N_c^{eff} . From the Table we see that (i) the dominant coefficients are a_1, a_2 for current-current amplitudes, a_4 and a_6 for QCD penguin-induced amplitudes, and a_9 for electroweak penguin-induced amplitudes, and (ii) a_1, a_4, a_6 and a_9 are N_c^{eff} -stable, while the others depend strongly on N_c^{eff} . Therefore, for charmless B decays whose decay amplitudes depend dominantly on N_c^{eff} -stable coefficients, their decay rates can be reliably predicted within the factorization approach even in the absence of information on nonfactorizable effects.

B. Factorized amplitudes and their classification

Applying the effective Hamiltonian (2.1), the factorizable decay amplitudes of $B_u, B_d \rightarrow PP, VP, VV$ obtained within the generalized factorization approach are tabulated in the

Table III. Numerical values for the effective coefficients a_i^{eff} for $b \rightarrow s$ transition at $N_c^{\text{eff}} = 2, 3, 5, \infty$ (in units of 10^{-4} for a_3, \dots, a_{10}). For simplicity we will drop the superscript “eff” henceforth.

	$N_c^{\text{eff}} = 2$	$N_c^{\text{eff}} = 3$	$N_c^{\text{eff}} = 5$	$N_c^{\text{eff}} = \infty$
a_1	0.985	1.046	1.095	1.168
a_2	0.219	0.024	-0.131	-0.365
a_3	$-4.15 - 22.8i$	72	$133 + 18.1i$	$225 + 45.3i$
a_4	$-345 - 113i$	$-383 - 121i$	$-413 - 127i$	$-458 - 136i$
a_5	$-107 - 22.7i$	-27	$36.7 + 18.2i$	$133 + 45.4i$
a_6	$-413 - 113i$	$-435 - 121i$	$-453 - 127i$	$-480 - 136i$
a_7	$-0.22 - 2.73i$	$-0.89 - 2.73i$	$-1.43 - 2.73i$	$-2.24 - 2.73i$
a_8	$2.93 - 1.37i$	$3.30 - 0.91i$	$3.60 - 0.55i$	4
a_9	$-87.9 - 2.71i$	$-93.9 - 2.71i$	$-98.6 - 2.71i$	$-105 - 2.71i$
a_{10}	$-17.3 - 1.36i$	$0.32 - 0.90i$	$14.4 - 0.54i$	36

Appendix. Note that while our factorized amplitudes agree with that presented in [10], we do include W -exchange, W -annihilation and spacelike penguin matrix elements in the expressions of decay amplitudes, though they are usually neglected in practical calculations of decay rates. Nevertheless, whether or not W -exchange and W -annihilation are negligible should be tested and the negligence of spacelike penguins (i.e. the terms $X^{(B, M_1 M_2)}$ multiplied by penguin coefficients) is actually quite questionable (see Sec. V.H. for discussion). Therefore, we keep trace of annihilation terms and spacelike penguins in the Appendix.

All the penguin contributions to the decay amplitudes can be derived from Table IV by studying the underlying b quark weak transitions [4,36]. To illustrate this, let $X^{(BM_1, M_2)}$ denote the factorizable amplitude with the meson M_2 being factored out:

$$X^{(BM_1, M_2)} = \langle M_2 | (\bar{q}_2 q_3)_{V-A} | 0 \rangle \langle M_1 | (\bar{q}_1 b)_{V-A} | \bar{B} \rangle. \quad (4.5)$$

In general, when M_2 is a charged state, only a_{even} penguin terms contribute. For example, from Table IV we obtain

$$\begin{aligned} A(\bar{B}_d \rightarrow \pi^+ K^-)_{\text{peng}} &\propto [a_4 + a_{10} + (a_6 + a_8)R] X^{(\bar{B}_d \pi^+, K^-)}, \\ A(\bar{B}_d \rightarrow \pi^+ K^{*-})_{\text{peng}} &\propto [a_4 + a_{10}] X^{(\bar{B}_d \pi^+, K^{*-})}, \\ A(\bar{B}_d \rightarrow \rho^+ K^-)_{\text{peng}} &\propto [a_4 + a_{10} - (a_6 + a_8)R'] X^{(\bar{B}_d \rho^+, K^-)}, \end{aligned} \quad (4.6)$$

with $R' \approx R \approx m_K^2 / (m_b m_s)$. When M_2 is a flavor neutral meson with $I_3 = 0$, namely, $M_2 = \pi^0, \rho^0, \omega$ and $\eta^{(\prime)}$, a_{odd} penguin terms start to contribute. From Table IV we see that the decay amplitudes of $\bar{B} \rightarrow M\pi^0$, $\bar{B} \rightarrow M\rho^0$, $\bar{B} \rightarrow M\omega$, $\bar{B} \rightarrow M\eta^{(\prime)}$ ($\bar{B} = B_u^-, \bar{B}_d$) contain the following respective factorizable terms:

$$\begin{aligned} &\frac{3}{2}(-a_7 + a_9)X_u^{(BM, \pi^0)}, \\ &\frac{3}{2}(a_7 + a_9)X_u^{(BM, \rho^0)}, \end{aligned}$$

$$\begin{aligned}
& (2a_3 + 2a_5 + \frac{1}{2}a_7 + \frac{1}{2}a_9)X_u^{(BM,\omega)}, \\
& (2a_3 - 2a_5 - \frac{1}{2}a_7 + \frac{1}{2}a_9)X_u^{(BM,\eta^{(\prime)})},
\end{aligned} \tag{4.7}$$

where the subscript u denotes the $u\bar{u}$ quark content of the neutral meson:

$$X_u^{(BM,\pi^0)} = \langle \pi^0 | (\bar{u}u)_{V-A} | 0 \rangle \langle M_1 | (\bar{q}_1 b)_{V-A} | \bar{B} \rangle. \tag{4.8}$$

In deriving Eq. (4.7) we have used the fact that the $d\bar{d}$ wave function in the π^0, ρ^0 ($\omega, \eta^{(\prime)}$) has a sign opposite to (the same as) that of the $u\bar{u}$ one. QCD penguins contribute to all charmless B_u and B_d decays except for $B_u^- \rightarrow \pi^- \pi^0, \rho^- \rho^0$ which only receive $\Delta I = \frac{3}{2}$ contributions. Applying the rules of Table IV, it is easily seen that

$$A(B_u^- \rightarrow \pi^- \pi^0)_{\text{peng}} \propto \frac{3}{2} \left[-a_7 + a_9 + a_{10} + a_8 \frac{m_\pi^2}{m_d(m_b - m_d)} \right] X^{(B^- \pi^-, \pi^0)}. \tag{4.9}$$

Table IV. Penguin contributions to the factorizable $B \rightarrow PP, VP, VV$ decay amplitudes multiplied by $-(G_F/\sqrt{2})V_{tb}V_{tq}^*$, where $q = d, s$. The notation $B \rightarrow M_1, M_2$ means that the meson M_2 can be factored out under the factorization approximation. In addition to the a_{even} terms, the rare B decays also receive contributions from a_{odd} penguin effects when M_2 is a flavor neutral meson. Except for η or η' production, the coefficients R and R' are given by $R = 2m_P^2/[(m_1+m_2)(m_b-m_3)]$ and $R' = -2m_P^2/[(m_1+m_2)(m_b+m_3)]$, respectively.

Decay	$b \rightarrow qu\bar{u}, b \rightarrow qc\bar{c}$	$b \rightarrow qd\bar{d}, b \rightarrow qs\bar{s}$
$B \rightarrow P, P$	$a_4 + a_{10} + (a_6 + a_8)R$	$a_4 - \frac{1}{2}a_{10} + (a_6 - \frac{1}{2}a_8)R$
$B \rightarrow V, P$	$a_4 + a_{10} + (a_6 + a_8)R'$	$a_4 - \frac{1}{2}a_{10} + (a_6 - \frac{1}{2}a_8)R'$
$B \rightarrow P, V$	$a_4 + a_{10}$	$a_4 - \frac{1}{2}a_{10}$
$B \rightarrow V, V$	$a_4 + a_{10}$	$a_4 - \frac{1}{2}a_{10}$
$B \rightarrow P, P^0$	$a_3 - a_5 - a_7 + a_9$	$a_3 - a_5 + \frac{1}{2}a_7 - \frac{1}{2}a_9$
$B \rightarrow V, P^0$	$a_3 - a_5 - a_7 + a_9$	$a_3 - a_5 + \frac{1}{2}a_7 - \frac{1}{2}a_9$
$B \rightarrow P, V^0$	$a_3 + a_5 + a_7 + a_9$	$a_3 + a_5 - \frac{1}{2}a_7 - \frac{1}{2}a_9$
$B \rightarrow V, V^0$	$a_3 + a_5 + a_7 + a_9$	$a_3 + a_5 - \frac{1}{2}a_7 - \frac{1}{2}a_9$

Just as the charm decays or B decays into the charmed meson, the tree-dominated amplitudes for hadronic charmless B decays are customarily classified into three classes [6]:

- Class-I for the decay modes dominated by the external W -emission characterized by the parameter a_1 . Examples are $\bar{B}_d \rightarrow \pi^+ \pi^-, \rho^+ \pi^-, B_u^- \rightarrow K^{0(*)} K^{0(*)}, \dots$.
- Class-II for the decay modes dominated by the color-suppressed internal W -emission characterized by the parameter a_2 . Examples are $\bar{B}_d \rightarrow \pi^0 \pi^0, \omega \pi^0, \dots$.
- Class-III decays involving both external and internal W emissions. Hence the class-III amplitude is of the form $a_1 + r a_2$. Examples are $B_u^- \rightarrow \pi^- \pi^0, \rho^- \pi^0, \omega \pi^-, \dots$.

Likewise, penguin-dominated charmless B decays can be classified into three categories:[§]

- Class-IV for those decays whose amplitudes are governed by the QCD penguin parameters a_4 and a_6 in the combination $a_4 + Ra_6$, where the coefficient R arises from the $(S - P)(S + P)$ part of the operator O_6 . In general, $R = 2m_{P_b}^2/[(m_1 + m_2)(m_b - m_3)]$ for $B \rightarrow P_a P_b$ with the meson P_b being factored out under the factorization approximation, $R = -2m_{P_b}^2/[(m_1 + m_2)(m_b + m_3)]$ for $B \rightarrow V_a P_b$, and $R = 0$ for $B \rightarrow P_a V_b$ and $B \rightarrow V_a V_b$. Note that a_4 is always accompanied by a_{10} , and a_6 by a_8 . In short, class-IV modes are governed by a_{even} penguin terms. Examples are $\overline{B}_d \rightarrow K^- \pi^+$, $K^- \rho^+$, $B_u^- \rightarrow \overline{K}^0 \pi^-$, $K^- K^0$, \dots .
- Class-V modes for those decays whose amplitudes are governed by the effective coefficients a_3, a_5, a_7 and a_9 (i.e. a_{odd} penguin terms) in the combinations $a_3 \pm a_5$ and/or $a_7 \pm a_9$ (see Table IV). Examples are $\overline{B}_d \rightarrow \phi \pi^0$, $\phi \eta^{(\prime)}$, $B_u^- \rightarrow \phi \pi^-$, $\phi \rho^-$.
- Class-VI modes involving the interference of a_{even} and a_{odd} terms, e.g. $\overline{B}_d \rightarrow \overline{K}^0 \pi^0$, $\overline{K}^0 \phi$, $B_u^- \rightarrow K^- \pi^0$, $K^- \phi$, \dots .

Sometimes the tree and penguin contributions are comparable. In this case, the interference between penguin and spectator amplitudes is at work. There are several such decay modes. For example, $B^0 \rightarrow \pi^0 \pi^0$, $\eta^{(\prime)} \eta^{(\prime)}$ involve class-II and -VI amplitudes, $B^- \rightarrow \rho^0 K^-$, ωK^- consist of class-III and -VI amplitudes, and $\overline{B}^0 \rightarrow \rho^+ K^-$ receives contributions from class-I and class-IV amplitudes (see Tables V and VI).

Using the BSW model for form factors, we have computed the relative magnitudes of tree, QCD and electroweak penguin amplitudes for all charmless decay modes of B_u and B_d mesons shown in Tables V-VII as a function of $N_c^{\text{eff}}(LR)$ with two different considerations for $N_c^{\text{eff}}(LL)$: (a) $N_c^{\text{eff}}(LL)$ being fixed at the value of 2, and (b) $N_c^{\text{eff}}(LL) = N_c^{\text{eff}}(LR)$. Because of space limitation, results for CP-conjugate modes are not listed in these tables. For tree-dominated decays, we have normalized the tree amplitude to unity. Likewise, the QCD penguin amplitude is normalized to unity for penguin-dominated decays.

V. RESULTS FOR BRANCHING RATIOS AND DISCUSSIONS

With the factorized decay amplitudes tabulated in the Appendix and the input parameters for decay constants, form factors, ..., etc., shown in Sec. III, it is ready to compute the decay rates given by

$$\begin{aligned} \Gamma(B \rightarrow P_1 P_2) &= \frac{p_c}{8\pi m_B^2} |A(B \rightarrow P_1 P_2)|^2, \\ \Gamma(B \rightarrow VP) &= \frac{p_c^3}{8\pi m_V^2} |A(B \rightarrow VP)/(\varepsilon \cdot p_B)|^2, \end{aligned} \quad (5.1)$$

[§]Our classification of factorized penguin amplitudes is slightly different from that in [10]; we introduce three new classes similar to the classification for tree-dominated decays.

where

$$p_c = \frac{\sqrt{[m_B^2 - (m_1 + m_2)^2][m_B^2 - (m_1 - m_2)^2]}}{2m_B} \quad (5.2)$$

is the c.m. momentum of the decay particles. For simplicity, we consider a single factorizable amplitude for $B \rightarrow VV$: $A(B \rightarrow V_1 V_2) = \alpha X^{(BV_1, V_2)}$. Then

$$\Gamma(B \rightarrow V_1 V_2) = \frac{p_c}{8\pi m_B^2} |\alpha(m_B + m_1)m_2 f_{V_2} A_1^{BV_1}(m_2^2)|^2 H, \quad (5.3)$$

with

$$H = (a - bx)^2 + 2(1 + c^2 y^2), \quad (5.4)$$

and

$$\begin{aligned} a &= \frac{m_B^2 - m_1^2 - m_2^2}{2m_1 m_2}, & b &= \frac{2m_B^2 p_c^2}{m_1 m_2 (m_B + m_1)^2}, & c &= \frac{2m_B p_c}{(m_B + m_1)^2}, \\ x &= \frac{A_2^{BV_1}(m_2^2)}{A_1^{BV_1}(m_2^2)}, & y &= \frac{V^{BV_1}(m_2^2)}{A_1^{BV_1}(m_2^2)}, \end{aligned} \quad (5.5)$$

where m_1 (m_2) is the mass of the vector meson V_1 (V_2).

Branching ratios for all charmless nonleptonic two-body decays of B_u^- and \overline{B}_d^0 mesons are displayed in Tables VIII-X with $N_c^{\text{eff}}(LR) = 2, 3, 5, \infty$ and two different considerations for $N_c^{\text{eff}}(LL)$. For the B meson lifetimes, we use [37]

$$\tau(B_d^0) = (1.57 \pm 0.03) \times 10^{-12} s, \quad \tau(B_u^-) = (1.67 \pm 0.03) \times 10^{-12} s. \quad (5.6)$$

Note that the branching ratios listed in Tables VIII-X are meant to be averaged over CP-conjugate modes:

$$\begin{aligned} &\frac{1}{2} [\mathcal{B}(B^- \rightarrow M_1 M_2) + \mathcal{B}(B^+ \rightarrow \overline{M}_1 \overline{M}_2)], \\ &\frac{1}{2} [\mathcal{B}(B^0 \rightarrow M_1 M_2) + \mathcal{B}(\overline{B}^0 \rightarrow \overline{M}_1 \overline{M}_2)]. \end{aligned} \quad (5.7)$$

To compute the decay rates we choose two representative form-factor models: the BSW and LCSR models (see Sec. III.D). From Eq. (A1) we see that the decay rate of $B \rightarrow PP$ depends on the form factor F_0 , $B \rightarrow PV$ on F_1 and/or A_0 , while $B \rightarrow VV$ on A_1, A_2 and V . It is interesting to note that the branching ratios of $B \rightarrow VV$ predicted by the LCSR are always larger than that by the BSW model by a factor of $1.6 \sim 2$ (see Table X). This is because the $B \rightarrow VV$ rate is very sensitive to the form-factor ratio $x = A_2/A_1$ at the appropriate q^2 . This form-factor ratio is almost equal to unity in the BSW model, but it is less than unity in the LCSR (see Table II). Consider the decay $\overline{B}^0 \rightarrow K^{*-} \rho^+$ as an example. Its decay rate is proportional to $A_1^{B\rho}(m_{K^*}^2)[(a - bx)^2 + 2(1 + c^2 y^2)]$, where $a = 19.3$, $b = 13.9$, $c = 0.72$, $x = A_2^{B\rho}(m_{K^*}^2)/A_1^{B\rho}(m_{K^*}^2)$ and $y = V^{B\rho}(m_{K^*}^2)/A_1^{B\rho}(m_{K^*}^2)$. We find $x = 1.03$ and 0.87 in the BSW and LCSR models, respectively. It is easily seen that the prediction of $\mathcal{B}(\overline{B}^0 \rightarrow K^{*-} \rho^+)$ in the LCSR is about 1.6 times as large as that in the BSW model (see Table X).

A. Spectator-dominated rare B decays

The class I-III charmless B decays proceed at the tree level through the b quark decay $b \rightarrow u\bar{u}d$ and at the loop level via the $b \rightarrow d$ penguin diagrams. Since

$$V_{ub}V_{ud}^* = A\lambda^3(\rho - i\eta), \quad V_{cb}V_{cd}^* = -A\lambda^3, \quad V_{tb}V_{td}^* = A\lambda^3(1 - \rho + i\eta), \quad (5.8)$$

in terms of the Wolfenstein parametrization [see Eq. (3.1)], are of the same order of magnitude, it is clear that the rare B decays of this type are tree-dominated as the penguin contributions are suppressed by the smallness of penguin coefficients. As pointed out in [10], the decays $B^0 \rightarrow \pi^0\eta^{(\prime)}$ are exceptional because their tree amplitudes are proportional to

$$a_2 \left[\langle \eta^{(\prime)} | (\bar{u}u)_{V-A} | 0 \rangle \langle \pi^0 | (\bar{d}b)_{V-A} | \bar{B}^0 \rangle + \langle \pi^0 | (\bar{u}u)_{V-A} | 0 \rangle \langle \eta^{(\prime)} | (\bar{d}b)_{V-A} | \bar{B}^0 \rangle \right]. \quad (5.9)$$

The matrix element $\langle \pi^0 | (\bar{d}b)_{V-A} | \bar{B}^0 \rangle$ has a sign opposite to that of $\langle \eta^{(\prime)} | (\bar{d}b)_{V-A} | \bar{B}^0 \rangle$ because of the wave functions: $\pi^0 = (\bar{u}u - \bar{d}d)/\sqrt{2}$ and $\eta^{(\prime)} \propto (\bar{u}u + \bar{d}d)$. The large destructive interference of the tree amplitudes renders the penguin contributions dominant (see Table V for the relative amplitudes). This explains why $B^0 \rightarrow \pi^0\eta'$ has the smallest branching ratio, of order 10^{-7} , in charmless $B \rightarrow PP$ decays. Likewise, the branching ratios of $B^0 \rightarrow \rho^0\eta^{(\prime)}$ are also very small. There is another exceptional one: $B^0 \rightarrow \rho^0\omega$ whose tree amplitude is proportional to

$$a_2 \left[X_u^{(B_d\rho^0,\omega)} + X_u^{(B_d\omega,\rho^0)} \right]. \quad (5.10)$$

Again, a large destructive interference occurs because $\rho^0 = (\bar{u}u - \bar{d}d)/\sqrt{2}$ and $\omega = (\bar{u}u + \bar{d}d)/\sqrt{2}$: the matrix element for $B_d \rightarrow \rho^0$ transition has a sign opposite to that for $B_d \rightarrow \omega$. Consequently, this decay is dominated by the penguin contribution and belongs to the class-VI mode.

Experimentally, $B^- \rightarrow \rho^0\pi^-$ is the only tree-dominated charmless B decay that has been observed very recently. If $N_c^{\text{eff}}(LL)$ is treated as a free parameter, it is easily seen that the decay rates of class-I modes increase with $N_c^{\text{eff}}(LL)$ since $a_1 = c_1^{\text{eff}} + c_2^{\text{eff}}/N_c^{\text{eff}}(LL)$ and c_2^{eff} is negative. Because a_2 is positive at $N_c^{\text{eff}}(LL) < 3.2$ and it becomes negative when $N_c^{\text{eff}}(LL) > 3.2$, the magnitude of a_2 has a minimum at $N_c^{\text{eff}}(LL) = 3.2$. Therefore, the branching ratio of class-II channels will decrease with $N_c^{\text{eff}}(LL)$ until it reaches the minimum at $1/N_c^{\text{eff}}(LL) = 0.31$ and then increases again. The class-III decays involve interference between external and internal W -emission amplitudes. It is obvious that the branching ratios of class-III modes will decrease with $N_c^{\text{eff}}(LL)$. On the contrary, when $N_c^{\text{eff}}(LL)$ is fixed, the branching ratios for most of class-I to class-III modes are insensitive to $N_c^{\text{eff}}(LR)$. This means that penguin contributions are generally small.

Theoretically, some expectation on the effective parameters a_1^{eff} and a_2^{eff} is as follows. We see from Table III that a_2 is very sensitive to the nonfactorized effects. Since the effective number of colors, $N_c^{\text{eff}}(LL)$, inferred from the Cabibbo-allowed decays $B \rightarrow (D, D^*)(\pi, \rho)$ is in the vicinity of 2 (see Eq. (4.3); for a recent work, see [35]) and since the energy released in the energetic two-body charmless B decays is in general slightly larger than that in $B \rightarrow D\pi$ decays, it is thus expected that

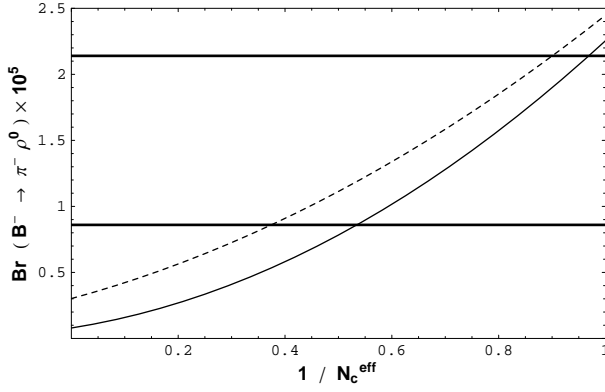


FIG. 2. The branching ratio of $B^- \rightarrow \rho^0 \pi^-$ versus $1/N_c^{\text{eff}}$. The solid (dotted) curve is calculated using the BSW (LCSR) model, while the solid thick lines are the CLEO measurements with one sigma errors.

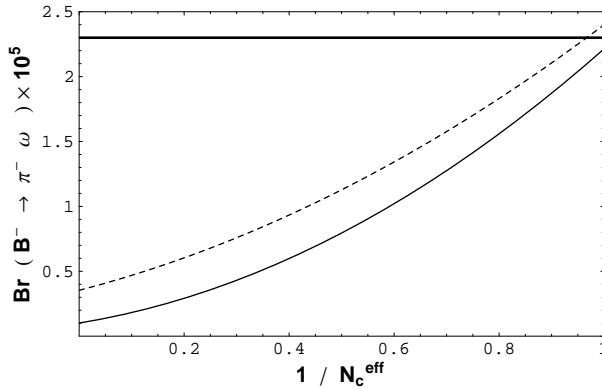


FIG. 3. The branching ratio of $B^- \rightarrow \pi^- \omega$ versus $1/N_c^{\text{eff}}$. The solid (dotted) curve is calculated using the BSW (LCSR) model, while the solid thick line is the CLEO upper limit.

$$|\chi(\text{two-body rare B decay})| \lesssim |\chi(B \rightarrow D\pi)|, \quad (5.11)$$

and hence $N_c^{\text{eff}}(LL) \approx N_c^{\text{eff}}(B \rightarrow D\pi) \sim 2$. This implies that the values of a_1 and a_2 are anticipated to be $a_1 \sim 0.986$ and $a_2 \sim 0.22$.

Very recently CLEO has made the first observation of a hadronic $b \rightarrow u$ decay, namely $B^\pm \rightarrow \rho^0 \pi^\pm$ [38]. The preliminary measurement yields:

$$\mathcal{B}(B^\pm \rightarrow \rho^0 \pi^\pm) = (1.5 \pm 0.5 \pm 0.4) \times 10^{-5}. \quad (5.12)$$

From Fig. 2 or Table IX it is clear that this class-III mode which receives external and internal W -emission contributions is sensitive to $1/N_c^{\text{eff}}$ if $N_c^{\text{eff}}(LL)$ is treated as a free parameter, namely, $N_c^{\text{eff}}(LR) = N_c^{\text{eff}}(LL) = N_c^{\text{eff}}$; it has the lowest value of order 1×10^{-6} and then grows with $1/N_c^{\text{eff}}$. We see from Fig. 2 that $0.38 \leq 1/N_c^{\text{eff}} \leq 0.96$. Since the tree diagrams make the dominant contributions, we then have

$$1.1 \leq N_c^{\text{eff}}(LL) \leq 2.6 \quad \text{from } B^\pm \rightarrow \rho^0 \pi^\pm. \quad (5.13)$$

Therefore, $N_c^{\text{eff}}(LL)$ is favored to be less than 3, as expected.

There is an additional experimental hint that favors the choice $N_c^{\text{eff}}(LL) \sim 2$ or a smaller N_c^{eff} : the class-III decay $B^\pm \rightarrow \pi^\pm \omega$. This mode is very similar to $\rho^0 \pi^\pm$ as its decay amplitude differs from that of $\omega \pi^\pm$ only in the penguin terms proportional to $X_u^{(B\pi^\pm, \omega)}$ (see Appendix E) which are not only small but also subject to the quark-mixing angle suppression. Therefore, the decay rates of $\omega \pi^\pm$ and $\rho^0 \pi^\pm$ are very similar. Although experimentally only the upper limit $\mathcal{B}(B^\pm \rightarrow \pi^\pm \omega) < 2.3 \times 10^{-5}$ is quoted by CLEO [39], the CLEO measurements $\mathcal{B}(B^\pm \rightarrow K^\pm \omega) = (1.5_{-0.6}^{+0.7} \pm 0.2) \times 10^{-5}$ and $\mathcal{B}(B^\pm \rightarrow h^\pm \omega) = (2.5_{-0.7}^{+0.8} \pm 0.3) \times 10^{-5}$ with $h = \pi, K$ indicate that the central value of $\mathcal{B}(B^\pm \rightarrow \pi^\pm \omega)$ is about 1×10^{-5} . A fit of the model calculations to this central value yields $0.4 < 1/N_c^{\text{eff}}(LL) < 0.6$ (see Fig. 3) or $1.7 < N_c^{\text{eff}}(LL) < 2.5$. The prediction for $N_c^{\text{eff}}(LL) = 2$ is $\mathcal{B}(B^\pm \rightarrow \omega \pi^\pm) = 0.8 \times 10^{-5}$ and 1.1×10^{-5} in the BSW model and the LCSR, respectively.

In analogue to the decays $B \rightarrow D^{(*)} \pi(\rho)$, the ratio a_2/a_1 can be inferred from the interference effect of spectator amplitudes in class-III charmless B decays by measuring the ratios of charged to neutral branching fractions:

$$\begin{aligned} R_1 &\equiv 2 \frac{\mathcal{B}(B^- \rightarrow \pi^- \pi^0)}{\mathcal{B}(\overline{B}^0 \rightarrow \pi^- \pi^+)}, & R_2 &\equiv 2 \frac{\mathcal{B}(B^- \rightarrow \rho^- \pi^0)}{\mathcal{B}(\overline{B}^0 \rightarrow \rho^- \pi^+)}, \\ R_3 &\equiv 2 \frac{\mathcal{B}(B^- \rightarrow \pi^- \rho^0)}{\mathcal{B}(\overline{B}^0 \rightarrow \pi^- \rho^+)}, & R_4 &\equiv 2 \frac{\mathcal{B}(B^- \rightarrow \rho^- \rho^0)}{\mathcal{B}(\overline{B}^0 \rightarrow \rho^- \rho^+)}. \end{aligned} \quad (5.14)$$

Since penguin contributions to R_i are small as we have checked explicitly, to a good approximation we have

$$\begin{aligned} R_1 &\cong \frac{\tau(B^-)}{\tau(B_d^0)} \left(1 + \frac{a_2}{a_1}\right)^2, \\ R_2 &\cong \frac{\tau(B^-)}{\tau(B_d^0)} \left(1 + \frac{f_\pi}{f_\rho} \frac{A_0^{B\rho}(m_\pi^2)}{F_1^{B\pi}(m_\rho^2)} \frac{a_2}{a_1}\right)^2, \\ R_3 &\cong \frac{\tau(B^-)}{\tau(B_d^0)} \left(1 + \frac{f_\rho}{f_\pi} \frac{F_1^{B\pi}(m_\rho^2)}{A_0^{B\rho}(m_\pi^2)} \frac{a_2}{a_1}\right)^2, \\ R_4 &\cong \frac{\tau(B^-)}{\tau(B_d^0)} \left(1 + \frac{a_2}{a_1}\right)^2. \end{aligned} \quad (5.15)$$

Evidently, the ratios R_i are greater (less) than unity when the interference is constructive (destructive). From Table XI we see that a measurement of R_i (in particular R_3) will constitute a very useful test on the effective number of colors $N_c^{\text{eff}}(LL)$.

A very recent CLEO analysis of $B^0 \rightarrow \pi^+ \pi^-$ presents an improved upper limit [40]

$$\mathcal{B}(B^0 \rightarrow \pi^+ \pi^-) < 0.84 \times 10^{-5}. \quad (5.16)$$

It is evident from Fig. 4 that $N_c^{\text{eff}}(LL)$ is preferred to be smaller and that the predicted branching ratio seems to be too large compared to experiment. Indeed, most known model predictions in the literature tend to predict a $\mathcal{B}(B^0 \rightarrow \pi^+ \pi^-)$ much larger than the current limit. There are several possibilities for explaining the data: (i) The CKM matrix element

Table XI. The predictions of the ratios R_i at $N_c^{\text{eff}} = 2$ and $N_c^{\text{eff}} = \infty$, respectively, in the BSW [LCSR] model.

	R_1	R_2	R_3	R_4
$N_c^{\text{eff}} = 2$	1.52 [1.52]	1.25 [1.34]	2.27 [1.84]	1.57 [1.57]
$N_c^{\text{eff}} = \infty$	0.48 [0.48]	0.86 [0.76]	0.16 [0.35]	0.50 [0.50]

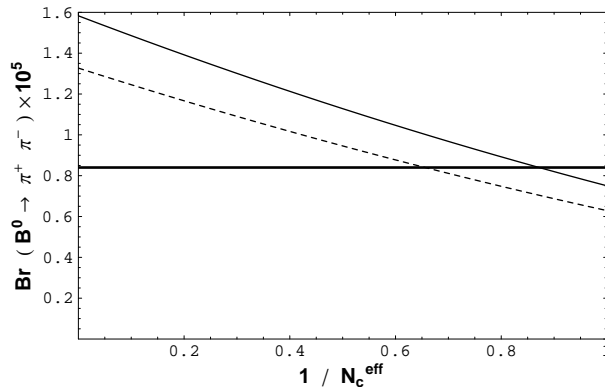


FIG. 4. The branching ratio of $B^0 \rightarrow \pi^+\pi^-$ versus $1/N_c^{\text{eff}}$ where use of $N_c^{\text{eff}}(LL) = N_c^{\text{eff}}(LR) = N_c^{\text{eff}}$ has been made. The solid (dotted) curve is calculated using the BSW (LCSR) model, while the solid thick line is the CLEO upper limit.

$|V_{ub}|$ (or the value of $\sqrt{\rho^2 + \eta^2}$) and/or the form factor $F_0^{B\pi}(0)$ are smaller than the conventional values. However, one has to bear in mind that the product $V_{ub}F_0^{B\pi}$ is constrained by the measured semileptonic $B \rightarrow \pi\ell\nu$ rate: A smaller V_{ub} will be correlated to a larger $B \rightarrow \pi$ form factor and vice versa. (ii) Final-state interactions may play an essential role. We shall see in Sec. VI that if the isospin phase shift difference is nonzero and larger than 70° , the decay rate of $\pi^+\pi^-$ will be significantly suppressed whereas the mode $\pi^0\pi^0$ is substantially enhanced (see Fig. 14). (iii) The unitarity angle γ is larger than 90° , or the Wolfenstein parameter ρ is negative, an interesting possibility pointed out recently in [41]. It is clear from Fig. 5 that the experimental limit of $\pi^+\pi^-$ can be accommodated by $\gamma > 105^\circ$. From Eq. (5.8) and Appendix B for the factorized amplitude of $B \rightarrow \pi^+\pi^-$, it is easily seen that the interference between tree and penguin amplitudes is suppressed when ρ is negative. We also see from Fig. 5 that the $\pi^-\pi^0$ mode is less sensitive to γ as it does not receive QCD penguin contributions and electroweak penguins are small. The current limit on $\pi^-\pi^0$ is $\mathcal{B}(B^- \rightarrow \pi^-\pi^0) < 1.6 \times 10^{-5}$ [40].

Three remarks are in order before ending this section. First, it is interesting to note that the tree-dominated class I-III modes which have branching ratios of order 10^{-5} or larger must have either one vector meson in the final state because of the larger vector-meson decay constant $f_V > f_P$ or two final-state vector mesons because of the larger spin phase space available due to the existence of three different polarization states for the vector meson. For example, it is expected that

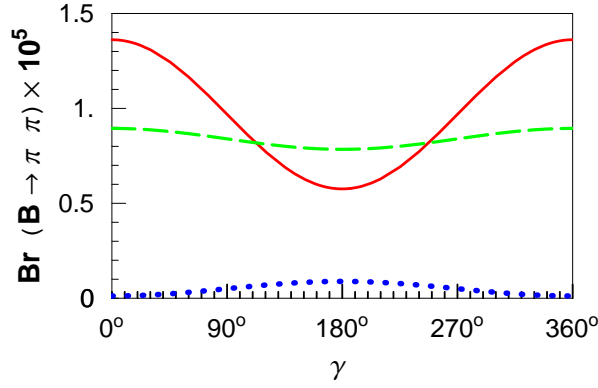


FIG. 5. Branching ratios of $B \rightarrow \pi\pi$ modes versus the unitarity angle γ , where the solid, dashed, and dotted curves correspond to $\pi^+\pi^-$, $\pi^-\pi^0$, and $\pi^0\pi^0$, respectively. Uses of $N_c^{\text{eff}}(LL) = 2$, $N_c^{\text{eff}}(LR) = 5$ and the BSW model for form factors have been made.

$$\begin{aligned}
\mathcal{B}(\overline{B}^0 \rightarrow \rho^-\rho^+) &\sim \mathcal{B}(\overline{B}^0 \rightarrow \rho^-\pi^+) > \mathcal{B}(\overline{B}^0 \rightarrow \pi^-\rho^+) \sim 1 \times 10^{-5}, \\
\mathcal{B}(B^- \rightarrow \rho^-\rho^0) &\sim \mathcal{B}(B^- \rightarrow \rho^-\pi^0) > \mathcal{B}(B^- \rightarrow \pi^-\rho^0) \sim 1 \times 10^{-5}, \\
\mathcal{B}(B^- \rightarrow \omega\rho^-) &> \mathcal{B}(B^- \rightarrow \omega\pi^-) \sim 1 \times 10^{-5}.
\end{aligned}
\tag{5.17}$$

The $\rho^-\pi^+$ ($\rho^-\pi^0$) decay has a larger rate than the $\rho^+\pi^-$ ($\rho^0\pi^-$) mode mainly because of the difference of the decay constants f_ρ and f_π so that $f_\rho F_1^{B\rho} > f_\pi A_0^{B\rho}$. Second, it is well known that the unitarity angle α can be determined from measuring the CP asymmetry in $(B^0, \overline{B}^0) \rightarrow \pi^+\pi^-$ decays provided that penguin contributions are negligible. But we see from Table V that the QCD penguin contribution is important for $B^0 \rightarrow \pi^0\pi^0$ and moderate for $B^0 \rightarrow \pi^+\pi^-$. Nevertheless, if isospin is a good symmetry, an isospin analysis of $B^0 \rightarrow \pi^+\pi^-$, $\pi^0\pi^0$, $B^+ \rightarrow \pi^+\pi^0$ and their CP-conjugate modes can lead to the extraction of 2α without electroweak penguin pollution. However, isospin symmetry is broken by electroweak penguins and also by the u and d quark mass difference which will contaminate the model-independent determination of $\sin 2\alpha$ [42]. Third, as mentioned before, the branching ratio of the class-II modes is very sensitive to the value of N_c^{eff} : it has a minimum at $N_c^{\text{eff}} = 3.2$. Our preferred prediction is made at the value $N_c^{\text{eff}}(LL) = 2$ and hence the branching ratio is not very small. Nevertheless, the decay rates of class-II channels are in general significantly smaller than that of class-I and class-III ones. As a result, W -exchange, W -annihilation and final-state interactions, which have been neglected thus far, could be important for class-II decays and they may even overwhelm the usual factorized contributions.

B. General features of QCD-penguin dominated B decays

For penguin-dominated class IV-VI decay modes, some general observations are the following:

1. Class-IV modes involve the QCD penguin parameters a_4 and a_6 in the combination $a_4 + Ra_6$, where $R > 0$ for $B \rightarrow P_a P_b$, $R = 0$ for $P_a V_b$ and $V_a V_b$ final states, and $R < 0$ for

$B \rightarrow V_a P_b$, where P_b or V_b is factorizable under the factorization assumption. Therefore, the decay rates of class-IV decays are expected to follow the pattern:

$$\Gamma(B \rightarrow P_a P_b) > \Gamma(B \rightarrow P_a V_b) \sim \Gamma(B \rightarrow V_a V_b) > \Gamma(B \rightarrow V_a P_b), \quad (5.18)$$

as a consequence of various possibilities of interference between the a_4 and a_6 penguin terms. From Tables VIII-X, we see that

$$\begin{aligned} \mathcal{B}(\overline{B}^0 \rightarrow K^- \pi^+) &> \mathcal{B}(\overline{B}^0 \rightarrow K^{*-} \pi^+) \sim \mathcal{B}(\overline{B}^0 \rightarrow K^{*-} \rho^+) > \mathcal{B}(\overline{B}^0 \rightarrow K^- \rho^+), \\ \mathcal{B}(B^- \rightarrow \overline{K}^0 \pi^-) &> \mathcal{B}(B^- \rightarrow \overline{K}^{*0} \pi^-) \sim \mathcal{B}(B^- \rightarrow \overline{K}^{*0} \rho^-) > \mathcal{B}(B^- \rightarrow \overline{K}^0 \rho^-), \\ \mathcal{B}(\overline{B}^0 \rightarrow K^0 \overline{K}^0) &> \mathcal{B}(\overline{B}^0 \rightarrow K^0 \overline{K}^{*0}) \sim \mathcal{B}(\overline{B}^0 \rightarrow K^{*0} \overline{K}^{*0}) > \mathcal{B}(\overline{B}^0 \rightarrow K^{*0} \overline{K}^0), \\ \mathcal{B}(B^- \rightarrow K^- K^0) &> \mathcal{B}(B^- \rightarrow K^- K^{*0}) \sim \mathcal{B}(B^- \rightarrow K^{*-} K^{*0}) > \mathcal{B}(B^- \rightarrow K^{*-} K^0). \end{aligned} \quad (5.19)$$

Note that the above hierarchy is opposite to the pattern $\mathcal{B}(B \rightarrow P_a V_b) > \mathcal{B}(B \rightarrow P_a P_b)$, as often seen in tree-dominated decays. It implies that the spin phase-space suppression of the penguin-dominated decay $B \rightarrow P_a P_b$ over $B \rightarrow P_a V_b$ or $B \rightarrow V_a P_b$ is overcome by the constructive interference between the penguin amplitudes in the former. Recall that the coefficient R is obtained by applying equations of motion to the hadronic matrix elements of pseudoscalar densities induced by penguin operators. Hence, a test of the hierarchy shown in (5.19) is important for understanding the penguin matrix elements.

2. Contrary to tree-dominated decays, the penguin-dominated charmless B decays have the largest branching ratios in the PP mode. Theoretically, the class-VI decay modes $B^- \rightarrow \eta' K^-, \overline{B}_d \rightarrow \eta' \overline{K}^0$ have branching ratios of order 4.5×10^{-5} . These decay modes receive two different sets of penguin terms proportional to $a_4 + R a_6$ with $R > 0$. The other penguin-dominated decay modes which have branching ratios of order 10^{-5} are $\overline{B}^0 \rightarrow K^- \pi^+, B^- \rightarrow K^- \pi^0, \overline{K}^0 \pi^-$; all of them have been observed by CLEO.

3. We will encounter hadronic matrix elements of pseudoscalar densities when evaluating the penguin amplitudes. Care must be taken to consider the pseudoscalar matrix element for $\eta^{(\prime)} \rightarrow$ vacuum transition: The anomaly effects must be included in order to ensure a correct chiral behavior for the pseudoscalar matrix element [8]. The results are [43,9]

$$\begin{aligned} \langle \eta^{(\prime)} | \bar{s} \gamma_5 s | 0 \rangle &= -i \frac{m_{\eta^{(\prime)}}^2}{2m_s} (f_{\eta^{(\prime)}}^s - f_{\eta^{(\prime)}}^u), \\ \langle \eta^{(\prime)} | \bar{u} \gamma_5 u | 0 \rangle &= \langle \eta^{(\prime)} | \bar{d} \gamma_5 d | 0 \rangle = r_{\eta^{(\prime)}} \langle \eta^{(\prime)} | \bar{s} \gamma_5 s | 0 \rangle, \end{aligned} \quad (5.20)$$

with [8]

$$\begin{aligned} r_{\eta'} &= \frac{\sqrt{2f_0^2 - f_8^2} \cos \theta + \frac{1}{\sqrt{2}} \sin \theta}{\sqrt{2f_8^2 - f_0^2} \cos \theta - \sqrt{2} \sin \theta}, \\ r_\eta &= -\frac{1}{2} \frac{\sqrt{2f_0^2 - f_8^2} \cos \theta - \sqrt{2} \sin \theta}{\sqrt{2f_8^2 - f_0^2} \cos \theta + \frac{1}{\sqrt{2}} \sin \theta}. \end{aligned} \quad (5.21)$$

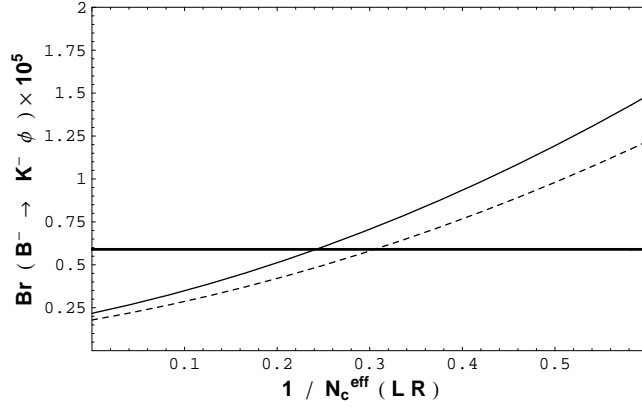


FIG. 6. The branching ratio of $B^- \rightarrow \phi K^-$ versus $1/N_c^{\text{eff}}(LR)$ with $N_c^{\text{eff}}(LL)$ being fixed at 2. The solid (dotted) curve is calculated using the BSW (LCSR) model, while the solid thick line is the CLEO upper limit.

4. We shall see below that nonfactorized effects in penguin-dominated decays are favored to be $N_c^{\text{eff}}(LR) > 3$, as implied by the decay modes $B \rightarrow \phi K$ and $B \rightarrow \eta' K$, contrary to the tree-dominated case where $N_c^{\text{eff}}(LL) < 3$. From Eqs. (4.3) and (5.11) it is anticipated that $N_c^{\text{eff}}(LL) \approx N_c^{\text{eff}}(B \rightarrow D\pi) \sim 2$ and $N_c^{\text{eff}}(LR) \sim 2 - 6$, depending on the sign of χ . Since $N_c^{\text{eff}}(LR) > N_c^{\text{eff}}(LL)$ implied by the data, therefore, we conjecture that [4]

$$N_c^{\text{eff}}(LR) \lesssim 6. \quad (5.22)$$

C. $B \rightarrow \phi K, \phi K^*$ decays

The decay amplitudes of the class-VI penguin-dominated modes $B \rightarrow \phi K$ and $B \rightarrow \phi K^*$ are governed by the effective coefficients $[a_3 + a_4 + a_5 - \frac{1}{2}(a_7 + a_9 + a_{10})]$ (see Appendixes C-G). As noted in passing, the QCD penguin coefficients a_3 and a_5 are sensitive to $N_c^{\text{eff}}(LL)$ and $N_c^{\text{eff}}(LR)$, respectively. We see from Figs. 6 and 7 that the decay rates of $B \rightarrow \phi K^{(*)}$ increase with $1/N_c^{\text{eff}}(LR)$ irrespective of the value of $N_c^{\text{eff}}(LL)$. The new CLEO upper limit [38]

$$\mathcal{B}(B^\pm \rightarrow \phi K^\pm) < 0.59 \times 10^{-5} \quad (5.23)$$

at 90% C.L. implies that (see Fig. 6)

$$N_c^{\text{eff}}(LR) \geq \begin{cases} 4.2 & \text{BSW,} \\ 3.2 & \text{LCSR,} \end{cases} \quad (5.24)$$

with $N_c^{\text{eff}}(LL)$ being fixed at the value of 2. Note that this constraint is subject to the corrections from spacelike penguin and W -annihilation contributions. At any rate, it is safe to conclude that $N_c^{\text{eff}}(LR) > 3 > N_c^{\text{eff}}(LL)$.

CLEO has seen a 3σ evidence for the decay $B \rightarrow \phi K^*$. Its branching ratio, the average of ϕK^{*-} and ϕK^{*0} modes, is reported to be [39]

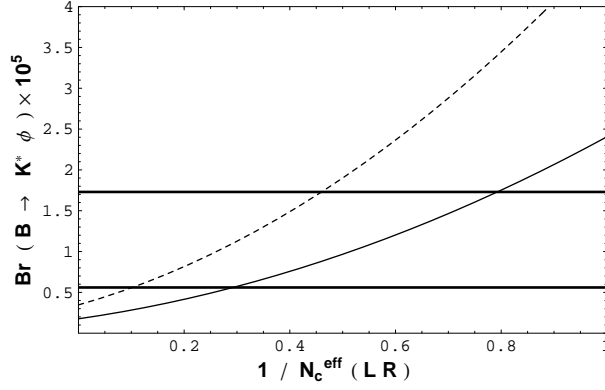


FIG. 7. The branching ratio of $B \rightarrow \phi K^*$ vs $1/N_c^{\text{eff}}(LR)$ with $N_c^{\text{eff}}(LL)$ being fixed at the value of 2. The solid (dotted) curve is calculated using the BSW (LCSR) model. The solid thick lines are the CLEO measurements with one sigma errors.

$$\mathcal{B}(B \rightarrow \phi K^*) \equiv \frac{1}{2} [\mathcal{B}(B^\pm \rightarrow \phi K^{*\pm}) + \mathcal{B}(B^0 \rightarrow \phi K^{*0})] = (1.1_{-0.5}^{+0.6} \pm 0.2) \times 10^{-5}. \quad (5.25)$$

Using $N_c^{\text{eff}}(LL) = 2$ and the constraint (5.24), we find that

$$\mathcal{B}(B \rightarrow \phi K^*) \leq \begin{cases} 0.4 \times 10^{-5} & \text{BSW,} \\ 1.2 \times 10^{-5} & \text{LCSR,} \end{cases} \quad (5.26)$$

and that the ratio $\Gamma(B \rightarrow \phi K^*)/\Gamma(B^\pm \rightarrow \phi K^\pm)$ is 0.76 in the BSW model, while it is equal to 1.9 in the LCSR. This is because $\Gamma(B \rightarrow \phi K^*)$ is very sensitive to the form factor ratio $x = A_2^{BK^*}(m_\phi^2)/A_1^{BK^*}(m_\phi^2)$, which is equal to 0.875 (1.03) in the LCSR (BSW) model [see the discussion after Eq. (5.7)]. In particular, $\mathcal{B}(B \rightarrow \phi K^*) = 0.74 \times 10^{-5}$ is predicted by the LCSR for $N_c^{\text{eff}}(LL) = 2$ and $N_c^{\text{eff}}(LR) = 5$, which is in accordance with experiment. It is evident from Figs. 6 and 7 that the data of $B \rightarrow \phi K$ and $B \rightarrow \phi K^*$ can be simultaneously accommodated in the LCSR analysis. Therefore, the non-observation of $B \rightarrow \phi K$ does not necessarily invalidate the factorization hypothesis; it could imply that the form-factor ratio A_2/A_1 is less than unity. Of course, it is also possible that the absence of $B \rightarrow \phi K$ events is a downward fluctuation of the experimental signal. At any rate, in order to clarify this issue and to pin down the effective number of colors $N_c^{\text{eff}}(LR)$, measurements of $B \rightarrow \phi K$ and $B \rightarrow \phi K^*$ are urgently needed with sufficient accuracy.

D. $B \rightarrow \eta' K^{(*)}$ and $\eta K^{(*)}$ decays

The published CLEO results [44] on the decay $B \rightarrow \eta' K$

$$\begin{aligned} \mathcal{B}(B^\pm \rightarrow \eta' K^\pm) &= (6.5_{-1.4}^{+1.5} \pm 0.9) \times 10^{-5}, \\ \mathcal{B}(B^0 \rightarrow \eta' K^0) &= (4.7_{-2.0}^{+2.7} \pm 0.9) \times 10^{-5}, \end{aligned} \quad (5.27)$$

are several times larger than earlier theoretical predictions [2,45,46] in the range of $(1 - 2) \times 10^{-5}$. It was pointed out in past two years by several authors [9,43,47] that the decay

rate of $B \rightarrow \eta' K$ will get enhanced because of the small running strange quark mass at the scale m_b and sizable $SU(3)$ breaking in the decay constants f_8 and f_0 .^{**} Ironically, it was also realized around a year ago that [43,9] the above-mentioned enhancement is partially washed out by the anomaly effect in the matrix element of pseudoscalar densities, an effect overlooked before. Specifically, $\langle \eta' | \bar{s} \gamma_5 s | 0 \rangle = -i(m_{\eta'}^2/2m_s) (f_{\eta'}^s - f_{\eta'}^u)$ [see Eq. (5.20)], where the QCD anomaly effect is manifested by the decay constant $f_{\eta'}^u$. Since $f_{\eta'}^u \sim \frac{1}{2} f_{\eta'}^s$ [cf. Eq. (3.13)], it is obvious that the decay rate of $B \rightarrow \eta' K$ induced by the $(S - P)(S + P)$ penguin interaction is suppressed by the anomaly term in $\langle \eta' | \bar{s} \gamma_5 s | 0 \rangle$. As a consequence, the net enhancement is not large. If we treat $N_c^{\text{eff}}(LL)$ to be the same as $N_c^{\text{eff}}(LR)$, as assumed in previous studies, we would obtain $\mathcal{B}(B^\pm \rightarrow \eta' K^\pm) = (2.7 - 4.7) \times 10^{-5}$ at $0 < 1/N_c^{\text{eff}} < 0.5$ for $m_s(m_b) = 90$ MeV and $F_0^{BK}(0) = 0.38$ (see the dashed curve in Fig. 8). It is easily seen that the experimental branching ratios can be accommodated by a smaller strange quark mass, say $m_s(m_b) = 60$ MeV, and/or a large form factor F_0^{BK} , for instance $F_0^{BK}(0) = 0.60$. However, it is very important to keep in mind that it is dangerous to adjust the form factors and/or light quark masses in order to fit a few particular modes; the comparison between theory and experiment should be done using the same set of parameters for all channels [48]. Indeed, a too small $m_s(m_b)$ will lead to a too large $B \rightarrow K\pi$, while a too large $F_0^{BK}(0)$ will break the $SU(3)$ -symmetry relation $F_0^{BK} = F_0^{B\pi}$ very badly as the form-factor $F_0^{B\pi}(0)$ larger than 0.33 is disfavored by the current limit on $B^0 \rightarrow \pi^+ \pi^-$ (see Sec. V.B).

What is the role played by the intrinsic charm content of the η' to $B \rightarrow \eta' K$? It has been advocated that the new internal W -emission contribution coming from the Cabibbo-allowed process $b \rightarrow c\bar{c}s$ followed by a conversion of the $c\bar{c}$ pair into the η' via two gluon exchanges is potentially important since its mixing angle $V_{cb}V_{cs}^*$ is as large as that of the penguin amplitude and yet its Wilson coefficient a_2 is larger than that of penguin operators. As noted in Sec. III.C, the decay constant $f_{\eta'}^c$ lies in the range $-2.0 \text{ MeV} \leq f_{\eta'}^c \leq -18.4 \text{ MeV}$. The sign of $f_{\eta'}^c$ is crucial for the η' charm content contribution. For a negative $f_{\eta'}^c$, its contribution to $B \rightarrow \eta' K$ is constructive for $a_2 > 0$. Since a_2 depends strongly on $N_c^{\text{eff}}(LL)$,

^{**}To demonstrate how the decay rate of $B^- \rightarrow \eta' K^-$ is enhanced, we first use the parameters $F_0^{BK}(0) = 0.38$, $\sqrt{3}F_0^{B\eta_0}(0) = \sqrt{6}F_0^{B\eta_8}(0) = F_0^{B\pi}(0)$, $m_s = 140$ MeV, $f_0 = f_8 = f_\pi$, $\theta_8 = \theta_0 = \theta = -20^\circ$, which in turn imply $f_{\eta'}^u = 53$ MeV, $f_{\eta'}^s = 108$ MeV and $F_0^{B\eta'}(0) = 0.133$. With the above inputs, we obtain $\mathcal{B}(B^- \rightarrow \eta' K^-) = (1.0 - 1.5) \times 10^{-5}$ at $0 < 1/N_c^{\text{eff}} < 0.5$ where $N_c^{\text{eff}}(LR) = N_c^{\text{eff}}(LR) = N_c^{\text{eff}}$. Then we consider some possible effects of enhancement. First of all, the penguin amplitude of $B \rightarrow \eta' K$ proportional to a_6 and a_8 will get enhanced by a factor of 1.6 if $m_s = 90$ MeV, the strange quark mass at $\mu = m_b$, instead of $m_s = 140$ MeV, the mass at 1 GeV, is employed. Second, $SU(3)$ breaking in the decay constants f_8 and f_0 [see Eq. (3.12)] and the two-mixing angle formulation for the decay constants f_η and $f_{\eta'}$ [see Eq. (3.11)] lead to $f_{\eta'}^u = 63$ MeV and $f_{\eta'}^s = 137$ MeV. Consequently, the factorized terms $X_u^{(BK,\eta')}$ and $X_s^{(BK,\eta')}$ (see Appendix C) are enhanced by a factor of 1.17 and 1.27, respectively. Third, for $\theta = -15.4^\circ$ [see Eq. (3.11)] we obtain $F_0^{B\eta'}(0) = 0.148$. Thus, $X^{(B\eta',K)}$ is increased by a factor of 1.11. As a result of an accumulation of above several small enhancements, the branching ratio eventually becomes $\mathcal{B}(B^- \rightarrow \eta' K^-) = (2.7 - 4.7) \times 10^{-5}$.

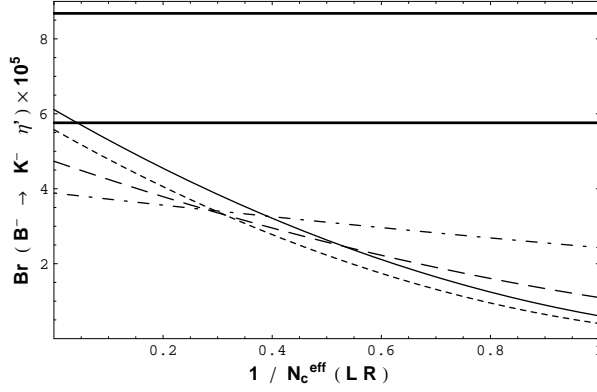


FIG. 8. The branching ratio of $B^\pm \rightarrow \eta' K^\pm$ as a function of $1/N_c^{\text{eff}}(LR)$ with $N_c^{\text{eff}}(LL)$ being fixed at the value of 2 and $\eta = 0.370$, $\rho = 0.175$, $m_s(m_b) = 90$ MeV. The calculation is done using the BSW model for form factors. The charm content of the η' with $f_{\eta'}^c = -6.3$ MeV contributes to the solid curve but not to the dotted curve. The anomaly contribution to $\langle \eta' | \bar{s} \gamma_5 s | 0 \rangle$ is included. For comparison, predictions for $N_c^{\text{eff}}(LL) = N_c^{\text{eff}}(LR)$ as depicted by the dashed curve with $f_{\eta'}^c = 0$ and dot-dashed curve with $f_{\eta'}^c = -6.3$ MeV are also shown. The solid thick lines are the preliminary updated CLEO measurements (5.29) with one sigma errors.

we see that the $c\bar{c} \rightarrow \eta'$ mechanism contributes constructively at $1/N_c^{\text{eff}}(LL) > 0.31$ where $a_2 > 0$, whereas it contributes destructively at $1/N_c^{\text{eff}}(LL) < 0.31$ where a_2 becomes negative. In order to explain the abnormally large branching ratio of $B \rightarrow \eta' K$, an enhancement from the $c\bar{c} \rightarrow \eta'$ mechanism is certainly welcome in order to improve the discrepancy between theory and experiment. This provides another strong support for $N_c^{\text{eff}}(LL) \approx 2$. If $N_c^{\text{eff}}(LL) = N_c^{\text{eff}}(LR)$ is adopted, then $\mathcal{B}(B \rightarrow \eta' K)$ will be *suppressed* at $1/N_c^{\text{eff}} \leq 0.31$ and *enhanced* at $1/N_c^{\text{eff}} > 0.31$ (see the dot-dashed curve in Fig. 8 for $f_{\eta'}^c = -6.3$ MeV). If the preference for N_c^{eff} is $1/N_c^{\text{eff}} \lesssim 0.2$ (see e.g. [10]), then it is quite clear that the contribution from the η' charm content will make the theoretical prediction even worse at the small values of $1/N_c^{\text{eff}}$! On the contrary, if $N_c^{\text{eff}}(LL) \approx 2$, the $c\bar{c}$ admixture in the η' will always lead to a constructive interference irrespective of the value of $N_c^{\text{eff}}(LR)$ (see the solid curve in Fig. 8).

At this point, we see that the branching ratio of $B \rightarrow K\eta'$ of order $(2.7 - 4.7) \times 10^{-5}$ at $0 < 1/N_c^{\text{eff}} < 0.5$ for $N_c^{\text{eff}}(LL) = N_c^{\text{eff}}(LR)$ and it becomes $(3.5 - 3.8) \times 10^{-5}$ when the η' charm content contribution with $f_{\eta'}^c = -6.3$ MeV is taken into account. However, the discrepancy between theory and experiment is largely improved by treating $N_c^{\text{eff}}(LL)$ and $N_c^{\text{eff}}(LR)$ differently. Setting $N_c^{\text{eff}}(LL) = 2$, we find that (see Fig. 8) the decay rates of $B \rightarrow \eta' K$ are considerably enhanced especially at small $1/N_c^{\text{eff}}(LR)$. Specifically, $\mathcal{B}(B^\pm \rightarrow \eta' K^\pm)$ at $1/N_c^{\text{eff}}(LR) \leq 0.2$ is enhanced from $(3.6 - 3.8) \times 10^{-5}$ to $(4.6 - 6.1) \times 10^{-5}$ due to three enhancements. First, the η' charm content contribution $a_2 X_c^{(BK, \eta')}$ now always contributes in the right direction to the decay rate irrespective of the value of $N_c^{\text{eff}}(LR)$. Second, the interference in the spectator amplitudes of $B^\pm \rightarrow \eta' K^\pm$ is constructive. Third, the term proportional to

$$2(a_3 - a_5)X_u^{(BK, \eta')} + (a_3 + a_4 - a_5)X_s^{(BK, \eta')} \quad (5.28)$$

is enhanced when $(N_c^{\text{eff}})_3 = (N_c^{\text{eff}})_4 = 2$.

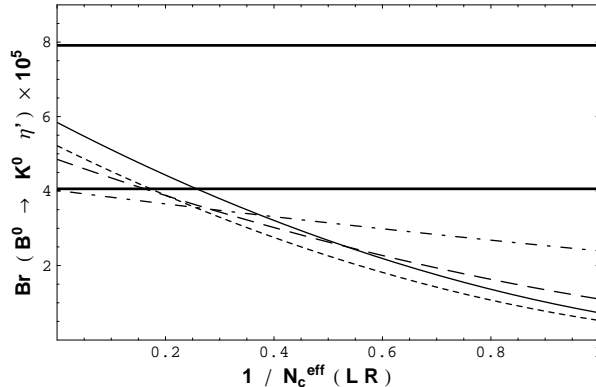


FIG. 9. Same as Fig. 8 except for $B^0 \rightarrow K^0 \eta'$.

A recent CLEO reanalysis of $B \rightarrow \eta' K$ using a data sample 80% larger than in previous studies yields the preliminary results [49,40]:

$$\begin{aligned} \mathcal{B}(B^\pm \rightarrow \eta' K^\pm) &= (7.4^{+0.8}_{-1.3} \pm 1.0) \times 10^{-5}, \\ \mathcal{B}(B_d^0 \rightarrow \eta' K^0) &= (5.9^{+1.8}_{-1.6} \pm 0.9) \times 10^{-5}, \end{aligned} \quad (5.29)$$

suggesting that the original measurements (5.27) were not an upward statistical fluctuation. It is evident from Fig. 9 that the measurement of $\overline{B}^0 \rightarrow \eta' \overline{K}^0$ is well explained in the present framework based on the Standard Model. Contrary to some early claims, we see that it is not necessary to invoke some new mechanisms, say the SU(3)-singlet contribution S' [50], to explain the data. The agreement with experiment provides another strong support for $N_c^{\text{eff}}(LL) \sim 2$ and for the relation $N_c^{\text{eff}}(LR) > N_c^{\text{eff}}(LL)$.

Thus far, the calculation is carried out using $m_s(m_b) = 90$ MeV and the prediction of $\mathcal{B}(B^- \rightarrow \eta' K^-)$ is on the lower side of the experimental data. The discrepancy between theory and experiment can be further improved by using a smaller strange quark mass, say $m_s(m_b) = 70$ MeV. However, as stressed before, the calculation should be consistently carried out using the same set of parameters for all channels [48]. Indeed, a too small $m_s(m_b)$ will lead to a too large $B \rightarrow K\pi$,

From the face values of the data, it appears that the branching ratio of the charged mode $\eta' K^-$ is slightly larger than that of the neutral mode $\eta' K^0$, though they are in agreement within one sigma error. Note that the neutral mode does not receive contributions from external W -emission and W -annihilation diagrams. Since the external W -emission is small due to small mixing angles, it is naively anticipated that both decays should have very similar rates unless W -annihilation plays some role. However, if the two branching values are confirmed not to converge when experimental errors are improved and refined in the future, a plausible explanation is ascribed to a negative Wolfenstein's ρ parameter. We see from Fig. 10 that the charged $\eta' K^-$ mode is significantly enhanced at $\gamma > 90^\circ$, whereas the neutral $\eta' K^0$ mode remains steady.

Contrary to the abnormally large decay rate of $B \rightarrow \eta' K$, the branching ratio of $B \rightarrow \eta K$ is very small because of the destructive interference in penguin amplitudes due to the opposite sign between the factorized terms $X^{(B\eta,K)}$ and $a_6 X_s^{(BK,\eta)}$; that is, the $(\bar{u}u + \bar{d}d)$ and $\bar{s}s$

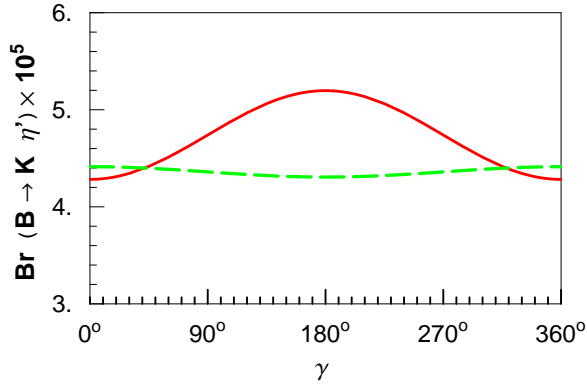


FIG. 10. Branching ratios of $B \rightarrow \eta' K$ modes versus the unitarity angle γ , where the solid and dashed curves correspond to $\eta' K^-$ and $\eta' K^0$, respectively. Uses of $N_c^{\text{eff}}(LL) = 2$, $N_c^{\text{eff}}(LR) = 5$ and the BSW model for form factors have been made.

components interfere destructively for the η but constructively for the η' . From Table VIII we obtain

$$\frac{\mathcal{B}(B \rightarrow \eta' K)}{\mathcal{B}(B \rightarrow \eta K)} = \begin{cases} 34 & \text{charged } B; \\ 58 & \text{neutral } B. \end{cases} \quad (5.30)$$

Since the sign of $a_6 X_s^{(BK^*, \eta^{(\prime)})}$ is flipped in $B \rightarrow \eta^{(\prime)} K^*$ decays, the interference effect becomes the other way around: constructive in $B \rightarrow \eta K^*$ and destructive in $B \rightarrow \eta' K^*$:

$$\frac{\mathcal{B}(B \rightarrow \eta' K^*)}{\mathcal{B}(B \rightarrow \eta K^*)} = \begin{cases} 0.13 & \text{charged } B; \\ 0.11 & \text{neutral } B. \end{cases} \quad (5.31)$$

It has been argued in [20] that $\mathcal{B}(B \rightarrow \eta' K^*)$ is about twice larger than that of $B \rightarrow \eta' K$, a prediction not borne out by the current limit $\mathcal{B}(B^0 \rightarrow \eta' K^{*0}) < 2.0 \times 10^{-5}$ [38] and the measurement of $\mathcal{B}(B^0 \rightarrow \eta' K^0)$ (5.29). Note that it has been advocated that the two-gluon fusion mechanism may account for the observed large decay rate of $B \rightarrow \eta' K$ [51,52]. Using the same gluon-fusion mechanism, large branching fractions of $B \rightarrow \eta' K^*$ of order 3×10^{-5} are found in [53], to be compared with 7×10^{-7} in our calculations. Therefore, it is important to measure the processes $B^- \rightarrow \eta' K^{*-}$ and $B^0 \rightarrow \eta' K^{*0}$ to test the two-gluon fusion mechanism.

E. $B \rightarrow K\pi$ decays

There are four $K\pi$ modes in $B_{u,d}$ decays: $\bar{B}^0 \rightarrow K^- \pi^+$, $B^- \rightarrow \bar{K}^0 \pi^-$, $B^- \rightarrow K^- \pi^0$, and $\bar{B}^0 \rightarrow \bar{K}^0 \pi^0$. Theoretically, the following pattern is expected:

$$\Gamma(B^- \rightarrow \bar{K}^0 \pi^-) \gtrsim \Gamma(\bar{B}^0 \rightarrow K^- \pi^+) > \Gamma(B^- \rightarrow K^- \pi^0) > \Gamma(\bar{B}^0 \rightarrow \bar{K}^0 \pi^0). \quad (5.32)$$

This pattern arises based on the following observations: (1) Since the tree contributions are CKM suppressed, these decays are penguin dominated. (2) Because of the π^0 wave function, it is generally anticipated that the first two channels are larger than the last two

and $\mathcal{B}(B^- \rightarrow K^- \pi^0)/\mathcal{B}(B^- \rightarrow K^- \pi^\pm) \approx 1/2$. (3) The small electroweak penguin effect makes the first two processes almost the same. The slight difference between $\overline{K}^0 \pi^-$ and $K^- \pi^+$ comes from the destructive interference between the tree and QCD penguin amplitudes in the latter; such an interference is absent in the former as it proceeds only through penguin diagrams. (4) Though it can be neglected in the first two modes, the electroweak penguin plays a role in the last two. With a moderate electroweak penguin contribution, the constructive (destructive) interference between electroweak and QCD penguins in $K^- \pi^0$ and $\overline{K}^0 \pi^0$ explains why the former is larger than the latter.

Experimentally, a substantial difference in the first two decay modes implied by the earlier data makes the Fleischer-Mannel bound [54] on the unitarity angle γ interesting. An improvement of the data samples and a new decay mode observed by CLEO [55,40] indicate nearly equal branching ratios for the three modes $K^- \pi^+$, $\overline{K}^0 \pi^-$ and $K^- \pi^0$:

$$\begin{aligned}\mathcal{B}(\overline{B}^0 \rightarrow K^- \pi^+) &= (1.4 \pm 0.3 \pm 0.2) \times 10^{-5}, \\ \mathcal{B}(B^- \rightarrow \overline{K}^0 \pi^-) &= (1.4 \pm 0.5 \pm 0.2) \times 10^{-5}, \\ \mathcal{B}(B^- \rightarrow K^- \pi^0) &= (1.5 \pm 0.4 \pm 0.3) \times 10^{-5}.\end{aligned}\tag{5.33}$$

While the improvement on the first two decay modes is in accordance with the theoretical expectation, the central value of the new measured decay mode $B^- \rightarrow K^- \pi^0$ is larger than the naive anticipation. Of course, one has to await the experimental improvement to clarify this issue. If the present data persist, an interesting interpretation based on the revived idea of a negative ρ is pointed out recently in [56]. To see the impact of a negative ρ or the dependence on the unitarity angle γ , we plot in Fig. 11 the branching ratios of $K\pi$ modes versus γ . It is clear that (i) the aforementioned pattern $\overline{K}^0 \pi^- > K^- \pi^+ > K^- \pi^0$ is modified to $K^- \pi^+ > \overline{K}^0 \pi^- > K^- \pi^0$ when $\gamma > 90^\circ$, (ii) the decay rate of $K^- \pi^0$ is close to that of $\overline{K}^0 \pi^-$ when γ approaches to 180° , and (iii) the purely-penguin decay mode $\overline{K}^0 \pi^-$ is insensitive to the change of γ , as expected.

A rise of the $K^- \pi^+$ and $K^- \pi^0$ decay rates from their minima at $\gamma = 0^\circ$ and 360° (or $|\rho| = \rho_{\max} = 0.41$ and $\eta = 0$) to the maxima at $\gamma = 180^\circ$ (or $\rho = 0$ and $\eta = -0.41$) can be understood as follows: The interference between tree and penguin contributions in these two decay processes is destructive for negative ρ and becomes largest at $\gamma = 0^\circ$ and then decreases with increasing γ . When the sign of ρ is flipped, the interference becomes constructive and has its maximal strength at $\gamma = 180^\circ$. It is obvious from the above discussion that a negative ρ alone is not adequate to explain the nearly-equality of $K\pi$ modes since an increase of $K^- \pi^0$ is always accompanied by a rise of $K^- \pi^+$. Therefore, final state interactions are probably needed to explain the central values of the data.

Finally we remark that it is anticipated that $K^- \pi^+ > K^{*-} \pi^+$ (likewise, $\overline{K}^0 \pi^- > \overline{K}^{*0} \pi^-$; see Eq. (5.19)) owing to the absence of the a_6 penguin term in the latter. The branching ratio of $K^{*-} \pi^+$ and $\overline{K}^{*0} \pi^-$ is predicted to be of order 0.5×10^{-5} at $\gamma = 65^\circ$ (see Table IX) and $\sim 1.0 \times 10^{-5}$ at $\gamma = 90^\circ$. As noted in passing, $K^- \rho^+$ and $\overline{K}^0 \rho^-$ have smaller branching ratios, typically of order 1×10^{-6} , as the a_6 penguin term contributes destructively.

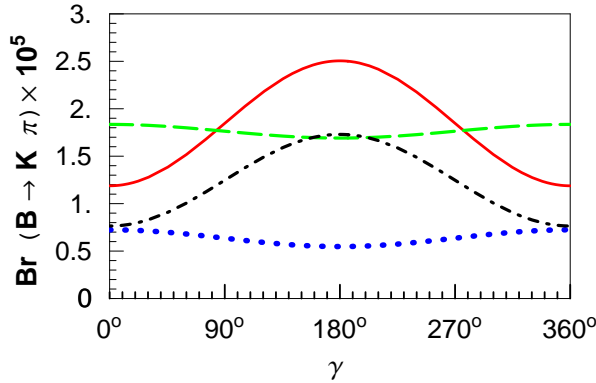


FIG. 11. Branching ratios of $K\pi$ modes versus the unitarity angle γ , where the solid, dashed, dotdashed and dotted curves correspond to $B \rightarrow K^- \pi^+$, $\bar{K}^0 \pi^-$, $K^- \pi^0$ and $\bar{K}^0 \pi^0$, respectively. Uses of $N_c^{\text{eff}}(LL) = 2$, $N_c^{\text{eff}}(LR) = 5$ and the BSW model for form factors have been made.

F. $B^\pm \rightarrow \omega K^\pm$ and $B^\pm \rightarrow \rho^0 K^\pm$ decays

The CLEO observation [39] of a large branching ratio for $B^\pm \rightarrow \omega K^\pm$

$$\mathcal{B}(B^\pm \rightarrow \omega K^\pm) = \left(1.5_{-0.6}^{+0.7} \pm 0.2\right) \times 10^{-5}, \quad (5.34)$$

is rather difficult to explain at first sight. Its factorizable amplitude is of the form (see Appendix E)

$$\begin{aligned} A(B^- \rightarrow \omega K^-) &= V_{ub}V_{us}^* \left\{ a_1 X^{(B\omega, K)} + a_2 X_u^{(BK, \omega)} \right\} - V_{tb}V_{ts}^* \left\{ [a_4 + a_{10} + R(a_6 + a_8)] X^{(B\omega, K)} \right. \\ &\quad \left. + [2a_3 + 2a_5 + \frac{1}{2}(a_7 + a_9)] X^{(BK, \omega)} + \dots \right\}, \end{aligned} \quad (5.35)$$

with $R \cong -2m_K^2/(m_b m_s)$, where ellipses represent contributions from W -annihilation and spacelike penguin diagrams. It is instructive to compare this decay mode closely with $B^- \rightarrow \rho^0 K^-$:

$$\begin{aligned} A(B^- \rightarrow \rho^0 K^-) &= V_{ub}V_{us}^* \left\{ a_1 X^{(B\rho^0, K)} + a_2 X_u^{(BK, \rho^0)} \right\} \\ &\quad - V_{tb}V_{ts}^* \left\{ [a_4 + a_{10} + R'(a_6 + a_8)] X^{(B\rho^0, K)} + \frac{3}{2}(a_7 + a_9) X_u^{(BK, \rho^0)} + \dots \right\}, \end{aligned} \quad (5.36)$$

with $R' \cong -2m_\rho^2/(m_b m_s)$. Although the tree amplitude is suppressed by the mixing angle, $|V_{ub}V_{us}^*/V_{tb}V_{ts}^*| = \lambda^2$, the destructive interference between a_4 and a_6 penguin terms renders the penguin contribution small. Consequently, the relative weight of tree and penguin contributions to ωK^- and $\rho^0 K^-$ depends on the values of N_c^{eff} (see Table VI). At our favored values $N_c^{\text{eff}}(LL) = 2$ and $N_c^{\text{eff}}(LR) = 5$, we see that the tree contribution is important for both channels. It is also clear from Table VI that the electroweak penguin contribution to $\rho^0 K^-$ is as important as the tree diagram. The branching ratio of $B^\pm \rightarrow \rho^0 K^\pm$ is estimated to be of order $(0.5 - 0.9) \times 10^{-6}$ (see Table IX). This prediction is relatively stable against N_c^{eff} . While the current bound is $\mathcal{B}(B^- \rightarrow \rho^0 K^-) < 2.2 \times 10^{-5}$ [38], the preliminary measurement of $B^- \rightarrow \rho^0 K^-$ shows a large event yield $14.8_{-7.7}^{+8.8}$ [38]. If the branching ratio of this decay is found to be, say, of order 0.5×10^{-5} , then it is a serious challenge to theorists.

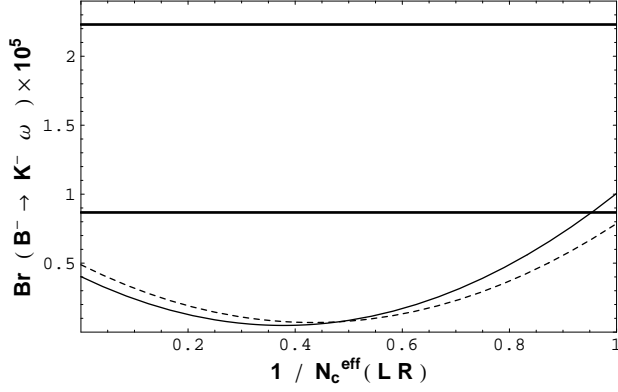


FIG. 12. The branching ratio of $B^- \rightarrow \omega K^-$ vs $1/N_c^{\text{eff}}(LR)$ with $N_c^{\text{eff}}(LL)$ being fixed at the value of 2. The solid (dotted) curve is calculated using the BSW (LCSR) model. The solid thick lines are the CLEO measurements with one sigma errors.

Since the ωK^- amplitude differs from that of $\rho^0 K^-$ only in the QCD penguin term proportional to $(a_3 + a_5)$ and in the electroweak penguin term governed by a_9 , it is naively anticipated that their branching ratios are similar if the contributions from a_3, a_5, a_9 are negligible. The question is then why is the observed rate of the ωK^- mode much larger than the theoretical estimate of the $\rho^0 K^-$ mode? By comparing (5.35) with (5.36), it is natural to contemplate that the penguin contribution proportional to $(2a_3 + 2a_5)$ accounts for the large enhancement of $B^\pm \rightarrow \omega K^\pm$. However, this is not the case: The coefficients a_3 and a_5 , whose magnitudes are smaller than a_4 and a_6 , are not large enough to accommodate the data unless $N_c^{\text{eff}}(LR) < 1.2$ (see Fig. 12). It is evident that the predicted branching ratio of $B^- \rightarrow \omega K^-$ is in general too small if $N_c^{\text{eff}}(LL)$ is fixed at the value of 2 and $1/N_c^{\text{eff}}(LR) < 0.5$. If $N_c^{\text{eff}}(LL)$ is assumed to be the same as $N_c^{\text{eff}}(LR)$, then the branching ratio can rise above 1×10^{-5} at the small value of $1/N_c^{\text{eff}} \cong 0$ [10] since $a_3 + a_5$ has its maximum at $N_c^{\text{eff}} = \infty$ (see Table III). However, it seems to us that $N_c^{\text{eff}} \rightarrow \infty$ for hadronic B decays is very unlikely.

So far we have neglected three effects in the consideration of $B^\pm \rightarrow \omega K^\pm, \rho^0 K^\pm$ decays: W -annihilation, spacelike penguin diagrams and final-state interactions. The first two mechanisms play the same role for both modes and they will lead to the decay rate of ωK^- similar to $\rho^0 K^-$. If the latter is observed to have a similar rate as the former, it is plausible that W -annihilation and spacelike penguins could play a prominent role to both modes. However, if $\mathcal{B}(B^- \rightarrow \rho^0 K^-) \ll \mathcal{B}(B^- \rightarrow \omega K^-)$ is observed experimentally, then one possibility is that FSI may explain the disparity between $\rho^0 K^-$ and ωK^- modes, as elaborated on in Sec. VI. At any rate, it is crucial to measure the branching ratios of both modes in order to understand their underlying mechanism.

G. Electroweak penguins

Electroweak penguin diagrams contribute to all charmless B decays. The relative importance of electroweak penguin amplitudes can be read directly from Tables V-VII. ^{††} In order to study their effects, we need to focus on those modes in which QCD penguins do not contribute or their effects are small. It is known that in the rare B_s decays, the decay modes

$$B_s \rightarrow \eta\pi, \eta'\pi, \eta\rho, \eta'\rho, \phi\pi, \phi\rho \quad (5.38)$$

do not receive any QCD penguin contributions [57] (for a detailed discussion, see [4]) . Therefore, these six decay modes are predominantly governed by the largest electroweak penguin coefficient a_9 . By contrast, there are only two channels in charmless B_u and B_d decays that do not receive QCD penguin contributions, namely $B^- \rightarrow \pi^-\pi^0$ and $B^- \rightarrow \rho^-\rho^0$, and they are dominated by tree diagrams. Nevertheless, there do exist several channels in which the QCD penguin contribution is small. From the Appendix we see that the amplitudes of the class-V decays

$$B_d^0 \rightarrow \phi\pi^0, \phi\eta, \phi\eta', \phi\rho^0, \phi\omega, \quad B^+ \rightarrow \phi\pi^+, \phi\rho^+ \quad (5.39)$$

are proportional to $[a_3 + a_5 - \frac{1}{2}(a_7 + a_9)]$. Since the effective coefficients a_3 and a_5 are N_c^{eff} sensitive, the decay rates depend very sensitively on N_c^{eff} and are governed by electroweak penguins at $N_c^{\text{eff}}(LL) \sim 2$, $N_c^{\text{eff}}(LR) \sim 5$ or $N_c^{\text{eff}}(LL) \sim N_c^{\text{eff}}(LR) \sim 3$ where the QCD penguin contribution characterized by $a_3 + a_5$ is close to its minimum (see Table III). Unfortunately, their branching ratios are very small (see Tables VIII-X), of order $(1 - 6) \times 10^{-9}$. We also see that the electroweak penguin in

$$B_d^0 \rightarrow K^0\rho^0, \quad B^+ \rightarrow K^+\rho^0 \quad (5.40)$$

is as important as the QCD penguin diagram because the latter is proportional to $[a_4 - 2a_6m_K^2/(m_b m_s)]$ which involves a large cancellation. The branching ratio of the above two modes is of order $(0.5 - 1.0) \times 10^{-6}$.

H. Theoretical uncertainties

The calculation of charmless hadronic B decay rates suffers from many theoretical uncertainties. Most of them have been discussed before and it is useful to make a short summary below.

^{††}The relative importance of electroweak penguin effects in penguin-dominated B decays is studied in [10] by computing the ratio

$$R_W = \frac{\mathcal{B}(B \rightarrow h_1 h_2)(\text{with } a_7, \dots, a_{10} = 0)}{\mathcal{B}(B \rightarrow h_1 h_2)}. \quad (5.37)$$

However, because of variously possible interference of the electroweak penguin amplitude with the tree and QCD penguin contributions, R_W is not the most suitable quantity for measuring the relative importance of electroweak penguin effects; see [4] and an example in Sec. VII.

- Heavy-to-light form factors and their q^2 dependence. We have considered in the present paper two different form-factor models: the BSW model and the LCSR approach. It turns out that $\mathcal{B}(B \rightarrow VV)$ is very sensitive to the form-factor ratio A_2/A_1 .
- Decay constants. Since the decay constants for light pseudoscalar and vector mesons are well measured, the uncertainty due to this part is the least.
- Running quark masses at the scale m_b . The decay rates of penguin-dominated charmless B decays are generally sensitive to the value of $m_s(m_b)$. The light quark masses arise in the decay amplitude because equation of motion has been applied to the matrix element of $(S - P)(S + P)$ interactions obtained from the Fierz transformation of $(V - A)(V + A)$ penguin operators. Since the current quark masses are not known precisely, this will result in large uncertainties for branching ratios.^{‡‡} While the measured $B \rightarrow \eta' K$ favors a smaller strange quark mass, a too small value of $m_s(m_b)$ will lead to a too large $B \rightarrow K\pi$.
- Quark mixing matrix elements parametrized in terms of the parameters ρ, η, A, λ . The uncertainty due to the values of ρ, η and A is reflected on the uncertainty on the angles α, β, γ of the unitarity triangle.
- Nonfactorized contributions to hadronic matrix elements. The main result of the present paper is to show that $N_c^{\text{eff}}(LR) > 3 > N_c^{\text{eff}}(LL) \sim 2$ implied by the bulk of the data.
- The magnitude of the gluon momentum transfer in the timelike penguin diagram. We have employed $k^2 = m_b^2/2$ for calculating the effective Wilson coefficients, though in general k^2 lies in the range $m_b^2/4 \lesssim k^2 \lesssim m_b^2/2$ [58]. The common argument is that while CP violation is sensitive to the value of k^2 , this is not the case for the decay rate.
- Final-state interactions (FSI). This is the part least known. Nevertheless, some qualitative statement and discussion about FSI still can be made, as shown in the next section.
- W -annihilation contribution. It is commonly believed that this contribution is negligible due to helicity suppression. Moreover, W -exchange is subject to both color and helicity suppression. The helicity suppression is likely to work because of the large energy released in rare B decays.
- Spacelike penguin contribution. The spacelike penguin amplitude gains a large enhancement by a factor of $m_B^2/(m_b m_{u,d})$ or $m_B^2/(m_b m_s)$. Therefore, *a priori* there is

^{‡‡}In order to avoid the uncertainty originated from the light quark masses, an attempt of evaluating the $(S - P)(S + P)$ matrix element using the perturbative QCD method has been made in [53]. It is found that the results are comparatively smaller than that obtained using equations of motion.

no convincing reason to ignore this effect that has been largely overlooked in the literature. Unfortunately, we do not have a reliable method for estimating the spacelike penguins.

VI. FINAL-STATE INTERACTIONS

It is customarily argued that final-state interactions (FSI) are expected to play only a minor role in rare hadronic B decays due to the large energy released in the decay process. Nevertheless, phenomenologically their presence could be essential in some cases: (i) Inelastic scattering may account for the observed large branching ratio of $B^- \rightarrow \omega K^-$. (ii) Some channels, for instance $B^0 \rightarrow K^+ K^-$ receives direct contributions only from W -exchange and penguin-annihilation diagrams, can be induced from FSI. (iii) The tree-dominated neutral modes, e.g., $B^0 \rightarrow \pi^0 \pi^0$, $\pi^0 \rho^0$, $\rho^0 \rho^0$, may get large enhancement from FSI.

In general, the effects of FSI are important and dramatic for the weak decay $B \rightarrow X$ if there exists a channel $B \rightarrow Y$ with a sufficiently large decay rate, i.e. $\mathcal{B}(B \rightarrow Y) \gg \mathcal{B}(B \rightarrow X)$ and if X and Y modes couple through FSI. A famous example is the decay $D^0 \rightarrow \bar{K}^0 \pi^0$ which is naively expected to be very suppressed but it gets a large enhancement from the weak decay $D^0 \rightarrow K^- \pi^+$ followed by the FSI: $K^- \pi^+ \rightarrow \bar{K}^0 \pi^0$.

Inelastic scattering contribution to $B^\pm \rightarrow \omega K^\pm$

As shown in Sec. V.F, it is difficult to understand why the observed branching ratio of $B^- \rightarrow \omega K^-$ is one order of magnitude larger than the theoretical expectation $(1.2-1.8) \times 10^{-6}$ (see Table IX). There are three possible effects for enhancement: W -annihilation, spacelike penguin diagrams and FSI. If the pattern $\mathcal{B}(B^- \rightarrow \omega K^-) \gg \mathcal{B}(B^- \rightarrow \rho^0 K^-)$ is observed experimentally, FSI may account for the disparity between ωK^- and $\rho^0 K^-$ as the first two mechanisms contribute equally to both modes. The weak decays $B^- \rightarrow K^{*-} \pi^0$, $K^{*-} \eta^{(\prime)}$ via the penguin process $b \rightarrow su\bar{u}$ and $B^- \rightarrow \{K^{*-} \pi^0, K^{*-} \eta^{(\prime)}, K^{*0} \pi^-, K^- \rho^0, K^0 \rho^-\}$ via $b \rightarrow s\bar{d}\bar{d}$ followed by the quark rescattering reactions $\{K^{*-} \pi^0, K^{*-} \eta^{(\prime)}, K^{*0} \pi^-, K^- \rho^0, K^0 \rho^-\} \rightarrow \omega K^-$ contribute *constructively* to $B^- \rightarrow \omega K^-$ (see Fig. 13), but *destructively* to $B^- \rightarrow \rho K^-$. Since the branching ratios for $B^- \rightarrow K^{*-} \pi^0$, $K^{*-} \eta^{(\prime)}$ and $K^{*0} \pi^-$ are not small, of order $(0.3 - 0.7) \times 10^{-5}$, it is conceivable that a bulk of observed $B^\pm \rightarrow \omega K^\pm$ arises from FSI via inelastic scattering. However, it is not clear to us quantitatively if FSI are adequate to enhance the branching ratio by one order of magnitude.

Inelastic scattering contribution to $B^0 \rightarrow K^+ K^-$

The decay $B^0 \rightarrow K^+ K^-$ proceeds through the W -exchange and penguin annihilation diagrams and its factorized amplitude given in Appendix B is governed by the factorized term $\langle K^+ K^- | (\bar{q}q)_{V-A} | 0 \rangle \langle 0 | (\bar{d}b)_{V-A} | \bar{B}^0 \rangle$ with $q = u, s$. If helicity suppression works, then this factorized term and hence $\mathcal{B}(B^0 \rightarrow K^+ K^-)$ is anticipated to be very suppressed. Nevertheless, the final-state rescattering contribution to $B^0 \rightarrow K^+ K^-$ from $\rho^+ \rho^-$, $\pi^+ \pi^-$, \dots intermediate states could be sizable, in particular $B^0 \rightarrow \rho^+ \rho^-$ should have a large branching ratio of

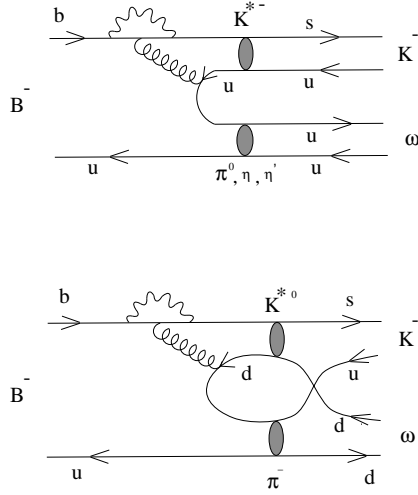


FIG. 13. Contributions to $B^- \rightarrow K^- \omega$ from final-state interactions via the weak decays $B^- \rightarrow K^{*-} \pi^0$, $K^{*-} \eta^{(\prime)}$ and $B^- \rightarrow K^{*0} \pi^-$ followed by quark rescattering.

order $(2 - 4) \times 10^{-5}$. Therefore, this decay is expected to be dominated by the rescattering effect [59]. A measurement of $B^0 \rightarrow K^+ K^-$ will provide information on the inelastic FSI. The present limit is $\mathcal{B}(B^0 \rightarrow K^+ K^-) < 2.3 \times 10^{-6}$ [38]. Another example is the decay $B^0 \rightarrow \phi \phi$ which proceeds via the spacelike penguin diagram (see Appendix F). It receives indirect contributions arising from the weak decays $B^0 \rightarrow \eta^{(\prime)} \eta^{(\prime)}$ followed by the rescattering $\eta^{(\prime)} \eta^{(\prime)} \rightarrow \phi \phi$.

Elastic FSI on $B \rightarrow \pi \pi$

In order to understand the effect of FSI on $B \rightarrow \pi \pi$ decays, we decompose the decay amplitudes into their isospin amplitudes

$$\begin{aligned}
 \mathcal{M}(B^0 \rightarrow \pi^0 \pi^0) &= \sqrt{\frac{1}{3}} A_0 e^{i\delta_0} - \sqrt{\frac{2}{3}} A_2 e^{i\delta_2}, \\
 \mathcal{M}(B^0 \rightarrow \pi^+ \pi^-) &= \sqrt{\frac{2}{3}} A_0 e^{i\delta_0} + \sqrt{\frac{1}{3}} A_2 e^{i\delta_2}, \\
 \mathcal{M}(B^- \rightarrow \pi^- \pi^0) &= \sqrt{\frac{3}{2}} A_2 e^{i\delta_2},
 \end{aligned} \tag{6.1}$$

where A_0 and A_2 are isospin 0 and 2 amplitudes, respectively, and δ_0, δ_2 are the corresponding S -wave $\pi \pi$ scattering isospin phase shifts. Note that the amplitudes (6.1) for $\pi^+ \pi^-$ and $\pi^- \pi^0$ are the same as the usual invariant amplitudes, but $\mathcal{A}(B^0 \rightarrow \pi^0 \pi^0) = \sqrt{2} \mathcal{M}(B^0 \rightarrow \pi^0 \pi^0)$. To proceed we shall assume that inelasticity is absent or negligible so that the isospin phase shifts are real and the magnitude of the isospin amplitudes is not affected by elastic FSI. Theoretically, A_0 and A_2 are of the same sign. As stressed in Sec. V.A, model calculations tend to predict a branching ratio of $B^0 \rightarrow \pi^+ \pi^-$ larger than the present limit. One possibility is that the isospin phase difference $\delta = \delta_0 - \delta_2$ is nonzero. In Fig. 14 we plot the branching ratios of $\pi \pi$ modes versus δ . It is evident that the suppression of $\pi^+ \pi^-$ and enhancement of $\pi^0 \pi^0$ become most severe when $\delta \gtrsim 70^\circ$ and furthermore the latter becomes overwhelming

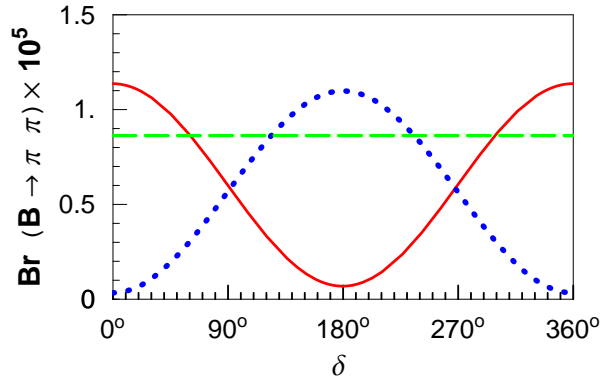


FIG. 14. Branching ratios of $B \rightarrow \pi\pi$ modes versus the isospin phase shift difference δ , where the solid, dashed, and dotted curves correspond to $\pi^+\pi^-$, $\pi^-\pi^0$, and $\pi^0\pi^0$, respectively. Uses of $N_c^{\text{eff}}(LL) = 2$, $N_c^{\text{eff}}(LR) = 5$ and the BSW model for form factors have been made.

at $\delta > 90^\circ$. Note that using the Regge analysis, $\delta_{\pi\pi}$ is estimated to be 11° in [60].

VII. COMPARISON WITH LITERATURE

In this section we would like to compare our framework and results with the excellent paper by Ali, Kramer and Lü (AKL) [10] in which nonleptonic charmless B decays are studied in a great detail. Our expressions for the factorized decay amplitudes of all two-body hadronic decays of B_u and B_d mesons are in agreement with AKL except that we have also included W -exchange, W -annihilation and spacelike penguin matrix elements in the expressions of factorized decay amplitudes, though they are usually neglected in the conventional calculation. Basically, our framework differs from AKL in the choice of the input parameters:^{§§} (i) The effective Wilson coefficients c_i^{eff} are obtained from the μ -dependent Wilson coefficient functions $c_i(\mu)$ at $\mu = m_b$ in the present paper and at $\mu = m_b/2$ by AKL. Although c_i^{eff} obtained by AKL and by us are scheme and scale independent, our effective Wilson coefficients are gauge invariant and free of the infrared singularity. (ii) As explained in detail before, we treat $N_c^{\text{eff}}(LL)$ and $N_c^{\text{eff}}(LR)$ differently for nonfactorized effects, while $N_c^{\text{eff}}(LL) = N_c^{\text{eff}}(LR) = N_c^{\text{eff}}$ is assumed by AKL with the preference $1/N_c^{\text{eff}} \leq 0.2$ or $N_c^{\text{eff}} \geq 5$. (iii) For the Wolfenstein parameters ρ and η , we use $\rho = 0.175$ and $\eta = 0.370$, corresponding to $(\rho^2 + \eta^2)^{1/2} = 0.41$, while $\rho = 0.12$, $\eta = 0.34$ and $(\rho^2 + \eta^2)^{1/2} = 0.36$ are employed by AKL. (iv) To evaluate the pseudoscalar matrix element arising from the penguin interactions, we apply equations of motion and use the light quark masses at $\mu = m_b$, while $m_q(\mu = m_b/2)$ is employed by AKL. (v) We apply the usual one-mixing angle formulation to the $\eta - \eta'$ mixing and two-mixing angle formulation to the decay constants of the η and η' , whereas

^{§§}Using the same values of input parameters as [10], we are able to reproduce all the branching ratios of AKL except for the decays $B^0 \rightarrow \rho^0\rho^0$, $\rho^0\omega$. This discrepancy is resolved after numerical corrections are made in [10] (private communication with C.D. Lü).

AKL use the two-angle parametrization for both $\eta - \eta'$ mixing and decay constants. (vi) The pseudoscalar matrix elements of $\eta^{(\prime)}$ -vacuum transition, characterized by the parameters r_η and $r_{\eta'}$ in (5.21), have different expressions in the present paper and in AKL.

In spite of the differences in the aforementioned input parameters, our work does agree with AKL in most cases. Some noticeable differences are as follows:

1. While our expressions for factorized amplitudes agree with AKL, we do have included W -annihilation and spacelike penguin contributions. For example, the decay amplitudes of $B^0 \rightarrow K^{+(\ast)}K^{-(\ast)}$, which proceed only through W -annihilation and spacelike penguin diagrams, are displayed in our Tables.
2. Employing the same values of N_c^{eff} as AKL, our predictions of branching ratios for tree-dominated decay modes are in general larger than that of AKL by a factor of 1.3 due to the difference in the use of $(\rho^2 + \eta^2)$ or $|V_{ub}|^2$.
3. It was advocated by AKL that the branching ratios of the decays $B^- \rightarrow \phi K^-$, $B^0 \rightarrow \phi K^0$, $B^- \rightarrow \phi K^{*-}$, $B^0 \rightarrow \phi K^{*0}$ are almost equal in the factorization approach, whereas we found that the decay rate of $B \rightarrow \phi K^*$ is very sensitive to the form-factor ratio $x = A_2^{BK^*}(m_\phi^2)/A_1^{BK^*}(m_\phi^2)$ and that the data of $B \rightarrow \phi K$ and $B \rightarrow \phi K^*$ can be simultaneously accommodated in the generalized factorization approach using the LCSR form factors (see Figs. 6 and 7).
4. We have argued that theoretically and phenomenologically the effective number of colors for $(V - A)(V - A)$ and $(V - A)(V + A)$ four-quark operators should be treated differently. The data of tree-dominated decays $B^- \rightarrow \rho^0\pi^-$, $\omega\pi^-$ indicate $N_c^{\text{eff}}(LL) < 3$, while the penguin-dominated modes $B^- \rightarrow \phi K^-$, $\eta'K^-$ clearly imply $N_c^{\text{eff}}(LR) > 3$. If using $N_c^{\text{eff}}(LL) = N_c^{\text{eff}}(LR) = N_c^{\text{eff}}$ as adopted by AKL, we found that the data of $B^- \rightarrow \phi K^-$ and $B^- \rightarrow \rho^0\pi^-$ cannot be accommodated simultaneously.
5. Our prediction for $B \rightarrow \eta'K$ is significantly different from that of AKL at the small value of $1/N_c^{\text{eff}}$. As illustrated in Fig. 8, the branching ratio of $B^- \rightarrow \eta'K^-$ predicted by AKL for $N_c^{\text{eff}}(LL) = N_c^{\text{eff}}(LR)$, corresponding to the dashed curve in Fig. 8, is largely enhanced at small $1/N_c^{\text{eff}}(LR)$ provided that $N_c^{\text{eff}}(LL)$ is fixed at the value of 2. Therefore, without adjusting other input parameters, the prediction of AKL will be significantly improved if $N_c^{\text{eff}}(LL)$ and $N_c^{\text{eff}}(LR)$ are treated differently. Moreover, we have shown that it is natural to have $\eta'K^\pm > \eta'K^0$ if $\gamma > 90^\circ$.
6. We found that in the absence of FSI, the branching ratio of $B^- \rightarrow \omega K^-$ is expected to be of the same order as $\mathcal{B}(B^- \rightarrow \rho^0 K^-) \sim (0.5 - 1.0) \times 10^{-6}$, whereas the branching ratio predicted by AKL rises above 1×10^{-5} at the small values of $1/N_c^{\text{eff}}$, $1/N_c^{\text{eff}} \approx 0$. We argue that if $\mathcal{B}(B^- \rightarrow \omega K^-) \gg \mathcal{B}(B^- \rightarrow \rho^0 K^-)$ is observed experimentally, then inelastic final-state rescattering may account for the disparity between ωK^- and $\rho^0 K^-$.
7. It is claimed by AKL that the decay $B^0 \rightarrow \rho^0 K^0$ is completely dominated by the electroweak penguin transitions for all values of N_c^{eff} and that a measurement of this mode will enable one to determine the largest electroweak penguin coefficient

a_9 . We found that the QCD penguin contribution to $\rho^0 K^0$ is not small compared to the electroweak penguin. To illustrate this point, we compute the ratio R_W defined in Eq. (5.37) and obtain $R_W(\rho^0 K^0) = 0.12$ averaged over CP-conjugate modes for $N_c^{\text{eff}}(LL) = N_c^{\text{eff}}(LR) = 2$, to be compared with the value 0.08 predicted by AKL for the same values of N_c^{eff} . It thus appears that the $\rho^0 K^0$ mode is almost completely dominated by the electroweak penguin. However, at the amplitude level, we found

$$\text{tree} : \text{QCD penguin} : \text{electroweak penguin} = -0.18 + 0.54i : 1 : 1.8 - 0.14i \quad (7.1)$$

for $\overline{B}^0 \rightarrow \rho^0 \overline{K}^0$ (see Table VI) and

$$\text{tree} : \text{QCD penguin} : \text{electroweak penguin} = -0.32 - 0.47i : 1 : 1.8 - 0.14i \quad (7.2)$$

for $B^0 \rightarrow \rho^0 K^0$, where the QCD penguin amplitude has been normalized to unity. It is evident that although Eqs. (7.1) and (7.2) lead to $R_W = 0.12$, the electroweak penguin contribution to the amplitude is largely contaminated by the QCD penguin one. Therefore, we conclude that only the B_s decay modes listed in (5.38) can provide a direct and unambiguous determination of a_9 .

VIII. CONCLUSIONS

Using the next-to-leading order QCD-corrected effective Hamiltonian and gauge-invariant, scheme- and scale-independent effective Wilson coefficients, we have systematically studied hadronic charmless two-body decays of B_u and B_d mesons within the framework of generalized factorization. Nonfactorizable effects are parametrized in terms of $N_c^{\text{eff}}(LL)$ and $N_c^{\text{eff}}(LR)$, the effective numbers of colors arising from $(V-A)(V-A)$ and $(V-A)(V+A)$ 4-quark operators, respectively. The branching ratios are calculated as a function of $N_c^{\text{eff}}(LR)$ with two different considerations for $N_c^{\text{eff}}(LL)$: (i) $N_c^{\text{eff}}(LL)$ being fixed at the value of 2, and (ii) $N_c^{\text{eff}}(LL) = N_c^{\text{eff}}(LR)$. Depending on the sensitivity of the effective coefficients a_i^{eff} on N_c^{eff} , we have classified the tree and penguin transitions into six different classes. Our main results are the following:

- To avoid the gauge and infrared problems connected with effective Wilson coefficients, we have worked in the on-shell scheme to obtain gauge invariant, infrared finite c_i^{eff} . The infrared pole is consistently absorbed into universal bound-state wave functions.
- The relative magnitudes of tree, QCD penguin and electroweak penguin amplitudes of all charmless B decays are tabulated in Tables V-VII for $N_c^{\text{eff}}(LR) = 2, 3, 5, \infty$ and $N_c^{\text{eff}}(LL) = 2$ as well as $N_c^{\text{eff}}(LL) = N_c^{\text{eff}}(LR)$. The predicted branching ratios are summarized in Tables VIII-X.
- Hadronic charmless B decays without strangeness in the final state are dominated by the tree $b \rightarrow u\bar{d}$ transition. The exceptional modes are $B^0 \rightarrow \pi^0 \eta, \pi^0 \eta', \rho^0 \omega$ which proceed mainly through the penguin diagram. The first measurement of the hadronic

$b \rightarrow u$ decay $B^- \rightarrow \rho^0 \pi^-$ by CLEO indicates that $1.1 \leq N_c^{\text{eff}}(LL) \leq 2.6$. Therefore, $N_c^{\text{eff}}(LL)$ is preferred to be smaller than 3. Moreover, the current experimental information on $B^- \rightarrow \omega \pi^-$ and $B^0 \rightarrow \pi^+ \pi^-$ also favors a small $N_c^{\text{eff}}(LL)$. For example, the former implies $1.7 < N_c^{\text{eff}}(LL) < 2.5$. The fact that $N_c^{\text{eff}}(LL) \approx 2$ is favored is also consistent with the nonfactorizable term extracted from $B \rightarrow (D, D^*)(\pi, \rho)$ decays, $N_c^{\text{eff}}(B \rightarrow D\pi) \approx 2$. The measurement of the ratios R_{1-4} of charged to neutral branching fractions [see Eq. (5.14)] is useful for determining $N_c^{\text{eff}}(LL)$.

- The tree-dominated class I-III modes that have branching ratios of order 10^{-5} or larger must have one or two vector mesons in the final state. For example, it is expected that $\mathcal{B}(\overline{B}^0 \rightarrow \rho^- \rho^+) \sim \mathcal{B}(\overline{B}^0 \rightarrow \rho^- \pi^+) > \mathcal{B}(\overline{B}^0 \rightarrow \pi^- \rho^+) \sim 1 \times 10^{-5}$. By contrast, the decay rates of penguin-dominated class-IV decays follow the pattern: $\Gamma(\overline{B} \rightarrow P_a P_b) > \Gamma(\overline{B} \rightarrow P_a V_b) \sim \Gamma(\overline{B} \rightarrow V_a V_b) > \Gamma(\overline{B} \rightarrow V_a P_b)$, where P_b or V_b is factorizable under the factorization assumption, because of various possibilities of interference between the penguin amplitudes governed by the QCD penguin parameters a_4 and a_6 . Moreover, the penguin-dominated charmless B decays have the largest branching ratios in the PP mode.
- The present limit on $B^\pm \rightarrow \phi K^\pm$ implies that $N_c^{\text{eff}}(LR) \gtrsim 3.2$ and 4.2 in the BSW and LCSR models, respectively. The data of $B \rightarrow \phi K$ and $B \rightarrow \phi K^*$ can be accommodated simultaneously if the form-factor ratio $A_2^{BK^*}(m_\phi^2)/A_1^{BK^*}(m_\phi^2)$ is less than unity. We found that the ratio $\Gamma(B \rightarrow \phi K^*)/\Gamma(B^\pm \rightarrow \phi K^\pm)$ is 0.76 in the BSW model, while it is equal to 1.9 in the LCSR analysis.
- If $N_c^{\text{eff}}(LL)$ is treated to be the same as $N_c^{\text{eff}}(LR)$, we showed that $\mathcal{B}(B^- \rightarrow \eta' K^-) \sim (2.7-4.7) \times 10^{-5}$ at $0 < 1/N_c^{\text{eff}} < 0.5$ and becomes even smaller at small $1/N_c^{\text{eff}}$ when the charm content contribution of the η' is taken into account. We have demonstrated that the discrepancy between theory and experiment is significantly improved by setting $N_c^{\text{eff}}(LL) \sim 2$. In particular, the η' charm content contribution is in the right direction. Therefore, the data of $B \rightarrow K \eta'$ provide a strong support for $N_c^{\text{eff}}(LL) \sim 2$ and the relation $N_c^{\text{eff}}(LR) > N_c^{\text{eff}}(LL)$. The mode $B \rightarrow \eta' K$ has the largest branching ratio in the two-body charmless B decays due mainly to the constructive interference between the penguin contributions arising from the $(\bar{u}u + \bar{d}d)$ and $\bar{s}s$ components of the η' . By contrast, the destructive interference for the η production leads to a much smaller decay rate for $B \rightarrow \eta K$. If the disparity between $\eta' K^\pm$ and $\eta' K^0$ is confirmed in the future, it could be attributed to a negative Wolfenstein's ρ parameter.
- The penguin-dominated class-V modes $\overline{B}_d^0 \rightarrow \phi \pi^0, \phi \eta, \phi \eta', \phi \rho^0, \phi \omega, B^+ \rightarrow \phi \pi^+, \phi \rho^+$ depend very sensitively on N_c^{eff} and are dominated by electroweak penguins at $N_c^{\text{eff}}(LL) \sim 2$, $N_c^{\text{eff}}(LR) \sim 5$ or $N_c^{\text{eff}}(LL) \sim N_c^{\text{eff}}(LR) \sim 3$. The electroweak penguin effect in the decays $\overline{B}^0 \rightarrow \overline{K}^0 \rho^0, B^- \rightarrow K^- \rho^0$ is as important as the QCD penguin contribution.
- Final-state interactions (FSI) are conventionally believed to play only a minor role in hadronic charmless B decays due to the large energy released in the decay. We showed

that in the absence of FSI, the branching ratio of $B^+ \rightarrow \omega K^+$ is expected to be of the same order as $\mathcal{B}(B^+ \rightarrow \rho^0 K^+) \sim (0.5 - 1.0) \times 10^{-6}$, while experimentally it is of order 1.5×10^{-5} . We argued that $B^+ \rightarrow \omega K^+$ may receive a sizable final-state rescattering contribution from the intermediate states $K^{*-}\pi^0, K^{*-}\eta^{(\prime)}, K^{*0}\pi^-, K^-\rho^0, K^0\rho^-$ which interfere constructively, whereas the analogous rescattering effect on $B^+ \rightarrow \rho^0 K^+$ is very suppressed. However, if the measured branching ratio $\rho^0 K^+$ is similar to that of ωK^+ , then W -annihilation and spacelike penguins could play a prominent role. Likewise, the decay mode $B^0 \rightarrow K^+ K^-$ is expected to be dominated by inelastic rescattering from $\rho^+\rho^-, \pi^+\pi^-$ intermediate states, and $B^0 \rightarrow \phi\phi$ is governed by the $\eta^{(\prime)}\eta^{(\prime)}$ intermediate channels.

- A negative Wolfenstein parameter ρ or a unitarity angle γ larger than 90° is helpful for explaining the $\pi^+\pi^-, K\pi$ and $\eta'K$ data. All the known model calculations predict a too large $\pi^+\pi^-$ rate compared to the recently improved limit. We have shown that either $\gamma > 105^\circ$ or an isospin phase shift difference $\delta_{\pi\pi} > 70^\circ$ can account for the data of $B \rightarrow \pi^+\pi^-$. Moreover, the disparity between the $\eta'K^-$ and $\eta'K^0$ modes can be accommodated by $\rho < 0$. The expected hierarchy pattern $\bar{K}^0\pi^- > K^-\pi^+ > K^-\pi^0$ predicted at $\gamma = 65^\circ$ will be modified to $K^-\pi^+ > \bar{K}^0\pi^- > K^-\pi^0$ at $\gamma > 90^\circ$ and $K^-\pi^0$ becomes close to $K^-\pi^+$ when γ approaches to 180° .
- Theoretical calculations suggest that the following decay modes of B_u^- and \bar{B}_d^0 have branching ratios are of order 10^{-5} or in the range of a few times of 10^{-5} : $\eta'K^-, \eta'K^0, \rho^+\rho^-, \rho^-\pi^+, \rho^-\rho^0, \rho^-\omega, \rho^-\pi^0, K^-\pi^+, \bar{K}^0\pi^-, K^-\pi^0, \rho^+\pi^-, \rho^0\pi^-, \omega\pi^-, \rho^-\eta$. Some of them have been observed and the rest will have a good chance to be seen soon.

Note added: Recently CLEO has reported two new measurements on the $\rho^\pm\pi^\mp$ and $K^{*\pm}\pi^\mp$ modes of the neutral B mesons [38]: $\mathcal{B}(\bar{B}^0 \rightarrow \rho^+\pi^- + \rho^-\pi^+) = (3.5_{-1.0}^{+1.1} \pm 0.5) \times 10^{-5}$ and $\mathcal{B}(\bar{B}^0 \rightarrow K^{*-}\pi^+) = (2.2_{-0.6-0.5}^{+0.8+0.4}) \times 10^{-5}$. We see from Table IX that while the prediction $\mathcal{B}(\bar{B}^0 \rightarrow \rho^+\pi^- + \rho^-\pi^+) = 3.7 \times 10^{-5}$ is in good agreement with experiment, the observation that $K^{*-}\pi^+ \gtrsim K^-\pi^+$ is opposite to the theoretical expectation (see the discussion in Sec. V.E.).

ACKNOWLEDGMENTS

We are grateful to J. Smith for critically reading the manuscript and for useful comments. Two of us (B.T. and K.C.Y.) wish to thank the KEK theory group for their warm hospitality. This work is supported in part by the National Science Council of the Republic of China under Grants Nos. NSC88-2112-M001-006 and NSC88-2112-M006-013.

REFERENCES

- [1] For a review of CLEO measurements on charmless B decays, see K. Lingel, T. Skwarnicki, and J.G. Smith, *Annu. Rev. Nucl. Part. Sci.* **48**, 253 (1998).
- [2] L.L. Chau, H.Y. Cheng, W.K. Sze, H. Yao, and B. Tseng, *Phys. Rev.* **D43**, 2176 (1991); **D58**, (E)019902 (1998).
- [3] L.L. Chau and H.Y. Cheng, *Phys. Rev. Lett.* **56**, 1655 (1986); *Phys. Rev.* **D36**, 137 (1987); *Phys. Lett.* **B222**, 285 (1989).
- [4] Y.H. Chen, H.Y. Cheng, and B. Tseng, *Phys. Rev.* **D59**, 074003 (1999).
- [5] A.J. Buras and L. Silvestrini, *Nucl. Phys.* **B548**, 293 (1999).
- [6] M. Bauer, B. Stech, and M. Wirbel, *Z. Phys.* **C34**, 103 (1987).
- [7] H.Y. Cheng, H.n. Li, and K.C. Yang, hep-ph/9902239, to appear in *Phys. Rev. D*.
- [8] H.Y. Cheng and B. Tseng, *Phys. Rev. D* **58**, 094005 (1998).
- [9] A. Ali and C. Greub, *Phys. Rev.* **D57**, 2996 (1998).
- [10] A. Ali, G. Kramer, and C.D. Lü, *Phys. Rev.* **D58**, 094009 (1998).
- [11] G. Buchalla, A.J. Buras, and M.E. Lautenbacher, *Rev. Mod. Phys.* **68**, 1125 (1996).
- [12] A.J. Buras, hep-ph/9806471.
- [13] L. Wolfenstein, *Phys. Rev. Lett.* **13**, 562 (1984).
- [14] L.L. Chau and W.Y. Keung, *Phys. Rev. Lett.* **53**, 1802 (1984).
- [15] F. Parodi, P. Roudeau, and A. Stocchi, hep-ex/9903063; F. Parodi, invited talk presented at the XXIX International Conference on High Energy Physics, Vancouver, July 23-28, 1998; A. Stocchi, hep-ex/9902004.
- [16] S. Mele, *Phys. Rev.* **D59**, 113011 (1999).
- [17] H. Fusaoku and Y. Koide, *Phys. Rev.* **D57**, 3986 (1998).
- [18] H. Leutwyler, *Nucl. Phys. B (Proc. Suppl.)* **64**, 223 (1998).
- [19] T. Feldmann, P. Kroll, and B. Stech, *Phys. Rev.* **D58**, 114006 (1998); *Phys. Lett.* **B449**, 339 (1999).
- [20] I. Halperin and A. Zhitnitsky, *Phys. Rev.* **D56**, 7247 (1997); E.V. Shuryak and A. Zhitnitsky, *Phys. Rev.* **D57**, 2001 (1998).
- [21] A. Ali, J. Chay, C. Greub, and P. Ko, *Phys. Lett.* **B424**, 161 (1998).
- [22] F. Araki, M. Musakhanov, and H. Toki, *Phys. Rev.* **D59**, 037501 (1999); hep-ph/9808290.

- [23] M. Franz, P.V. Pobylitsa, M.V. Polyakov, and K. Goeke, hep-ph/9810343.
- [24] A.A. Petrov, *Phys. Rev.* **D58**, 054003 (1998).
- [25] T. Feldmann and P. Kroll, *Eur. Phys. J.* **C5**, 327 (1998).
- [26] J. Cao, F.G. Cao, T. Huang, and B.Q. Ma, *Phys. Rev.* **D58**, 113006 (1998).
- [27] M.R. Ahmady and E. Kou, hep-ph/9903335.
- [28] M. Wirbel, B. Stech, and M. Bauer, *Z. Phys.* **C29**, 637 (1985).
- [29] P. Ball and V.M. Braun, *Phys. Rev.* **D58**, 094016 (1998); P. Ball, *J. High Energy Phys.* **9809**, 005 (1998) [hep-ph/9802394].
- [30] H.Y. Cheng, C.Y. Cheung, and C.W. Hwang, *Phys. Rev.* **D55**, 1559 (1997).
- [31] H.Y. Cheng, *Phys. Lett.* **B395**, 345 (1994); in *Particle Theory and Phenomenology*, XVII International Karimierz Meeting on Particle Physics, Iowa State University, May 1995, edited by K.E. Lassila *et al.* (World Scientific, Singapore, 1996), p.122.
- [32] A.N. Kamal and A.B. Santra, Alberta Thy-31-94 (1994); *Z. Phys.* **C72**, 91 (1996).
- [33] J.M. Soares, *Phys. Rev.* **D51**, 3518 (1995).
- [34] M. Neubert and B. Stech, in *Heavy Flavours*, edited by A.J. Buras and M. Lindner, 2nd ed. (World Scientific, Singapore, 1998), p.294.
- [35] H.Y. Cheng and K.C. Yang, *Phys. Rev.* **D59**, 092004 (1999).
- [36] B. Tseng, *Phys. Lett.* **B446**, 125 (1999).
- [37] For updated *B* meson lifetimes, see J. Alcaraz *et al.* (LEP *B* Lifetime Working Group), <http://wwwcn.cern.ch/~claires/lepblife.html>.
- [38] CLEO Collaboration, Y.S. Gao and F. Würthwein, hep-ex/9904008.
- [39] CLEO Collaboration, T. Bergfeld *et al.*, *Phys. Rev. Lett.* **81**, 272 (1998).
- [40] CLEO Collaboration, J. Roy, invited talk presented at the XXIX International Conference on High Energy Physics, Vancouver, July 23-28, 1998.
- [41] X.G. He, W.S. Hou, and K.C. Yang, hep-ph/9902256.
- [42] S. Gardner, *Phys. Rev.* **D59**, 077502 (1999).
- [43] A.L. Kagan and A.A. Petrov, UCHEP-27 [hep-ph/9707354].
- [44] CLEO Collaboration, B.H. Behrens *et al.*, *Phys. Rev. Lett.* **80**, 3710 (1998).
- [45] G. Kramer, W.F. Palmer, and H. Simma, *Z. Phys.* **C66**, 429 (1995); *Nucl. Phys.* **B428**, 77 (1994).
- [46] D.S. Du and L. Guo, *Z. Phys.* **C75**, 9 (1997); D.S. Du, M.Z. Yang, and D.Z. Zhang,

- Phys. Rev.* **D53**, 249 (1996).
- [47] N.G. Deshpande, B. Dutta, and S. Oh, *Phys. Rev.* **D57**, 5723 (1998); A. Datta, X.G. He, and S. Pakvasa, *Phys. Lett.* **B419**, 369 (1998).
- [48] H.Y. Cheng and B. Tseng, *Phys. Lett.* **B415**, 263 (1997).
- [49] CLEO Collaboration, B.H. Behrens *et al.*, CLEO CONF 98-09 (1998).
- [50] A.S. Dighe, M. Gronau, and J.L. Rosner, *Phys. Rev. Lett.* **79**, 4333 (1997).
- [51] M.R. Ahmady, E. Kou, and A. Sugamoto, *Phys. Rev.* **D58**, 014015 (1998).
- [52] D.S. Du, C.S. Kim, and Y.D. Yang, *Phys. Lett.* **B419**, 369 (1998).
- [53] D.S. Du, Y.D. Yang, and G. Zhu, *Phys. Rev.* **D59**, 014007 (1999); hep-ph/9901218.
- [54] R. Fleischer and T. Mannel, *Phys. Rev.* **D57**, 2752 (1998).
- [55] CLEO Collaboration, R. Godang *et al.*, *Phys. Rev. Lett.* **80**, 3456 (1998).
- [56] N.G. Deshpande, X.G. He, W.S. Hou, and S. Pakvasa, *Phys. Rev. Lett.* **82**, 2240 (1999).
- [57] R. Fleischer, *Phys. Lett.* **B332**, 419 (1994); N.G. Deshpande, X.G. He, and J. Trampetic, *Phys. Lett.* **B345**, 547 (1995).
- [58] N.G. Deshpande and J. Trampetic, *Phys. Rev.* **D41**, 2926 (1990); H. Simma and D. Wyler, *Phys. Lett.* **B272**, 395 (1991); J.-M. Gérard and W.S. Hou, *Phys. Rev.* **D43**, 2909 (1991).
- [59] M. Gronau and J.L. Rosner, *Phys. Rev.* **D58**, 113005 (1998).
- [60] J.-M. Gérard, J. Pestieau, and J. Weyers, *Phys. Lett.* **B436**, 363 (1998).

APPENDIX

A.

The factorized decay amplitudes of all charmless $B_{u,d} \rightarrow PP, VP, VV$ decays are tabulated in the Appendix. The factorized terms $X^{(BM_1, M_2)}$ have the expressions:

$$\begin{aligned}
X^{(BP_1, P_2)} &\equiv \langle P_2 | (\bar{q}_2 q_3)_{V-A} | 0 \rangle \langle P_1 | (\bar{q}_1 b)_{V-A} | \bar{B} \rangle = i f_{P_2} (m_B^2 - m_{P_1}^2) F_0^{BP_1} (m_{P_2}^2), \\
X^{(BP, V)} &\equiv \langle V | (\bar{q}_2 q_3)_{V-A} | 0 \rangle \langle P | (\bar{q}_1 b)_{V-A} | \bar{B} \rangle = 2 f_V m_V F_1^{BP} (m_V^2) (\varepsilon^* \cdot p_B), \\
X^{(BV, P)} &\equiv \langle P | (\bar{q}_2 q_3)_{V-A} | 0 \rangle \langle V | (\bar{q}_1 b)_{V-A} | \bar{B} \rangle = 2 f_P m_V A_0^{BV} (m_P^2) (\varepsilon^* \cdot p_B), \\
X^{(BV_1, V_2)} &\equiv \langle V_2 | (\bar{q}_2 q_3)_{V-A} | 0 \rangle \langle V_1 | (\bar{q}_1 b)_{V-A} | \bar{B} \rangle = -i f_{V_2} m_2 \left[(\varepsilon_1^* \cdot \varepsilon_2^*) (m_B + m_1) A_1^{BV_1} (m_2^2) \right. \\
&\quad \left. - (\varepsilon_1^* \cdot p_B) (\varepsilon_2^* \cdot p_B) \frac{2 A_2^{BV_1} (m_2^2)}{(m_B + m_1)} + i \epsilon_{\mu\nu\alpha\beta} \varepsilon_2^{*\mu} \varepsilon_1^{*\nu} p_B^\alpha p_1^\beta \frac{2 V^{BV_1} (m_2^2)}{(m_B + m_1)} \right], \tag{A1}
\end{aligned}$$

where ε^* is the polarization vector of the vector meson V . For a flavor-neutral M_2 with the quark content $(\bar{q}q + \dots)$, we will encounter the factorized term

$$X_q^{(BM_1, M_2)} \equiv \langle M_2 | (\bar{q}q)_{V-A} | 0 \rangle \langle M_1 | (\bar{q}_1 b)_{V-A} | \bar{B} \rangle. \tag{A2}$$

For example,

$$\begin{aligned}
X_s^{(B^- K^-, \eta')} &= \langle \eta' | (\bar{s}s)_{V-A} | 0 \rangle \langle K^- | (\bar{s}b)_{V-A} | B^- \rangle = i f_{\eta'}^s (m_B^2 - m_K^2) F_0^{BK} (m_{\eta'}^2), \\
X_u^{(B^- \pi^-, \rho^0)} &= \langle \rho^0 | (\bar{u}u)_{V-A} | 0 \rangle \langle \pi^- | (\bar{d}b)_{V-A} | B^- \rangle = \sqrt{2} f_\rho m_\rho F_1^{B\pi} (m_\rho^2) (\varepsilon^* \cdot p_B). \tag{A3}
\end{aligned}$$

For $\bar{B}_d^0 \rightarrow VV$ decays (see Appendix F), we have distinguished spacelike penguin matrix elements arising from $(V-A)(V+A)$ and $(V-A)(V-A)$ operators, e.g.,

$$\begin{aligned}
X_u^{(B^0, \rho^0 \omega)} &= \langle 0 | (\bar{d}b)_{V-A} | \bar{B}^0 \rangle \langle \rho^0 \omega | (\bar{u}u)_{V-A} | 0 \rangle, \\
\bar{X}_u^{(B^0, \rho^0 \omega)} &= \langle 0 | (\bar{d}b)_{V-A} | \bar{B}^0 \rangle \langle \rho^0 \omega | (\bar{u}u)_{V+A} | 0 \rangle. \tag{A4}
\end{aligned}$$

As stressed in Sec. IV.B, we have included W -exchange, W -annihilation and spacelike penguin matrix elements in the expressions of factorized decay amplitudes, though they are usually neglected in practical calculations of branching ratios.

Note that the hadronic matrix elements of scalar and pseudoscalar densities are conventionally evaluated by applying equations of motion. However, we encounter in $\bar{B}_d \rightarrow PP, VV$ decays terms like $\langle \pi\pi | \bar{d}d | 0 \rangle$ which cannot be directly related to the matrix element $\langle \pi\pi | \bar{d}\gamma_\mu d | 0 \rangle$ via the use of equation of motion

$$-i\partial^\mu (\bar{q}_1 \gamma_\mu q_2) = (m_1 - m_2) \bar{q}_1 q_2. \tag{A5}$$

Hence, the matrix element such as $\langle \pi\pi | \bar{d}d | 0 \rangle$ has to be evaluated using a different technique. Unfortunately, chiral perturbation theory, which has been employed to compute the same matrix element occurred in $K \rightarrow \pi\pi$ decay, is no longer applicable in energetic B decays. Since $\langle V | \bar{q}_1 q_2 | 0 \rangle = 0$, $B \rightarrow VV$ decays do not receive factorizable contributions from a_6 and a_8 penguin terms except for spacelike penguin diagrams (see Appendixes F and G).

All the amplitudes listed below should be multiplied by a factor of $G_F/\sqrt{2}$.

B. $\bar{B}_d^0 \rightarrow PP$ DECAYS

$$A(\bar{B}_d^0 \rightarrow K^- \pi^+) = \left\{ V_{ub}V_{us}^* a_1 - V_{tb}V_{ts}^* \left[a_4 + a_{10} + 2(a_6 + a_8) \frac{m_{K^-}^2}{(m_b - m_u)(m_u + m_s)} \right] \right\} X^{(\bar{B}_d^0 \pi^+, K^-)} \\ - V_{tb}V_{ts}^* \left[a_4 - \frac{1}{2}a_{10} + (2a_6 - a_8) \frac{m_{\bar{B}_d^0}^2}{(m_b + m_d)(m_s - m_d)} \right] X^{(\bar{B}_d^0, \pi^+ K^-)}, \quad (\text{B1})$$

$$A(\bar{B}_d^0 \rightarrow \bar{K}^0 \pi^0) = \left[V_{ub}V_{us}^* a_2 - V_{tb}V_{ts}^* \left(-\frac{3}{2}a_7 + \frac{3}{2}a_9 \right) \right] X_u^{(\bar{B}_d^0 \bar{K}^0, \pi^0)} \\ - V_{tb}V_{ts}^* \left[a_4 - \frac{1}{2}a_{10} + 2(a_6 - \frac{1}{2}a_8) \frac{m_{\bar{K}^0}^2}{(m_s + m_d)(m_b - m_d)} \right] X^{(\bar{B}_d^0 \pi^0, \bar{K}^0)} \\ + \left[a_4 - \frac{1}{2}a_{10} + (2a_6 - a_8) \frac{m_{\bar{B}_d^0}^2}{(m_b + m_d)(m_s - m_d)} \right] X^{(\bar{B}_d^0, \pi^0 \bar{K}^0)} \Big\}, \quad (\text{B2})$$

$$A(\bar{B}_d^0 \rightarrow \bar{K}^0 \eta^{(\prime)}) = V_{ub}V_{us}^* a_2 X_u^{(\bar{B}_d^0 \bar{K}^0, \eta^{(\prime)})} + V_{cb}V_{cs}^* a_2 X_c^{(\bar{B}_d^0 \bar{K}^0, \eta^{(\prime)})} \\ - V_{tb}V_{ts}^* \left\{ \left[2a_3 - 2a_5 - \frac{1}{2}a_7 + \frac{1}{2}a_9 \right] X_u^{(\bar{B}_d^0 \bar{K}^0, \eta^{(\prime)})} \right. \\ + \left[a_3 + a_4 - a_5 + (2a_6 - a_8) \frac{m_{\eta^{(\prime)}}^2}{2m_s(m_b - m_s)} \left(1 - \frac{f_{\eta^{(\prime)}}^u}{f_{\eta^{(\prime)}}^s} \right) \right. \\ \left. + \frac{1}{2}(a_7 - a_9 - a_{10}) \right] X_s^{(\bar{B}_d^0 \bar{K}^0, \eta^{(\prime)})} + [a_3 - a_5 - a_7 + a_9] X_c^{(\bar{B}_d^0 \bar{K}^0, \eta^{(\prime)})} \\ \left. + \left[a_4 - \frac{1}{2}a_{10} + (2a_6 - a_8) \frac{m_{\bar{K}^0}^2}{(m_s + m_d)(m_b - m_d)} \right] X^{(\bar{B}_d^0 \eta^{(\prime)}, \bar{K}^0)} \right. \\ \left. + \left[a_4 + a_{10} + 2(a_6 + a_8) \frac{m_{\bar{B}_d^0}^2}{(m_s - m_d)(m_b + m_d)} \right] X^{(\bar{B}_d^0, \bar{K}^0 \eta^{(\prime)})} \right\}, \quad (\text{B3})$$

$$A(\bar{B}_d^0 \rightarrow K^0 \bar{K}^0) = -V_{tb}V_{td}^* \left\{ \left[a_3 + a_4 + a_5 - \frac{1}{2}(a_7 + a_9 + a_{10}) \right] X_d^{(\bar{B}_d^0, K^0 \bar{K}^0)} \right. \\ + \left[a_3 + a_5 - \frac{1}{2}a_7 - \frac{1}{2}a_9 \right] X_s^{(\bar{B}_d^0, K^0 \bar{K}^0)} \\ + \left[a_4 - \frac{1}{2}a_{10} + (2a_6 - a_8) \frac{m_{\bar{K}^0}^2}{(m_s + m_d)(m_b - m_s)} \right] X^{(\bar{B}_d^0 K^0, \bar{K}^0)} \\ \left. - (2a_6 - a_8) \langle K^0 \bar{K}^0 | \bar{d}(1 + \gamma_5)d | 0 \rangle \langle 0 | \bar{d}(1 - \gamma_5)b | \bar{B}_d^0 \rangle \right\}, \quad (\text{B4})$$

$$A(\bar{B}_d^0 \rightarrow K^+ K^-) = V_{ub}V_{ud}^* a_2 X_u^{(\bar{B}_d^0, K^+ K^-)} - V_{tb}V_{td}^* \left\{ [a_3 + a_5 + a_7 + a_9] X_u^{(\bar{B}_d^0, K^+ K^-)} \right. \\ \left. + \left[a_3 + a_5 - \frac{1}{2}a_7 - \frac{1}{2}a_9 \right] X_s^{(\bar{B}_d^0, K^+ K^-)} \right\}, \quad (\text{B5})$$

$$\begin{aligned}
A(\bar{B}_d^0 \rightarrow \pi^+\pi^-) &= V_{ub}V_{ud}^* \left(a_1 X(\bar{B}_d^0 \pi^+, \pi^-) + a_2 X(\bar{B}_d^0, \pi^+\pi^-) \right) \\
&\quad - V_{tb}V_{td}^* \left\{ \left[a_4 + a_{10} + 2(a_6 + a_8) \frac{m_{\pi^-}^2}{(m_d + m_u)(m_b - m_u)} \right] X(\bar{B}_d^0 \pi^+, \pi^-) \right. \\
&\quad + \left[2a_3 + a_4 + 2a_5 + \frac{1}{2}(a_7 + a_9 - a_{10}) \right] X(\bar{B}_d^0, \pi^+\pi^-) \\
&\quad \left. - (2a_6 - a_8) \langle \pi^+\pi^- | \bar{d}(1 + \gamma_5)d | 0 \rangle \langle 0 | \bar{d}(1 - \gamma_5)b | \bar{B}_d^0 \rangle \right\}, \tag{B6}
\end{aligned}$$

$$\begin{aligned}
A(\bar{B}_d^0 \rightarrow \pi^0\pi^0) &= V_{ub}V_{ud}^* 2(a_2 X_u(\bar{B}_d^0 \pi^0, \pi^0) + a_2 X_u(\bar{B}_d^0, \pi^0\pi^0)) \\
&\quad - V_{tb}V_{td}^* 2 \left\{ \left[-a_4 + \frac{3}{2}(-a_7 + a_9) + \frac{1}{2}a_{10} - (2a_6 - a_8) \frac{m_{\pi^0}^2}{2m_d(m_b - m_d)} \right] X_u(\bar{B}_d^0 \pi^0, \pi^0) \right. \\
&\quad + \left[2a_3 + a_4 + 2a_5 + \frac{1}{2}(a_7 + a_9 - a_{10}) \right] X_u(\bar{B}_d^0, \pi^0\pi^0) \\
&\quad \left. - (2a_6 - a_8) \langle \pi^0\pi^0 | \bar{d}(1 + \gamma_5)d | 0 \rangle \langle 0 | \bar{d}(1 - \gamma_5)b | \bar{B}_d^0 \rangle \right\}, \tag{B7}
\end{aligned}$$

$$\begin{aligned}
A(\bar{B}_d^0 \rightarrow \pi^0\eta^{(\prime)}) &= V_{ub}V_{ud}^* a_2 (X_u(\bar{B}_d^0 \pi^0, \eta^{(\prime)}) + X_u(\bar{B}_d^0 \eta^{(\prime)}, \pi^0)) + V_{cb}V_{cd}^* a_2 X_c(\bar{B}_d^0 \pi^0, \eta^{(\prime)}) \\
&\quad - V_{tb}V_{td}^* \left\{ \left[2a_3 + a_4 - 2a_5 - \frac{1}{2}(a_7 - a_9 + a_{10}) \right. \right. \\
&\quad + (2a_6 - a_8) \frac{m_{\eta^{(\prime)}}^2}{2m_s(m_b - m_d)} \left(\frac{f_{\eta^{(\prime)}}^s}{f_{\eta^{(\prime)}}^u} - 1 \right) r_{\eta'} \left. \right] X_u(\bar{B}_d^0 \pi^0, \eta^{(\prime)}) \\
&\quad + [a_3 - a_5 - a_7 + a_9] X_c(\bar{B}_d^0 \pi^0, \eta^{(\prime)}) + \left[a_3 - a_5 + \frac{1}{2}a_7 - \frac{1}{2}a_9 \right] X_s(\bar{B}_d^0 \pi^0, \eta^{(\prime)}) \\
&\quad + \left[-a_4 - \frac{3}{2}(a_7 - a_9) + \frac{1}{2}a_{10} - (2a_6 - a_8) \frac{m_{\pi^0}^2}{2m_d(m_b - m_d)} \right] X_u(\bar{B}_d^0 \eta^{(\prime)}, \pi^0) \\
&\quad + [a_3 - a_5 - a_7 + a_9] X_c(\bar{B}_d^0, \pi^0\eta^{(\prime)}) + \left[a_3 - a_5 + \frac{1}{2}a_7 - \frac{1}{2}a_9 \right] X_s(\bar{B}_d^0, \pi^0\eta^{(\prime)}) \\
&\quad + \left[2a_3 + a_4 + 2a_5 + \frac{1}{2}(a_7 + a_9 - a_{10}) \right] X(\bar{B}_d^0, \pi^0\eta^{(\prime)}) \\
&\quad \left. - (2a_6 - a_8) \langle \eta^{(\prime)}\pi^0 | \bar{d}(1 + \gamma_5)d | 0 \rangle \langle 0 | \bar{d}(1 - \gamma_5)b | \bar{B}_d^0 \rangle \right\}, \tag{B8}
\end{aligned}$$

$$\begin{aligned}
A(\bar{B}_d^0 \rightarrow \eta\eta') &= V_{ub}V_{ud}^* a_2 (X_u(\bar{B}_d^0 \eta, \eta') + X_u(\bar{B}_d^0 \eta', \eta) + 2X(\bar{B}_d^0, \eta\eta')) \\
&\quad + V_{cb}V_{cd}^* a_2 (X_c(\bar{B}_d^0 \eta, \eta') + X_c(\bar{B}_d^0 \eta', \eta) + 2X_c(\bar{B}_d^0, \eta\eta')) \\
&\quad - V_{tb}V_{td}^* \left\{ \left[2a_3 + a_4 - 2a_5 - \frac{1}{2}a_7 + \frac{1}{2}a_9 - \frac{1}{2}a_{10} \right. \right. \\
&\quad + (2a_6 - a_8) \frac{m_{\eta'}^2}{2m_s(m_b - m_d)} \left(\frac{f_{\eta'}^s}{f_{\eta'}^u} - 1 \right) r_{\eta'} \left. \right] X_u(\bar{B}_d^0 \eta, \eta') \\
&\quad + \left[2a_3 + a_4 - 2a_5 - \frac{1}{2}a_7 + \frac{1}{2}a_9 - \frac{1}{2}a_{10} \right.
\end{aligned}$$

$$\begin{aligned}
& + (2a_6 - a_8) \frac{m_\eta^2}{2m_s(m_b - m_d)} \left(\frac{f_\eta^s}{f_\eta^u} - 1 \right) r_\eta \Big] X_u^{(\overline{B}_d^0 \eta', \eta)} \\
& + \left[a_3 - a_5 + \frac{1}{2}(a_7 - a_9) \right] (X_s^{(\overline{B}_d^0 \eta, \eta')} + X_s^{(\overline{B}_d^0 \eta', \eta)}) \\
& + [a_3 - a_5 - a_7 + a_9] (X_c^{(\overline{B}_d^0 \eta, \eta')} + X_c^{(\overline{B}_d^0 \eta', \eta)}) \\
& + \left[a_3 + a_5 - \frac{1}{2}(a_7 + a_9) \right] X_s^{(\overline{B}_d^0, \eta \eta')} + [a_3 + a_5 + a_7 + a_9] X_c^{(\overline{B}_d^0, \eta \eta')} \\
& + \left[2a_3 + a_4 + 2a_5 + \frac{1}{2}(a_7 + a_9 - a_{10}) \right] X^{(\overline{B}_d^0, \eta \eta')} \\
& - (2a_6 - a_8) \langle \eta' \eta | \bar{d}(1 + \gamma_5) d | 0 \rangle \langle 0 | \bar{d}(1 - \gamma_5) b | \overline{B}_d^0 \rangle \Big\}, \tag{B9}
\end{aligned}$$

$$\begin{aligned}
A(\overline{B}_d^0 \rightarrow \eta \eta) & = V_{ub} V_{ud}^* 2a_2 (X_u^{(\overline{B}_d^0 \eta, \eta)} + X^{(\overline{B}_d^0, \eta \eta)}) + V_{cb} V_{cd}^* 2a_2 (X_c^{(\overline{B}_d^0 \eta, \eta)} + X_c^{(\overline{B}_d^0, \eta \eta)}) \\
& - V_{tb} V_{td}^* 2 \left\{ \left[2a_3 + a_4 - 2a_5 - \frac{1}{2}a_7 + \frac{1}{2}a_9 - \frac{1}{2}a_{10} \right. \right. \\
& \left. \left. + (2a_6 - a_8) \frac{m_\eta^2}{2m_s(m_b - m_d)} \left(\frac{f_\eta^s}{f_\eta^u} - 1 \right) r_\eta \right] X_u^{(\overline{B}_d^0 \eta, \eta)} \right. \\
& + \left[a_3 - a_5 + \frac{1}{2}(a_7 - a_9) \right] X_s^{(\overline{B}_d^0 \eta, \eta)} + [a_3 - a_5 - a_7 + a_9] X_c^{(\overline{B}_d^0 \eta, \eta)} \\
& + \left[a_3 + a_5 - \frac{1}{2}(a_7 + a_9) \right] X_s^{(\overline{B}_d^0, \eta \eta)} + [a_3 + a_5 + a_7 + a_9] X_c^{(\overline{B}_d^0, \eta \eta)} \\
& + \left[2a_3 + a_4 + 2a_5 + \frac{1}{2}(a_7 + a_9 - a_{10}) \right] X^{(\overline{B}_d^0, \eta \eta)} \\
& \left. - (2a_6 - a_8) \langle \eta \eta | \bar{d}(1 + \gamma_5) d | 0 \rangle \langle 0 | \bar{d}(1 - \gamma_5) b | \overline{B}_d^0 \rangle \right\}, \tag{B10}
\end{aligned}$$

$$A(\overline{B}_d^0 \rightarrow \eta' \eta') \text{ is obtained from } A(\overline{B}_d^0 \rightarrow \eta \eta) \text{ with } \eta \rightarrow \eta'. \tag{B11}$$

C. $B_u^- \rightarrow PP$ DECAYS

$$\begin{aligned}
A(B_u^- \rightarrow \overline{K}^0 \pi^-) & = -V_{tb} V_{ts}^* \left\{ \left[a_4 + a_{10} + 2(a_6 + a_8) \frac{m_{B_u^-}^2}{(m_s - m_u)(m_b + m_u)} \right] X^{(B_u^-, \pi^- \overline{K}^0)} \right. \\
& \left. + \left[a_4 - \frac{1}{2}a_{10} + (2a_6 - a_8) \frac{m_{\overline{K}^0}^2}{(m_s + m_d)(m_b - m_d)} \right] X^{(B_u^-, \pi^-, \overline{K}^0)} \right\} \\
& + V_{ub} V_{us}^* a_1 X^{(B_u^-, \pi^- \overline{K}^0)}, \tag{C1}
\end{aligned}$$

$$\begin{aligned}
A(B_u^- \rightarrow K^- \pi^0) & = V_{ub} V_{us}^* (a_1 X^{(B_u^-, \pi^0, K^-)} + a_1 X^{(B_u^-, \pi^0 K^-)} + a_2 X_u^{(B_u^-, K^-, \pi^0)}) \\
& - V_{tb} V_{ts}^* \left\{ \left[a_4 + a_{10} + 2(a_6 + a_8) \frac{m_{K^-}^2}{(m_s + m_u)(m_b - m_u)} \right] X^{(B_u^-, \pi^0, K^-)} \right.
\end{aligned}$$

$$\begin{aligned}
& + \frac{3}{2} [-a_7 + a_9] X_u^{(B_u^- K^-, \pi^0)} \\
& + \left[a_4 + a_{10} + 2(a_6 + a_8) \frac{m_{B_u^-}^2}{(m_s - m_u)(m_b + m_u)} \right] X^{(B_u^-, K^-, \pi^0)} \Big\}, \quad (C2)
\end{aligned}$$

$$\begin{aligned}
A(B_u^- \rightarrow K^- \eta^{(\prime)}) &= V_{ub} V_{us}^* \left[a_1 X^{(B_u^- \eta^{(\prime)}, K^-)} + a_2 X_u^{(B_u^- K^-, \eta^{(\prime)})} + a_1 X_u^{(B_u^-, K^-, \eta^{(\prime)})} + a_1 X_s^{(B_u^-, K^-, \eta^{(\prime)})} \right] \\
& + V_{cb} V_{cs}^* a_2 X_c^{(B_u^- K^-, \eta^{(\prime)})} - V_{tb} V_{ts}^* \left\{ \left[2a_3 - 2a_5 - \frac{1}{2}a_7 + \frac{1}{2}a_9 \right] X_u^{(B_u^- K^-, \eta^{(\prime)})} \right. \\
& + [a_3 - a_5 - a_7 + a_9] X_c^{(B_u^- K^-, \eta^{(\prime)})} + \left[a_3 + a_4 - a_5 + \frac{1}{2}(a_7 - a_9 - a_{10}) \right. \\
& + (2a_6 - a_8) \frac{m_{\eta^{(\prime)}}^2}{2m_s(m_b - m_s)} \left. \left(1 - \frac{f_{\eta^{(\prime)}}^u}{f_{\eta^{(\prime)}}^s} \right) \right] X_s^{(B_u^- K^-, \eta^{(\prime)})} \\
& + \left[a_4 + a_{10} + 2(a_6 + a_8) \frac{m_{K^-}^2}{(m_s + m_u)(m_b - m_u)} \right] X^{(B_u^- \eta^{(\prime)}, K^-)} \\
& \left. + \left[a_4 + a_{10} + 2(a_6 + a_8) \frac{m_{B_u^-}^2}{(m_s - m_u)(m_b + m_u)} \right] X^{(B_u^-, K^-, \eta^{(\prime)})} \right\}, \quad (C3)
\end{aligned}$$

$$\begin{aligned}
A(B_u^- \rightarrow K^- K^0) &= \left\{ V_{ub} V_{ud}^* a_1 - V_{tb} V_{td}^* \left[a_4 + a_{10} + 2(a_6 + a_8) \frac{m_{B_u^-}^2}{(m_d - m_u)(m_b + m_u)} \right] \right\} X^{(B_u^-, K^-, K^0)} \\
& - V_{tb} V_{td}^* \left[a_4 - \frac{1}{2}a_{10} + (2a_6 - a_8) \frac{m_{K^0}^2}{(m_d + m_s)(m_b - m_s)} \right] X^{(B_u^- K^-, K^0)}, \quad (C4)
\end{aligned}$$

$$\begin{aligned}
A(B_u^- \rightarrow \pi^- \pi^0) &= V_{ub} V_{ud}^* \left[a_1 X^{(B_u^- \pi^0, \pi^-)} + a_2 X_u^{(B_u^- \pi^-, \pi^0)} \right] \\
& - V_{tb} V_{td}^* \left\{ \frac{3}{2} \left[-a_7 + a_9 + a_{10} + 2a_8 \frac{m_{\pi^0}^2}{(m_d + m_d)(m_b - m_d)} \right] X^{(B_u^- \pi^-, \pi^0)} \right\}, \quad (C5)
\end{aligned}$$

$$\begin{aligned}
A(B_u^- \rightarrow \pi^- \eta^{(\prime)}) &= V_{ub} V_{ud}^* \left[a_1 (X_u^{(B_u^- \eta^{(\prime)}, \pi^-)} + 2X^{(B_u^-, \pi^-, \eta^{(\prime)})}) + a_2 X_u^{(B_u^- \pi^-, \eta^{(\prime)})} \right] \\
& + V_{cb} V_{cd}^* a_2 X_c^{(B_u^- \pi^-, \eta^{(\prime)})} - V_{tb} V_{td}^* \left\{ \left[2a_3 + a_4 - 2a_5 + \frac{1}{2}(-a_7 + a_9 - a_{10}) \right. \right. \\
& + (2a_6 - a_8) \frac{m_{\eta^{(\prime)}}^2}{2m_s(m_b - m_d)} \left. \left(\frac{f_{\eta^{(\prime)}}^s}{f_{\eta^{(\prime)}}^u} - 1 \right) r_{\eta^{(\prime)}} \right] X_u^{(B_u^- \pi^-, \eta^{(\prime)})} \\
& + \left[a_3 - a_5 + \frac{1}{2}(a_7 - a_9) \right] X_s^{(B_u^- \pi^-, \eta^{(\prime)})} + [a_3 - a_5 - a_7 + a_9] X_c^{(B_u^- \pi^-, \eta^{(\prime)})} \\
& + \left[a_4 + a_{10} + 2(a_6 + a_8) \frac{m_{\pi^-}^2}{(m_u + m_d)(m_b - m_u)} \right] X_u^{(B_u^- \eta^{(\prime)}, \pi^-)} \\
& \left. + \left[a_4 + a_{10} - 2(a_6 + a_8) \frac{m_{B_u^-}^2}{(m_b + m_u)(m_d - m_u)} \right] X^{(B_u^-, \eta^{(\prime)} \pi^-)} \right\}. \quad (C6)
\end{aligned}$$

D. $\bar{B}_d^0 \rightarrow VP$ DECAYS

$$\begin{aligned}
A(\bar{B}_d^0 \rightarrow \bar{K}^0 \rho^0) &= V_{ub}V_{us}^* a_2 X_u^{(\bar{B}_d^0 \bar{K}^0, \rho^0)} - V_{tb}V_{ts}^* \left\{ \frac{3}{2}(a_7 + a_9) X_u^{(\bar{B}_d^0 \bar{K}^0, \rho^0)} \right. \\
&\quad + \left[a_4 - \frac{1}{2}a_{10} - (2a_6 - a_8) \frac{m_{\bar{K}^0}^2}{(m_s + m_d)(m_b + m_d)} \right] X^{(\bar{B}_d^0 \rho^0, \bar{K}^0)} \\
&\quad \left. + \left[a_4 - \frac{1}{2}a_{10} - (2a_6 - a_8) \frac{m_{\bar{B}_d^0}^2}{(m_s + m_d)(m_b + m_d)} \right] X^{(\bar{B}_d^0, \bar{K}^0 \rho^0)} \right\}, \quad (D1)
\end{aligned}$$

$$\begin{aligned}
A(\bar{B}_d^0 \rightarrow K^- \rho^+) &= V_{ub}V_{us}^* a_1 X^{(\bar{B}_d^0 \rho^+, K^-)} \\
&\quad - V_{tb}V_{ts}^* \left\{ \left[a_4 - \frac{1}{2}a_{10} - (2a_6 - a_8) \frac{m_{\bar{B}_d^0}^2}{(m_s + m_d)(m_b + m_d)} \right] X^{(\bar{B}_d^0, K^- \rho^+)} \right. \\
&\quad \left. + \left[a_4 + a_{10} - 2(a_6 + a_8) \frac{m_{K^-}^2}{(m_s + m_u)(m_b + m_u)} \right] X^{(\bar{B}_d^0 \rho^+, K^-)} \right\}, \quad (D2)
\end{aligned}$$

$$\begin{aligned}
A(\bar{B}_d^0 \rightarrow K^{*-} \pi^+) &= V_{ub}V_{us}^* a_1 X^{(\bar{B}_d^0 \pi^+, K^{*-})} - V_{tb}V_{ts}^* \left\{ [a_4 + a_{10}] X^{(\bar{B}_d^0 \pi^+, K^{*-})} \right. \\
&\quad \left. + \left[a_4 - \frac{1}{2}a_{10} - (2a_6 - a_8) \frac{m_{\bar{B}_d^0}^2}{(m_s + m_d)(m_b + m_d)} \right] X^{(\bar{B}_d^0, K^{*-} \pi^+)} \right\}, \quad (D3)
\end{aligned}$$

$$\begin{aligned}
A(\bar{B}_d^0 \rightarrow \bar{K}^{*0} \pi^0) &= V_{ub}V_{us}^* a_2 X^{(\bar{B}_d^0 K^{*0}, \pi^0)} - V_{tb}V_{ts}^* \left\{ \left[-\frac{3}{2}a_7 + \frac{3}{2}a_9 \right] X^{(\bar{B}_d^0 K^{*0}, \pi^0)} \right. \\
&\quad + \left[a_4 - \frac{1}{2}a_{10} - (2a_6 - a_8) \frac{m_{\bar{B}_d^0}^2}{(m_s + m_d)(m_b + m_d)} \right] X^{(\bar{B}_d^0, K^{*0} \pi^0)} \\
&\quad \left. + (a_4 - \frac{1}{2}a_{10}) X^{(\bar{B}_d^0 \pi^0, K^{*0})} \right\}, \quad (D4)
\end{aligned}$$

$$\begin{aligned}
A(\bar{B}_d^0 \rightarrow \bar{K}^0 \phi) &= -V_{tb}V_{ts}^* \left\{ \left[a_3 + a_4 + a_5 - \frac{1}{2}(a_7 + a_9 + a_{10}) \right] X^{(\bar{B}_d^0 \bar{K}^0, \phi)} \right. \\
&\quad \left. + \left[a_4 - \frac{1}{2}a_{10} - (2a_6 - a_8) \frac{m_{\bar{B}_d^0}^2}{(m_s + m_d)(m_b + m_d)} \right] X^{(\bar{B}_d^0, \bar{K}^0 \phi)} \right\}, \quad (D5)
\end{aligned}$$

$$\begin{aligned}
A(\bar{B}_d^0 \rightarrow \bar{K}^{*0} \eta^{(\prime)}) &= V_{ub}V_{us}^* a_2 X^{(\bar{B}_d^0 \bar{K}^{*0}, \eta^{(\prime)})} + V_{cb}V_{cs}^* a_2 X_c^{(\bar{B}_d^0 \bar{K}^{*0}, \eta^{(\prime)})} \\
&\quad - V_{tb}V_{ts}^* \left\{ \left[2(a_3 - a_5) - \frac{1}{2}(a_7 - a_9) \right] X_u^{(\bar{B}_d^0 \bar{K}^{*0}, \eta^{(\prime)})} \right. \\
&\quad \left. + \left[a_3 + a_4 - a_5 - \frac{1}{2}(-a_7 + a_9 + a_{10}) \right] \right\}
\end{aligned}$$

$$\begin{aligned}
& -(2a_6 - a_8) \frac{m_{\eta'}^2}{2m_s(m_b + m_s)} \left(1 - \frac{f_{\eta'}^u}{f_{\eta'}^s}\right) \left] X_s^{\overline{B}_d^0 \overline{K}^{*0}, \eta'} \right. \\
& + [a_3 - a_5 - a_7 + a_9] X_c^{\overline{B}_d^0 \overline{K}^{*0}, \eta'} + \left[a_4 - \frac{1}{2} a_{10} \right] X^{\overline{B}_d^0 \eta', \overline{K}^{*0}} \\
& \left. + \left[a_4 - a_{10} - (2a_6 - a_8) \frac{m_{\overline{B}_d^0}^2}{(m_s + m_d)(m_b + m_d)} \right] X^{\overline{B}_d^0, \overline{K}^{*0} \eta'} \right\}, \quad (D6)
\end{aligned}$$

$$\begin{aligned}
A(\overline{B}_d^0 \rightarrow \overline{K}^0 \omega) &= V_{ub} V_{us}^* a_2 X_u^{\overline{B}_d^0 \overline{K}^0, \omega} - V_{tb} V_{ts}^* \left\{ \left[2a_3 + 2a_5 + \frac{1}{2}(a_7 + a_9) \right] X_u^{\overline{B}_d^0 \overline{K}^0, \omega} \right. \\
& + \left[a_4 - \frac{1}{2} a_{10} - (2a_6 - a_8) \frac{m_K^2}{(m_s + m_d)(m_b + m_d)} \right] X^{\overline{B}_d^0 \omega, \overline{K}^0} \\
& \left. + \left[a_4 - \frac{1}{2} a_{10} - (2a_6 - a_8) \frac{m_{\overline{B}_d^0}^2}{(m_s + m_d)(m_b + m_d)} \right] X^{\overline{B}_d^0, \overline{K}^0 \omega} \right\}, \quad (D7)
\end{aligned}$$

$$\begin{aligned}
A(\overline{B}_d^0 \rightarrow \rho^- \pi^+) &= V_{ub} V_{ud}^* \left\{ a_1 X^{\overline{B}_d^0 \pi^+, \rho^-} + a_2 X^{\overline{B}_d^0, \rho^- \pi^+} \right\} - V_{tb} V_{td}^* \left\{ (a_4 + a_{10}) X^{\overline{B}_d^0 \pi^+, \rho^-} \right. \\
& + \left[2a_3 + a_4 - 2a_5 + \frac{1}{2}(-a_7 + a_9 - a_{10}) \right. \\
& \left. \left. - (2a_6 - a_8) \frac{m_{\overline{B}_d^0}^2}{2m_d(m_b + m_d)} \right] X^{\overline{B}_d^0, \rho^- \pi^+} \right\}, \quad (D8)
\end{aligned}$$

$$\begin{aligned}
A(\overline{B}_d^0 \rightarrow \rho^+ \pi^-) &= V_{ub} V_{ud}^* \left\{ a_1 X^{\overline{B}_d^0 \rho^+, \pi^-} + a_2 X^{\overline{B}_d^0, \rho^+ \pi^-} \right\} - V_{tb} V_{td}^* \left\{ \left[2a_3 + a_4 - 2a_5 \right. \right. \\
& - \frac{1}{2}(a_7 - a_9 + a_{10}) - (2a_6 - a_8) \frac{m_{\overline{B}_d^0}^2}{2m_d(m_b + m_d)} \left. \right] X^{\overline{B}_d^0, \rho^+ \pi^-} \\
& \left. + \left[a_4 + a_{10} - 2(a_6 + a_8) \frac{m_{\pi^-}^2}{(m_u + m_d)(m_b + m_u)} \right] X^{\overline{B}_d^0 \rho^+, \pi^-} \right\}, \quad (D9)
\end{aligned}$$

$$\begin{aligned}
A(\overline{B}_d^0 \rightarrow K^{*0} \overline{K}^0) &= -V_{tb} V_{td}^* \left\{ \left[a_4 - \frac{1}{2} a_{10} \right] X^{\overline{B}_d^0 \overline{K}^0, \overline{K}^{*0}} + \left[a_3 + a_4 + a_5 - \frac{1}{2}(a_7 + a_9 + a_{10}) \right. \right. \\
& \left. \left. - (2a_6 - a_8) \frac{m_{\overline{B}_d^0}^2}{2m_d(m_b + m_d)} \right] X^{\overline{B}_d^0, \overline{K}^0 \overline{K}^{*0}} \right\}, \quad (D10)
\end{aligned}$$

$$\begin{aligned}
A(\overline{B}_d^0 \rightarrow \overline{K}^{*0} K^0) &= -V_{tb} V_{td}^* \left\{ \left[a_4 - \frac{1}{2} a_{10} - (2a_6 - a_8) \frac{m_{\overline{K}^0}^2}{(m_s + m_d)(m_b + m_s)} \right] X^{\overline{B}_d^0 \overline{K}^{*0}, K^0} \right. \\
& + \left[a_3 + a_4 + a_5 - \frac{1}{2}(a_7 + a_9 + a_{10}) \right. \\
& \left. \left. - (2a_6 - a_8) \frac{m_{\overline{B}_d^0}^2}{2m_d(m_b + m_d)} \right] X^{\overline{B}_d^0, \overline{K}^{*0} K^0} \right\}, \quad (D11)
\end{aligned}$$

$$\begin{aligned}
A(\overline{B}_d^0 \rightarrow K^{*-} K^+) &= -V_{tb} V_{td}^* \left\{ \left[a_3 - a_5 - a_7 + a_9 + 2(a_6 + a_8) \frac{m_{\overline{B}_d^0}^2}{2m_u(m_b + m_d)} \right] X(\overline{B}_d^0, K^+ K^{*-}) \right. \\
&\quad \left. + \left[a_3 - a_5 - \frac{1}{2}(a_7 + a_9) + (2a_6 - a_8) \frac{m_{\overline{B}_d^0}^2}{2m_s(m_b + m_d)} \right] X_s(\overline{B}_d^0, K^+ K^{*-}) \right\} \\
&\quad + V_{ub} V_{ud}^* a_2 X(\overline{B}_d^0, K^+ K^{*-}), \tag{D12}
\end{aligned}$$

$$\begin{aligned}
A(\overline{B}_d^0 \rightarrow K^- K^{*+}) &= -V_{tb} V_{td}^* \left\{ \left[a_3 - a_5 - a_7 + a_9 + 2(a_6 + a_8) \frac{m_{\overline{B}_d^0}^2}{2m_u(m_b + m_d)} \right] X(\overline{B}_d^0, K^- K^{*+}) \right. \\
&\quad \left. + \left[a_3 - a_5 - \frac{1}{2}(a_7 + a_9) + (2a_6 - a_8) \frac{m_{\overline{B}_d^0}^2}{2m_s(m_b + m_d)} \right] X_s(\overline{B}_d^0, K^- K^{*+}) \right\} \\
&\quad + V_{ub} V_{ud}^* a_2 X(\overline{B}_d^0, K^- K^{*+}), \tag{D13}
\end{aligned}$$

$$\begin{aligned}
A(\overline{B}_d^0 \rightarrow \phi \eta^{(\prime)}) &= -V_{tb} V_{td}^* \left\{ \left[a_3 + a_5 - \frac{1}{2}(a_7 + a_9) \right] X(\overline{B}_d^0, \eta^{(\prime)}, \phi) \right. \\
&\quad \left. + \left[a_3 - a_5 + \frac{1}{2}(a_7 - a_9) \right] X_s(\overline{B}_d^0, \phi \eta^{(\prime)}) \right\}, \tag{D14}
\end{aligned}$$

$$A(\overline{B}_d^0 \rightarrow \phi \pi^0) = V_{tb} V_{td}^* \left\{ a_3 + a_5 - \frac{1}{2}(a_7 + a_9) \right\} X(\overline{B}_d^0, \pi^0, \phi), \tag{D15}$$

$$\begin{aligned}
A(\overline{B}_d^0 \rightarrow \rho^0 \pi^0) &= V_{ub} V_{ud}^* a_2 \left\{ X(\overline{B}_d^0, \rho^0 \pi^0) + X_u(\overline{B}_d^0, \rho^0, \pi^0) + X_u(\overline{B}_d^0, \pi^0, \rho^0) \right\} \\
&\quad - V_{tb} V_{td}^* \left\{ \left[2a_3 + a_4 - 2a_5 - \frac{1}{2}(a_7 - a_9 + a_{10}) \right. \right. \\
&\quad \left. \left. - (2a_6 - a_8) \frac{m_{\overline{B}_d^0}^2}{2m_d(m_b + m_d)} \right] X(\overline{B}_d^0, \rho^0 \pi^0) \right. \\
&\quad \left. + \left[-a_4 + (2a_6 - a_8) \frac{m_{\pi^0}^2}{2m_d(m_b + m_d)} - \frac{3}{2}a_7 + \frac{3}{2}a_9 + \frac{1}{2}a_{10} \right] X_u(\overline{B}_d^0, \rho^0, \pi^0) \right. \\
&\quad \left. + \left[-a_4 + \frac{3}{2}a_7 + \frac{3}{2}a_9 + \frac{1}{2}a_{10} \right] X_u(\overline{B}_d^0, \pi^0, \rho^0) \right\}, \tag{D16}
\end{aligned}$$

$$\begin{aligned}
A(\overline{B}_d^0 \rightarrow \rho^0 \eta^{(\prime)}) &= V_{ub} V_{ud}^* a_2 \left\{ X(\overline{B}_d^0, \rho^0 \eta^{(\prime)}) + X_u(\overline{B}_d^0, \rho^0, \eta^{(\prime)}) + X_u(\overline{B}_d^0, \eta^{(\prime)}, \rho^0) \right\} + V_{cb} V_{cd}^* a_2 X_c(\overline{B}_d^0, \rho^0, \eta^{(\prime)}) \\
&\quad - V_{tb} V_{td}^* \left\{ \left[2a_3 + a_4 - 2a_5 - \frac{1}{2}(a_7 - a_9 + a_{10}) \right. \right. \\
&\quad \left. \left. - (2a_6 - a_8) \frac{m_{\overline{B}_d^0}^2}{2m_d(m_b + m_d)} \right] X(\overline{B}_d^0, \rho^0 \eta^{(\prime)}) \right.
\end{aligned}$$

$$\begin{aligned}
& + \left[2a_3 + a_4 - 2a_5 - (2a_6 - a_8) \frac{m_{\eta^{(\prime)}}^2}{2m_s(m_b + m_d)} \left(\frac{f_{\eta^{(\prime)}}^s}{f_{\eta^{(\prime)}}^u} - 1 \right) r_{\eta^{(\prime)}} \right. \\
& - \frac{1}{2}(a_7 - a_9 + a_{10}) \left. \right] X_u^{(\overline{B}_d^0 \rho^0, \eta^{(\prime)})} + \left[-a_4 + \frac{1}{2}a_{10} + \frac{3}{2}(a_7 + a_9) \right] X_u^{(\overline{B}_d^0 \eta^{(\prime)}, \rho^0)} \\
& + \left[a_3 - a_5 + \frac{1}{2}a_7 - \frac{1}{2}a_9 \right] X_s^{(\overline{B}_d^0 \rho^0, \eta^{(\prime)})} + [a_3 - a_5 - a_7 + a_9] X_c^{(\overline{B}_d^0 \rho^0, \eta^{(\prime)})} \left. \right\}, \tag{D17}
\end{aligned}$$

$$\begin{aligned}
A(\overline{B}_d^0 \rightarrow \omega \pi^0) & = V_{ub} V_{ud}^* a_2 \left\{ X^{(\overline{B}_d^0, \omega \pi^0)} + X_u^{(\overline{B}_d^0 \omega, \pi^0)} + X_u^{(\overline{B}_d^0 \pi^0, \omega)} \right\} \\
& - V_{tb} V_{td}^* \left\{ \left[2a_3 + a_4 - 2a_5 - \frac{1}{2}(a_7 - a_9 + a_{10}) \right. \right. \\
& \left. \left. - (2a_6 - a_8) \frac{m_{\overline{B}_d^0}^2}{2m_d(m_b + m_d)} \right] X^{(\overline{B}_d^0, \omega \pi^0)} \right. \\
& + \left[a_4 - \frac{3}{2}a_7 + \frac{3}{2}a_9 - \frac{1}{2}a_{10} - (2a_6 - a_8) \frac{m_{\pi^0}^2}{2m_d(m_b + m_d)} \right] X_d^{(\overline{B}_d^0 \omega, \pi^0)} \\
& \left. + \left[2a_3 + a_4 + 2a_5 + \frac{1}{2}(a_7 + a_9 - a_{10}) \right] X_u^{(\overline{B}_d^0 \pi^0, \omega)} \right\}, \tag{D18}
\end{aligned}$$

$$\begin{aligned}
A(\overline{B}_d^0 \rightarrow \omega \eta^{(\prime)}) & = V_{ub} V_{ud}^* a_2 \left\{ X^{(\overline{B}_d^0, \omega \eta^{(\prime)})} + X_u^{(\overline{B}_d^0 \omega, \eta^{(\prime)})} + X_u^{(\overline{B}_d^0 \eta^{(\prime)}, \omega)} \right\} + V_{cb} V_{cd}^* a_2 X_c^{(\overline{B}_d^0 \omega, \eta^{(\prime)})} \\
& - V_{tb} V_{td}^* \left\{ 2 \left[2a_3 + a_4 - 2a_5 - (2a_6 - a_8) \frac{m_{\overline{B}_d^0}^2}{2m_d(m_b + m_d)} \right. \right. \\
& + \frac{1}{2}(-a_7 + a_9 - a_{10}) \left. \right] X_u^{(\overline{B}_d^0 \omega, \eta^{(\prime)})} + \left[2a_3 + a_4 - 2a_5 + \frac{1}{2}(-a_7 + a_9 - a_{10}) \right. \\
& - (2a_6 - a_8) \frac{m_{\eta^{(\prime)}}^2}{2m_d(m_b + m_d)} \left. \left(\frac{f_{\eta^{(\prime)}}^s}{f_{\eta^{(\prime)}}^u} - 1 \right) r_{\eta^{(\prime)}} \right] X_u^{(\overline{B}_d^0 \omega, \eta^{(\prime)})} \\
& + \left[a_3 - a_5 + \frac{1}{2}(a_7 - a_9) \right] X_s^{(\overline{B}_d^0 \omega, \eta^{(\prime)})} + [a_3 - a_5 - a_7 + a_9] X_c^{(\overline{B}_d^0 \omega, \eta^{(\prime)})} \\
& \left. + \left[2a_3 + a_4 + 2a_5 + \frac{1}{2}(a_7 + a_9 - a_{10}) \right] X_u^{(\overline{B}_d^0 \eta^{(\prime)}, \omega)} \right\}. \tag{D19}
\end{aligned}$$

E. $B_u^- \rightarrow VP$ DECAYS

$$\begin{aligned}
A(B_u^- \rightarrow K^- \rho^0) & = V_{ub} V_{us}^* \left\{ a_1 X^{(B_u^- \rho^0, K^-)} + a_1 X^{(B_u^-, \rho^0 K^-)} + a_2 X_u^{(B_u^- K^-, \rho^0)} \right\} \\
& - V_{tb} V_{ts}^* \left\{ \frac{3}{2} [a_7 + a_9] X_u^{(B_u^- K^-, \rho^0)} \right. \\
& + \left[a_4 + a_{10} - 2(a_6 + a_8) \frac{m_{K^-}^2}{(m_s + m_u)(m_b + m_u)} \right] X^{(B_u^- \rho^0, K^-)} \\
& \left. + \left[a_4 + a_{10} - 2(a_6 + a_8) \frac{m_{B_u^-}^2}{(m_s + m_u)(m_b + m_u)} \right] X^{(B_u^-, \rho^0 K^-)} \right\}, \tag{E1}
\end{aligned}$$

$$\begin{aligned}
A(B_u^- \rightarrow K^{*-} \pi^0) &= V_{ub} V_{us}^* \left\{ a_1 X^{(B_u^- \pi^0, K^{*-})} + a_1 X^{(B_u^-, \pi^0 K^{*-})} + a_2 X^{(B_u^- K^{*-}, \pi^0)} \right\} \\
&\quad - V_{tb} V_{ts}^* \left\{ \left[-\frac{3}{2} a_7 + \frac{3}{2} a_9 \right] X_u^{(B_u^- K^{*-}, \pi^0)} + (a_4 + a_{10}) X^{(B_u^- \pi^0, K^{*-})} \right. \\
&\quad \left. + \left[a_4 + a_{10} - 2(a_6 + a_8) \frac{m_{B_u^-}^2}{(m_s + m_u)(m_b + m_u)} \right] X^{(B_u^-, \pi^0 K^{*-})} \right\}, \quad (\text{E2})
\end{aligned}$$

$$\begin{aligned}
A(B_u^- \rightarrow \bar{K}^0 \rho^-) &= V_{ub} V_{us}^* a_1 X^{(B_u^-, K^0 \rho^-)} \\
&\quad - V_{tb} V_{ts}^* \left\{ \left[a_4 - \frac{1}{2} a_{10} - (2a_6 - a_8) \frac{m_{K^0}^2}{(m_s + m_d)(m_b + m_d)} \right] X^{(B_u^- \rho^-, K^0)} \right. \\
&\quad \left. + \left[a_4 + a_{10} - 2(a_6 + a_8) \frac{m_{B_u^-}^2}{(m_s + m_u)(m_b + m_u)} \right] X^{(B_u^-, \rho^- K^0)} \right\}, \quad (\text{E3})
\end{aligned}$$

$$\begin{aligned}
A(B_u^- \rightarrow \bar{K}^{*0} \pi^-) &= V_{ub} V_{us}^* a_1 X^{(B_u^-, K^{*0} \pi^-)} - V_{tb} V_{ts}^* \left\{ \left[a_4 - \frac{1}{2} a_{10} \right] X^{(B_u^- \pi^-, K^{*0})} \right. \\
&\quad \left. + \left[a_4 + a_{10} - 2(a_6 + a_8) \frac{m_{B_u^-}^2}{(m_s + m_u)(m_b + m_u)} \right] X^{(B_u^-, \pi^- K^{*0})} \right\}, \quad (\text{E4})
\end{aligned}$$

$$\begin{aligned}
A(B_u^- \rightarrow K^- \omega) &= V_{ub} V_{us}^* \left\{ a_1 X^{(B_u^- \omega, K^-)} + a_1 X^{(B_u^-, \omega K^-)} + a_2 X_u^{(B_u^- K^-, \omega)} \right\} \\
&\quad - V_{tb} V_{ts}^* \left\{ \left[2a_3 + 2a_5 + \frac{1}{2} a_7 + \frac{1}{2} a_9 \right] X_u^{(B_u^- K^-, \omega)} \right. \\
&\quad + \left[a_4 + a_{10} - 2(a_6 + a_8) \frac{m_{K^-}^2}{(m_s + m_u)(m_b + m_u)} \right] X^{(B_u^- \omega, K^-)} \\
&\quad \left. + \left[a_4 + a_{10} - 2(a_6 + a_8) \frac{m_{B_u^-}^2}{(m_s + m_u)(m_b + m_u)} \right] X^{(B_u^-, \omega K^-)} \right\}, \quad (\text{E5})
\end{aligned}$$

$$\begin{aligned}
A(B_u^- \rightarrow K^- \phi) &= V_{ub} V_{us}^* a_1 X^{(B_u^-, \phi K^-)} \\
&\quad - V_{tb} V_{ts}^* \left\{ \left[a_4 + a_{10} - 2(a_6 + a_8) \frac{m_{B_u^-}^2}{(m_s + m_u)(m_b + m_u)} \right] X^{(B_u^-, \phi K^-)} \right. \\
&\quad \left. + \left[a_3 + a_4 + a_5 - \frac{1}{2} (a_7 + a_9 + a_{10}) \right] X^{(B_u^- K^-, \phi)} \right\}, \quad (\text{E6})
\end{aligned}$$

$$\begin{aligned}
A(B_u^- \rightarrow K^{*-} \eta^{(\prime)}) &= V_{ub} V_{us}^* \left[a_1 X^{(B_u^- \eta^{(\prime)}, K^{*-})} + a_2 X_u^{(B_u^- K^{*-}, \eta^{(\prime)})} \right. \\
&\quad \left. + a_1 X_u^{(B_u^-, K^{*-} \eta^{(\prime)})} + a_1 X_s^{(B_u^-, K^{*-} \eta^{(\prime)})} \right] + V_{cb} V_{cs}^* a_2 X_c^{(B_u^- K^{*-}, \eta^{(\prime)})} \\
&\quad - V_{tb} V_{ts}^* \left\{ \left[2a_3 - 2a_5 - \frac{1}{2} a_7 + \frac{1}{2} a_9 \right] X_u^{(B_u^- K^{*-}, \eta^{(\prime)})} \right\}
\end{aligned}$$

$$\begin{aligned}
& + (a_3 - a_5 - a_7 + a_9)X_c^{(B_u^- K^{*-}, \eta^{(\prime)})} + \left[a_3 + a_4 - a_5 + \frac{1}{2}(a_7 - a_9 - a_{10}) \right. \\
& - (2a_6 - a_8) \frac{m_{\eta^{(\prime)}}^2}{2m_s(m_b + m_s)} \left(1 - \frac{f_{\eta^{(\prime)}}^u}{f_{\eta^{(\prime)}}^s} \right) \left. \right] X_s^{(B_u^- K^{*-}, \eta^{(\prime)})} + (a_4 + a_{10})X^{(B_u^- \eta^{(\prime)}, K^{*-})} \\
& + \left[a_4 + a_{10} - 2(a_6 + a_8) \frac{m_{B_u^-}^2}{(m_s + m_u)(m_b + m_u)} \right] X^{(B_u^-, K^{*-} \eta^{(\prime)})} \left. \right\}, \quad (E7)
\end{aligned}$$

$$\begin{aligned}
A(B_u^- \rightarrow \rho^- \pi^0) & = V_{ub}V_{ud}^* \left\{ a_1 X^{(B_u^- \pi^0, \rho^-)} + a_1 X^{(B_u^-, \pi^0 \rho^-)} + a_2 X_u^{(B_u^- \rho^-, \pi^0)} \right\} \\
& - V_{tb}V_{td}^* \left\{ \left[a_4 + \frac{3}{2}a_7 - \frac{3}{2}a_9 - \frac{1}{2}a_{10} - (2a_6 - a_8) \frac{m_{\pi^0}^2}{2m_d(m_b + m_d)} \right] X_d^{(B_u^- \rho^-, \pi^0)} \right. \\
& + [a_4 + a_{10}] X^{(B_u^- \pi^0, \rho^-)} \\
& + \left. \left[a_4 + a_{10} - 2(a_6 + a_8) \frac{m_{B_u^-}^2}{(m_u + m_d)(m_b + m_u)} \right] X^{(B_u^-, \pi^0 \rho^-)} \right\}, \quad (E8)
\end{aligned}$$

$$\begin{aligned}
A(B_u^- \rightarrow \rho^0 \pi^-) & = V_{ub}V_{ud}^* \left\{ a_1 X^{(B_u^- \rho^0, \pi^-)} + a_1 X^{(B_u^-, \pi^- \rho^0)} + a_2 X_u^{(B_u^- \pi^-, \rho^0)} \right\} \\
& - V_{tb}V_{td}^* \left\{ \left[-a_4 + \frac{3}{2}a_7 + \frac{3}{2}a_9 + \frac{1}{2}a_{10} \right] X_u^{(B_u^- \pi^-, \rho^0)} \right. \\
& + \left[a_4 + a_{10} - 2(a_6 + a_8) \frac{m_{\pi^-}^2}{(m_d + m_u)(m_b + m_u)} \right] X^{(B_u^- \rho^0, \pi^-)} \\
& + \left. \left[a_4 + a_{10} - 2(a_6 + a_8) \frac{m_{B_u^-}^2}{(m_u + m_d)(m_b + m_u)} \right] X^{(B_u^-, \pi^- \rho^0)} \right\}, \quad (E9)
\end{aligned}$$

$$\begin{aligned}
A(B_u^- \rightarrow \pi^- \omega) & = V_{ub}V_{ud}^* \left\{ a_1 X^{(B_u^- \omega, \pi^-)} + a_1 X^{(B_u^-, \pi^- \omega)} + a_2 X^{(B_u^- \pi^-, \omega)} \right\} \\
& - V_{tb}V_{td}^* \left\{ \left[2a_3 + a_4 + 2a_5 + \frac{1}{2}(a_7 + a_9 - a_{10}) \right] X_u^{(B_u^- \pi^-, \omega)} \right. \\
& + \left[a_4 + a_{10} - 2(a_6 + a_8) \frac{m_{\pi^-}^2}{(m_d + m_u)(m_b + m_u)} \right] X_u^{(B_u^- \omega, \pi^-)} \\
& + \left. \left[a_4 + a_{10} - 2(a_6 + a_8) \frac{m_{B_u^-}^2}{(m_u + m_d)(m_b + m_u)} \right] X^{(B_u^-, \pi^- \omega)} \right\}, \quad (E10)
\end{aligned}$$

$$\begin{aligned}
A(B_u^- \rightarrow \rho^- \eta^{(\prime)}) & = V_{ub}V_{ud}^* \left[a_1 (X_u^{(B_u^- \eta^{(\prime)}, \rho^-)} + X^{(B_u^-, \rho^- \eta^{(\prime)})}) + a_2 X_u^{(B_u^- \rho^-, \eta^{(\prime)})} \right] \\
& + V_{cb}V_{cd}^* a_2 X_c^{(B_u^- \rho^-, \eta^{(\prime)})} - V_{tb}V_{td}^* \left\{ \left[2a_3 + a_4 - 2a_5 + \frac{1}{2}(-a_7 + a_9 - a_{10}) \right. \right. \\
& \left. \left. - (2a_6 - a_8) \frac{m_{\eta^{(\prime)}}^2}{2m_s(m_b + m_d)} \left(\frac{f_{\eta^{(\prime)}}^s}{f_{\eta^{(\prime)}}^u} - 1 \right) r_{\eta^{(\prime)}} \right] X_u^{(B_u^- \rho^-, \eta^{(\prime)})} \right\}
\end{aligned}$$

$$\begin{aligned}
& + \left[2a_3 + a_4 - 2a_5 - \frac{1}{2}(a_7 - a_9) \right] X_s^{(B_u^- \rho^-, \eta^{(\prime)})} \\
& + [a_3 - a_5 - a_7 + a_9] X_c^{(B_u^- \rho^-, \eta^{(\prime)})} + (a_4 + a_{10}) X_u^{(B_u^- \eta^{(\prime)}, \rho^-)} \\
& + \left[a_4 + a_{10} - 2(a_6 + a_8) \frac{m_{B_u^-}^2}{(m_b + m_u)(m_d + m_u)} \right] X^{(B_u^-, \eta^{(\prime)} \rho^-)} \Big\}, \quad (\text{E11})
\end{aligned}$$

$$A(B_u^- \rightarrow \pi^- \phi) = -V_{tb} V_{td}^* \left\{ a_3 + a_5 - \frac{1}{2}(a_7 + a_9) \right\} X^{(B^- \pi^-, \phi)}, \quad (\text{E12})$$

$$\begin{aligned}
A(B_u^- \rightarrow K^{*-} K^0) &= V_{ub} V_{ud}^* a_1 X^{(B_u^-, K^{*-} K^0)} - V_{tb} V_{td}^* \left\{ \left[a_4 - \frac{1}{2} a_{10} \right. \right. \\
& \quad \left. \left. - (2a_6 - a_8) \frac{m_{K^0}^2}{(m_s + m_d)(m_b + m_s)} \right] X^{(B_u^- K^{*-}, K^0)} \right. \\
& \quad \left. + \left[a_4 + a_{10} - 2(a_6 + a_8) \frac{m_{B_u^-}^2}{(m_u + m_d)(m_b + m_u)} \right] X^{(B_u^-, K^{*-} K^0)} \right\}, \quad (\text{E13})
\end{aligned}$$

$$\begin{aligned}
A(B_u^- \rightarrow K^- K^{*0}) &= V_{ub} V_{ud}^* a_1 X^{(B_u^-, K^- K^{*0})} - V_{tb} V_{td}^* \left\{ \left[a_4 - \frac{1}{2} a_{10} \right] X^{(B_u^- K^-, K^{*0})} \right. \\
& \quad \left. + \left[a_4 + a_{10} - 2(a_6 + a_8) \frac{m_{B_u^-}^2}{(m_u + m_d)(m_b + m_u)} \right] X^{(B_u^-, K^- K^{*0})} \right\}. \quad (\text{E14})
\end{aligned}$$

F. $\bar{B}_d^0 \rightarrow VV$ DECAYS

$$\begin{aligned}
A(\bar{B}_d^0 \rightarrow K^{*-} \rho^+) &= V_{ub} V_{us}^* a_1 X^{(\bar{B}_d^0 \rho^+, K^{*-})} \\
& \quad - V_{tb} V_{ts}^* \left\{ (a_4 + a_{10}) X^{(\bar{B}_d^0 \rho^+, K^{*-})} + (a_4 - \frac{1}{2} a_{10}) X^{(\bar{B}_d^0, K^{*-} \rho^+)} \right. \\
& \quad \left. + (-2a_6 + a_8) \langle K^{*-} \rho^+ | \bar{s}(1 + \gamma_5) d | 0 \rangle \langle 0 | \bar{d}(1 - \gamma_5) b | \bar{B}_d^0 \rangle \right\}, \quad (\text{F1})
\end{aligned}$$

$$\begin{aligned}
A(\bar{B}_d^0 \rightarrow \bar{K}^{*0} \rho^0) &= V_{ub} V_{us}^* a_2 X_u^{(\bar{B}_d^0 \bar{K}^{*0}, \rho^0)} - V_{tb} V_{ts}^* \left\{ \frac{3}{2} (a_7 + a_9) X_u^{(\bar{B}_d^0 \bar{K}^{*0}, \rho^0)} \right. \\
& \quad + (a_4 - \frac{1}{2} a_{10}) X^{(\bar{B}_d^0 \rho^0, \bar{K}^{*0})} + (a_4 - \frac{1}{2} a_{10}) X^{(\bar{B}_d^0, \bar{K}^{*0} \rho^0)} \\
& \quad \left. + (-2a_6 + a_8) \langle \bar{K}^{*0} \rho^0 | \bar{s}(1 + \gamma_5) d | 0 \rangle \langle 0 | \bar{d}(1 - \gamma_5) b | \bar{B}_d^0 \rangle \right\}, \quad (\text{F2})
\end{aligned}$$

$$\begin{aligned}
A(\bar{B}_d^0 \rightarrow \bar{K}^{*0} \omega) &= V_{ub} V_{us}^* a_2 X_u^{(\bar{B}_d^0 \bar{K}^{*0}, \omega)} - V_{tb} V_{ts}^* \left\{ (2a_3 + 2a_5 + \frac{1}{2} a_7 + \frac{1}{2} a_9) X_u^{(\bar{B}_d^0 \bar{K}^{*0}, \omega)} \right. \\
& \quad + (a_4 - \frac{1}{2} a_{10}) X^{(\bar{B}_d^0 \omega, \bar{K}^{*0})} + (a_4 - a_{10}) X^{(\bar{B}_d^0, \bar{K}^{*0} \omega)} \\
& \quad \left. + (-2a_6 + a_8) \langle \bar{K}^{*0} \omega | \bar{s}(1 + \gamma_5) d | 0 \rangle \langle 0 | \bar{d}(1 - \gamma_5) b | \bar{B}_d^0 \rangle \right\}, \quad (\text{F3})
\end{aligned}$$

$$\begin{aligned}
A(\overline{B}_d^0 \rightarrow \overline{K}^{*0} \phi) &= -V_{tb}V_{ts}^* \left\{ [a_3 + a_4 + a_5 - \frac{1}{2}(a_7 + a_9 + a_{10})] X_s^{(\overline{B}_d^0 \overline{K}^{*0} \phi)} \right. \\
&\quad + (a_4 - \frac{1}{2}a_{10}) X^{(\overline{B}_d^0, \overline{K}^{*0} \phi)} \\
&\quad \left. + (-2a_6 + a_8) \langle \overline{K}^{*0} \phi | \bar{s}(1 + \gamma_5) d | 0 \rangle \langle 0 | \bar{d}(1 - \gamma_5) b | \overline{B}_d^0 \rangle \right\}, \tag{F4}
\end{aligned}$$

$$\begin{aligned}
A(\overline{B}_d^0 \rightarrow K^{*0} \overline{K}^{*0}) &= -V_{tb}V_{td}^* \left\{ [a_3 + a_4 + a_5 - \frac{1}{2}(a_7 + a_9 + a_{10})] X_d^{(\overline{B}_d^0, K^{*0} \overline{K}^{*0})} \right. \\
&\quad + [a_3 + a_5 - \frac{1}{2}a_7 - \frac{1}{2}a_9] X_s^{(\overline{B}_d^0, K^{*0} \overline{K}^{*0})} + (a_4 - \frac{1}{2}a_{10}) X^{(\overline{B}_d^0 K^{*0}, \overline{K}^{*0})} \\
&\quad \left. - (2a_6 - a_8) \langle K^{*0} \overline{K}^{*0} | \bar{d}(1 + \gamma_5) d | 0 \rangle \langle 0 | \bar{d}(1 - \gamma_5) b | \overline{B}_d^0 \rangle \right\}, \tag{F5}
\end{aligned}$$

$$\begin{aligned}
A(\overline{B}_d^0 \rightarrow K^{*+} K^{*-}) &= V_{ub}V_{ud}^* a_2 X_u^{(\overline{B}_d^0, K^{*+} K^{*-})} - V_{tb}V_{td}^* \left\{ (a_3 + a_5 + a_7 + a_9) X_u^{(\overline{B}_d^0, K^{*+} K^{*-})} \right. \\
&\quad \left. + (a_3 + a_5 - \frac{1}{2}a_7 - \frac{1}{2}a_9) X_s^{(\overline{B}_d^0, K^{*+} K^{*-})} \right\}, \tag{F6}
\end{aligned}$$

$$\begin{aligned}
A(\overline{B}_d^0 \rightarrow \rho^+ \rho^-) &= V_{ub}V_{ud}^* [a_1 X^{(\overline{B}_d^0 \rho^+, \rho^-)} + a_2 X_u^{(\overline{B}_d^0, \rho^+ \rho^-)}] - V_{tb}V_{td}^* \left\{ (a_4 + a_{10}) X^{(\overline{B}_d^0 \rho^+, \rho^-)} \right. \\
&\quad + [2a_3 + a_4 + \frac{1}{2}(a_9 - a_{10})] X_u^{(\overline{B}_d^0, \rho^+ \rho^-)} + (2a_5 + \frac{1}{2}a_7) \overline{X}_u^{(\overline{B}_d^0, \rho^+ \rho^-)} \\
&\quad \left. + (-2a_6 + a_8) \langle \rho^+ \rho^- | \bar{d}(1 + \gamma_5) d | 0 \rangle \langle 0 | \bar{d}(1 - \gamma_5) b | \overline{B}_d^0 \rangle \right\}, \tag{F7}
\end{aligned}$$

$$\begin{aligned}
A(\overline{B}_d^0 \rightarrow \rho^0 \rho^0) &= V_{ub}V_{ud}^* a_2 2 [X_u^{(\overline{B}_d^0 \rho^0, \rho^0)} + X_u^{(\overline{B}_d^0, \rho^0 \rho^0)}] \\
&\quad - V_{tb}V_{td}^* 2 \left\{ [-a_4 + \frac{1}{2}(3a_7 + 3a_9 + a_{10})] X_u^{(\overline{B}_d^0 \rho^0, \rho^0)} \right. \\
&\quad + [2a_3 + a_4 + \frac{1}{2}(a_9 - a_{10})] X_u^{(\overline{B}_d^0, \rho^0 \rho^0)} + (2a_5 + \frac{1}{2}a_7) \overline{X}_u^{(\overline{B}_d^0, \rho^0 \rho^0)} \\
&\quad \left. + (-2a_6 + a_8) \langle \rho^0 \rho^0 | \bar{d}(1 + \gamma_5) d | 0 \rangle \langle 0 | \bar{d}(1 - \gamma_5) b | \overline{B}_d^0 \rangle \right\}, \tag{F8}
\end{aligned}$$

$$\begin{aligned}
A(\overline{B}_d^0 \rightarrow \rho^0 \omega) &= V_{ub}V_{ud}^* a_2 [X_u^{(\overline{B}_d^0 \rho^0, \omega)} + X_u^{(\overline{B}_d^0 \omega, \rho^0)} + X_u^{(\overline{B}_d^0, \omega \rho^0)}] \\
&\quad - V_{tb}V_{td}^* \left\{ [2a_3 + a_4 + 2a_5 + \frac{1}{2}a_7 + \frac{1}{2}a_9 - \frac{1}{2}a_{10}] X_u^{(\overline{B}_d^0 \rho^0, \omega)} \right. \\
&\quad + [-a_4 + \frac{3}{2}a_7 + \frac{3}{2}a_9 + \frac{1}{2}a_{10}] X_u^{(\overline{B}_d^0 \omega, \rho^0)} + (-a_4 + \frac{3}{2}a_9 + \frac{1}{2}a_{10}) X_u^{(\overline{B}_d^0, \omega \rho^0)} \\
&\quad \left. + \frac{3}{2}a_7 \overline{X}_u^{(\overline{B}_d^0, \omega \rho^0)} + (-2a_6 + a_8) \langle \omega \rho^0 | \bar{d}(1 + \gamma_5) d | 0 \rangle \langle 0 | \bar{d}(1 - \gamma_5) b | \overline{B}_d^0 \rangle \right\}, \tag{F9}
\end{aligned}$$

$$\begin{aligned}
A(\bar{B}_d^0 \rightarrow \omega\omega) = & V_{ub}V_{ud}^* 2a_2 (X_u^{(\bar{B}_d^0, \omega, \omega)} + X_u^{(\bar{B}_d^0, \omega\omega)}) \\
& - V_{tb}V_{td}^* \left\{ (4a_3 + 2a_4 + 4a_5 + a_7 + a_9 - a_{10}) X_u^{(\bar{B}_d^0, \omega, \omega)} \right. \\
& + \left[2a_3 + a_4 + \frac{1}{2}(a_9 - a_{10}) \right] X_u^{(\bar{B}_d^0, \omega\omega)} + (2a_5 + \frac{1}{2}a_7) \bar{X}_u^{(\bar{B}_d^0, \omega\omega)} \\
& \left. + (-2a_6 + a_8) \langle \omega\omega | \bar{d}(1 + \gamma_5) d | 0 \rangle \langle 0 | \bar{d}(1 - \gamma_5) b | \bar{B}^0 \rangle \right\}, \tag{F10}
\end{aligned}$$

$$A(\bar{B}_d^0 \rightarrow \rho^0 \phi) = -V_{tb}V_{td}^* \left[a_3 + a_5 - \frac{1}{2}a_7 - \frac{1}{2}a_9 \right] X_s^{(\bar{B}_d^0, \rho^0, \phi)}, \tag{F11}$$

$$A(\bar{B}_d^0 \rightarrow \omega\phi) = -V_{tb}V_{td}^* \left[a_3 + a_5 - \frac{1}{2}a_7 - \frac{1}{2}a_9 \right] X_s^{(\bar{B}_d^0, \omega, \phi)}, \tag{F12}$$

$$A(\bar{B}_d^0 \rightarrow \phi\phi) = -V_{tb}V_{td}^* \left[a_3 + a_5 - \frac{1}{2}a_7 - \frac{1}{2}a_9 \right] X_s^{(\bar{B}_d^0, \phi\phi)}. \tag{F13}$$

G. $B_u^- \rightarrow VV$ DECAYS

$$\begin{aligned}
A(B_u^- \rightarrow K^{*-} \rho^0) = & V_{ub}V_{us}^* \left[a_1 X^{(B^- \rho^0, K^{*-})} + a_2 X_u^{(B^- K^{*-}, \rho^0)} + a_1 X^{(B^-, \rho^0 K^{*-})} \right] \\
& - V_{tb}V_{ts}^* \left\{ (a_4 + a_{10}) X^{(B^- \rho^0, K^{*-})} + \frac{3}{2}(a_7 + a_9) X_u^{(B^- K^{*-}, \rho^0)} \right. \\
& + (a_4 + a_{10}) X^{(B^-, \rho^0 K^{*-})} \\
& \left. - 2(a_6 + a_8) \langle K^{*-} \rho^0 | \bar{s}(1 + \gamma_5) u | 0 \rangle \langle 0 | \bar{u}(1 - \gamma_5) b | B^- \rangle \right\}, \tag{G1}
\end{aligned}$$

$$\begin{aligned}
A(B_u^- \rightarrow \bar{K}^{*0} \rho^-) = & -V_{tb}V_{ts}^* \left\{ (a_4 - \frac{1}{2}a_{10}) X^{(B^- \rho^-, \bar{K}^{*0})} + (a_4 + a_{10}) X^{(B^-, \rho^- \bar{K}^{*0})} \right. \\
& \left. - 2(a_6 + a_8) \langle \rho^- \bar{K}^{*0} | \bar{s}(1 + \gamma_5) u | 0 \rangle \langle 0 | \bar{u}(1 - \gamma_5) b | B^- \rangle \right\} \\
& + V_{ub}V_{us}^* a_1 X^{(B^-, \rho^- \bar{K}^{*0})}, \tag{G2}
\end{aligned}$$

$$\begin{aligned}
A(B_u^- \rightarrow K^{*-} \omega) = & V_{ub}V_{us}^* \left(a_1 X^{(B^- \omega, K^{*-})} + a_2 X_u^{(B^- K^{*-}, \omega)} + a_1 X^{(B^-, \omega K^{*-})} \right) \\
& - V_{tb}V_{ts}^* \left\{ (a_4 + a_{10}) X^{(B^- \omega, K^{*-})} + \left[2a_3 + 2a_5 + \frac{1}{2}a_7 + \frac{1}{2}a_9 \right] X_u^{(B^- K^{*-}, \omega)} \right. \\
& + (a_4 + a_{10}) X^{(B^-, \omega K^{*-})} \\
& \left. - 2(a_6 + a_8) \langle K^{*-} \omega | \bar{s}(1 + \gamma_5) u | 0 \rangle \langle 0 | \bar{u}(1 - \gamma_5) b | B^- \rangle \right\}, \tag{G3}
\end{aligned}$$

$$\begin{aligned}
A(B_u^- \rightarrow K^{*-} \phi) &= V_{ub} V_{us}^* a_1 X^{(B_u^-, \phi K^{*-})} - V_{tb} V_{ts}^* \left\{ [a_3 + a_4 + a_5 \right. \\
&\quad \left. - \frac{1}{2}(a_7 + a_9 + a_{10})] X_s^{(B^- K^{*-}, \phi)} + (a_4 + a_{10}) X^{(B^-, K^{*-} \phi)} \right. \\
&\quad \left. - 2(a_6 + a_8) \langle K^{*-} \phi | \bar{s}(1 + \gamma_5) u | 0 \rangle \langle 0 | \bar{u}(1 - \gamma_5) b | B^- \rangle \right\}, \tag{G4}
\end{aligned}$$

$$\begin{aligned}
A(B_u^- \rightarrow K^{*-} K^{*0}) &= V_{ub} V_{ud}^* a_1 X^{(B^-, K^{*-} K^{*0})} \\
&\quad - V_{tb} V_{td}^* \left\{ (a_4 - \frac{1}{2} a_{10}) X^{(B^- K^{*-}, K^{*0})} + (a_4 + a_{10}) X^{(B^-, K^{*-} K^{*0})} \right. \\
&\quad \left. - 2(a_6 + a_8) \langle K^{*-} K^{*0} | \bar{d}(1 + \gamma_5) u | 0 \rangle \langle 0 | \bar{u}(1 - \gamma_5) b | B^- \rangle \right\}, \tag{G5}
\end{aligned}$$

$$A(B_u^- \rightarrow \rho^- \phi) = -\sqrt{2} A(\bar{B}_d^0 \rightarrow \rho^0 \phi), \tag{G6}$$

$$\begin{aligned}
A(B_u^- \rightarrow \rho^- \rho^0) &= V_{ub} V_{ud}^* [a_1 X^{(B^- \rho^0, \rho^-)} + a_2 X_u^{(B^- \rho^-, \rho^0)}] \\
&\quad - V_{tb} V_{td}^* \left\{ \frac{3}{2} (a_7 + a_9 + a_{10}) X^{(B^- \rho^0, \rho^-)} + (a_4 + a_{10}) X_u^{(B^-, \rho^0 \rho^-)} \right. \\
&\quad \left. - 2(a_6 + a_8) \langle \rho^0 \rho^- | \bar{d}(1 + \gamma_5) u | 0 \rangle \langle 0 | \bar{u}(1 - \gamma_5) b | B^- \rangle \right\}, \tag{G7}
\end{aligned}$$

$$\begin{aligned}
A(B_u^- \rightarrow \rho^- \omega) &= V_{ub} V_{ud}^* [a_1 X^{(B^- \omega, \rho^-)} + a_2 (X_u^{(B^- \rho^-, \omega)} + X_u^{B^-, \rho^- \omega})] \\
&\quad - V_{tb} V_{td}^* \left\{ (a_4 + a_{10}) X^{(B^- \omega, \rho^-)} \right. \\
&\quad + \left[2a_3 + a_4 + 2a_5 + \frac{1}{2} a_7 + \frac{1}{2} a_9 - \frac{1}{2} a_{10} \right] X_u^{(B^- \rho^-, \omega)} + (a_4 + a_{10}) X_u^{(B^-, \rho^- \omega)} \\
&\quad \left. - 2(a_6 + a_8) \langle \rho^- \omega | \bar{d}(1 + \gamma_5) u | 0 \rangle \langle 0 | \bar{u}(1 - \gamma_5) b | B^- \rangle \right\}. \tag{G8}
\end{aligned}$$

Table V. Relative magnitudes of tree, QCD penguin and electroweak penguin amplitudes for charmless $B_{u,d} \rightarrow PP$ decays shown in first, second and third entries, respectively. Predictions are made for $k^2 = m_b^2/2$, $\eta = 0.370$, $\rho = 0.175$, and $N_c^{\text{eff}}(LR) = 2, 3, 5, \infty$ with $N_c^{\text{eff}}(LL)$ being fixed to be 2 in the first case and treated to be the same as $N_c^{\text{eff}}(LR)$ in the second case. The BSW model is used for heavy-to-light form factors. Results for CP-conjugate modes are not listed here. For tree-dominated decays, the tree amplitude is normalized to unity. Likewise, the QCD penguin amplitude is normalized to unity for penguin-dominated decays. Our preferred predictions are those for $N_c^{\text{eff}}(LL) = 2$ and $N_c^{\text{eff}}(LR) = 5$.

Decay	Class	$N_c^{\text{eff}}(LL) = 2$				$N_c^{\text{eff}}(LL) = N_c^{\text{eff}}(LR)$			
		2	3	5	∞	2	3	5	∞
$\overline{B}_d^0 \rightarrow \pi^+ \pi^-$	I	1	1	1	1	1	1	1	1
		-0.04+0.17i 0.004i	-0.04+0.17i 0.004i	-0.05+0.18i 0.004i	-0.05+0.18i 0.004i	-0.04+0.17i 0.004i	-0.04+0.17i -0.0004	-0.04+0.17i -0.003i	-0.04+0.18i -0.01i
$\overline{B}_d^0 \rightarrow \pi^0 \pi^0$	II,VI	1	1	1	1	1	1	1	1
		0.17-0.64i 0.15i	0.17-0.66i 0.14i	0.17-0.67i 0.14i	0.18-0.69i 0.14i	0.17-0.64i 0.15i	1.6-6.3i 0.05+1.3i	-0.31+1.2i -0.01-0.24i	-0.12+0.48i -0.08i
$\overline{B}_d^0 \rightarrow \eta \eta$	II,VI	1	1	1	1	1	1	1	1
		-0.17+0.84i 0.01+0.10i	-0.18+0.91i 0.01+0.10i	-0.19+0.97i 0.01+0.10i	-0.21+1.1i 0.01+0.09i	-0.17+0.84i 0.01+0.10i	-1.6+8.2i 0.12+1.0i	0.31-1.6i -0.02-0.2i	0.12-0.63i -0.01-0.08i
$\overline{B}_d^0 \rightarrow \eta \eta'$	II,VI	1	1	1	1	1	1	1	1
		-0.13+0.64i 0.012i	-0.16+0.85i 0.012i	-0.17+1.0i 0.012i	-0.2+1.3i 0.012i	-0.13+0.64i 0.012i	-1.2+6.4i 0.04+0.19i	0.23-1.3i -0.01-0.05i	0.09-0.51i -0.02i
$\overline{B}_d^0 \rightarrow \eta' \eta'$	II,VI	1	1	1	1	1	1	1	1
		-0.13+0.45i -0.01-0.06i	-0.14+0.79i -0.01-0.06i	-0.15+1.1i -0.01-0.06i	-0.17+1.5i -0.01-0.06i	-0.13+0.45i -0.01-0.06i	-1.1+4.7i -0.12-0.5i	0.21-0.97i 0.02+0.09i	0.07-0.40i 0.01+0.03i
$B^- \rightarrow \pi^- \pi^0$	III	1	1	1	1	1	1	1	1
		0 0.03i	0 0.03i	0 0.03i	0 0.03i	0 0.03i	0 0.03i	0 0.03i	0 0.03i
$B^- \rightarrow \pi^- \eta$	III	1	1	1	1	1	1	1	1
		-0.08+0.30i 0.02i	-0.08+0.32i 0.02i	-0.08+0.34i 0.02i	-0.09+0.36i 0.02i	-0.08+0.30i 0.02i	-0.10+0.38i 0.03i	-0.12+0.45i 0.03i	-0.18+0.61i 0.04i
$B^- \rightarrow \pi^- \eta'$	III	1	1	1	1	1	1	1	1
		-0.07+0.23i -0.01i	-0.09+0.31i -0.01i	-0.1+0.37i -0.01i	-0.12+0.46i -0.01i	-0.07+0.23i -0.01i	-0.1+0.3i -0.02i	-0.14+0.37i -0.02i	-0.24+0.52i -0.03i
$\overline{B}_d^0 \rightarrow K^- \pi^+$	IV	-0.04+0.22i	-0.04+0.22i	-0.04+0.21i	-0.04+0.21i	-0.04+0.22i	-0.04+0.22i	-0.04+0.22i	-0.04+0.22i
		1 0.02	1 0.02	1 0.02	1 0.02	1 0.02	1 0.002i	1 -0.02+0.01i	1 -0.03+0.01i
$B^- \rightarrow \overline{K}^0 \pi^-$	IV	0	0	0	0	0	0	0	0
		1 -0.01	1 -0.01	1 -0.01	1 -0.01	1 -0.01	1 -0.001i	1 0.002-0.001i	1 0.01
$B^- \rightarrow K^- K^0$	IV	0	0	0	0	0	0	0	0
		1 -0.01	1 -0.01	1 -0.01	1 -0.01	1 -0.01	1 -0.001i	1 0.01	1 0.02-0.01i

Table V. (continued)

Decay	Class	$N_c^{\text{eff}}(LL) = 2$				$N_c^{\text{eff}}(LL) = N_c^{\text{eff}}(LR)$			
		2	3	5	∞	2	3	5	∞
$\overline{B}_d^0 \rightarrow \pi^0 \eta$	VI	0.02-0.10i	0.02-0.09i	0.02-0.09i	0.02-0.08i	0.02-0.10i	-0.01i	-0.01+0.05i	-0.03+0.13i
		1	1	1	1	1	1	1	1
$\overline{B}_d^0 \rightarrow \pi^0 \eta'$	VI	-0.02+0.01i	-0.02+0.01i	-0.02+0.01i	-0.02+0.004i	-0.02+0.01i	-0.01	-0.001	0.01
		1	1	1	1	1	1	1	1
$\overline{B}_d^0 \rightarrow \overline{K}^0 \pi^0$	VI	0.11-0.27i	0.09-0.2i	0.08-0.16i	0.06-0.13i	0.11-0.27i	0.01-0.03i	-0.06+0.13i	-0.16+0.33i
		1	1	1	1	1	1	1	1
$\overline{B}_d^0 \rightarrow \overline{K}^0 \eta$	VI	-0.17+0.07i	-0.12+0.05i	-0.1+0.04i	-0.08+0.03i	-0.17+0.07i	-0.14+0.06i	-0.13+0.05i	-0.11+0.04i
		1	1	1	1	1	1	1	1
$\overline{B}_d^0 \rightarrow \overline{K}^0 \eta'$	VI	-0.14+0.04i	-0.14+0.04i	-0.13+0.04i	-0.13+0.04i	-0.14+0.04i	-0.13+0.04i	-0.12+0.04i	-0.11+0.03i
		1	1	1	1	1	1	1	1
$\overline{B}_d^0 \rightarrow K^0 \overline{K}^0$	VI	-0.10-0.05i	-0.11-0.05i	-0.11-0.06i	-0.12-0.06i	-0.10-0.05i	-0.01-0.01i	0.06+0.03i	0.15+0.07i
		1	1	1	1	1	1	1	1
$B^- \rightarrow K^- \pi^0$	VI	-0.19+0.05i	-0.20+0.05i	-0.21+0.05i	-0.22+0.06i	-0.19+0.05i	-0.18+0.05i	-0.18+0.05i	-0.17+0.05i
		1	1	1	1	1	1	1	1
$B^- \rightarrow K^- \eta$	VI	0.08-0.01i	0.07-0.01i	0.06-0.01i	0.06	0.08-0.01i	0.01	-0.04+0.01i	-0.11+0.01i
		1	1	1	1	1	1	1	1
$B^- \rightarrow K^- \eta'$	VI	-0.03+0.01i	-0.03+0.01i	-0.03+0.01i	-0.02+0.01i	-0.03+0.01i	-0.02+0.01i	-0.01+0.004i	-0.004
		0	0	0	0	0	0	0	0
$B^- \rightarrow K^- \pi^0$	VI	1	1	1	1	1	1	1	1
		-0.01	-0.01	-0.01	-0.01	-0.01	-0.001i	0.01	0.02-0.01i
$B^- \rightarrow K^- \eta$	VI	-0.05+0.27i	-0.05+0.26i	-0.04+0.26i	-0.04+0.25i	-0.05+0.27i	-0.04+0.23i	-0.04+0.2i	-0.03+0.15i
		1	1	1	1	1	1	1	1
$B^- \rightarrow K^- \eta'$	VI	0.15-0.04i	0.15-0.04i	0.14-0.04i	0.13-0.04i	0.15-0.04i	0.13-0.04i	0.11-0.03i	0.09-0.03i
		1	1	1	1	1	1	1	1
$B^- \rightarrow K^- \eta'$	VI	-0.03-0.40i	-0.03-0.43i	-0.04-0.45i	-0.04-0.48i	-0.03-0.40i	0.06-0.36i	0.13-0.33i	0.22-0.29i
		1	1	1	1	1	1	1	1
$B^- \rightarrow K^- \eta'$	VI	-0.24+0.05i	-0.25+0.06i	-0.26+0.06i	-0.27+0.07i	-0.24+0.05i	-0.19+0.04i	-0.14+0.04i	-0.09+0.02i
		1	1	1	1	1	1	1	1
$B^- \rightarrow K^- \eta'$	VI	0.07+0.07i	0.06+0.06i	0.06+0.05i	0.05+0.05i	0.07+0.07i	0.08i	-0.05+0.08i	-0.12+0.08i
		1	1	1	1	1	1	1	1
$B^- \rightarrow K^- \eta'$	VI	-0.02+0.01i	-0.02+0.01i	-0.02+0.01i	-0.02+0.01i	-0.02+0.01i	-0.02+0.01i	-0.02+0.01i	-0.02+0.01i
		1	1	1	1	1	1	1	1

Table VI. Same as Table V except for charmless $B_{u,d} \rightarrow VP$ decays.

Decay	Class	$N_c^{\text{eff}}(LL) = 2$				$N_c^{\text{eff}}(LL) = N_c^{\text{eff}}(LR)$			
		2	3	5	∞	2	3	5	∞
$\overline{B}_d^0 \rightarrow \rho^- \pi^+$	I	1	1	1	1	1	1	1	1
		-0.02+0.08i	-0.02+0.08i	-0.02+0.08i	-0.02+0.08i	-0.02+0.08i	-0.02+0.08i	-0.02+0.09i	-0.02+0.09i
		0.01i	0.01i	0.01i	0.01i	0.01i	0.001i	-0.002i	-0.006i
$\overline{B}_d^0 \rightarrow \rho^+ \pi^-$	I	1	1	1	1	1	1	1	1
		-0.01i	-0.01i	-0.02i	-0.02i	-0.01i	-0.004i	-0.002i	0.003i
		0.01i	0.01i	0.01i	0.01i	0.01i	0.001i	-0.002i	-0.006i
$\overline{B}_d^0 \rightarrow \rho^+ K^-$	I,IV	1	1	1	1	1	1	1	1
		0.23+0.7i	0.24+0.83i	0.26+0.95i	0.28+1.1i	0.23+0.7i	0.18+0.61i	0.15+0.55i	0.11+0.47i
		-0.05-0.1i	-0.05-0.11i	-0.05-0.11i	-0.05-0.11i	-0.05-0.1i	-0.01-0.03i	0.01+0.03i	0.05+0.1i
$\overline{B}_d^0 \rightarrow \rho^0 \pi^0$	II	1	1	1	1	1	1	1	1
		0.08-0.27i	0.08-0.27i	0.08-0.26i	0.08-0.26i	0.08-0.27i	0.77-2.7i	-0.15+0.55i	-0.06+0.22i
		0.15i	0.15i	0.15i	0.15i	0.15i	1.3i	-0.24i	-0.09i
$\overline{B}_d^0 \rightarrow \omega \pi^0$	II	1	1	1	1	1	1	1	1
		-0.5+1.6i	-0.36+1.0i	-0.29+0.72i	-0.18+0.26i	-0.5+1.6i	-2.7+7.3i	0.28-0.54i	-0.02+0.24i
		0.01+0.26i	0.01+0.23i	0.01+0.23i	0.01+0.23i	0.01+0.23i	0.06+2.5i	-0.01-0.52i	-0.01-0.22i
$\overline{B}_d^0 \rightarrow \omega \eta$	II	1	1	1	1	1	1	1	1
		-0.1+0.29i	-0.08+0.18i	-0.06+0.11i	-0.04-0.01i	-0.1+0.29i	-0.52+0.98i	0.04+0.05i	-0.02+0.14i
		0.06i	0.06i	0.06i	0.06i	0.06i	0.03+0.64i	-0.01-0.13i	-0.06i
$\overline{B}_d^0 \rightarrow \omega \eta'$	II	1	1	1	1	1	1	1	1
		-0.1+0.15i	-0.1+0.16i	-0.1+0.17i	-0.1+0.19i	-0.1+0.15i	-0.61-0.23i	0.07+0.26i	0.21i
		-0.004i	-0.01i	-0.004i	-0.004i	-0.004i	0.04-0.01i	-0.02i	-0.01i
$\overline{B}_d^0 \rightarrow \rho^0 \eta$	II	1	1	1	1	1	1	1	1
		0.25-0.5i	0.26-0.52i	0.26-0.54i	0.26-0.59i	0.25-0.5i	2.5-5.5i	-0.48+1.2i	-0.19+0.49i
		-0.03+0.21i	-0.03+0.22i	-0.03+0.22i	-0.03+0.22i	-0.03+0.2i	-0.27+1.8i	0.05-0.3i	0.02-0.10i
$\overline{B}_d^0 \rightarrow \rho^0 \eta'$	II,VI	1	1	1	1	1	1	1	1
		0.26	0.51-0.35i	0.71-0.67i	1.0-1.1i	0.26	2.8-0.72i	-0.6+0.3i	-0.26+0.20i
		-0.14+0.43i	-0.16+0.45i	-0.16+0.46i	-0.17+0.46i	-0.14+0.43i	-1.4+4.0i	0.26-0.73i	0.1-0.26i
$B^- \rightarrow \rho^0 \pi^-$	III	1	1	1	1	1	1	1	1
		0.03-0.12i	0.03-0.12i	0.03-0.12i	0.03-0.13i	0.03-0.12i	0.04-0.17i	0.06-0.23i	0.12-0.48i
		0.05i	0.05i	0.05i	0.05i	0.05i	0.06i	0.08i	0.14i
$B^- \rightarrow \rho^- \pi^0$	III	1	1	1	1	1	1	1	1
		-0.02+0.08i	-0.02+0.08i	-0.02+0.08i	-0.02+0.08i	-0.02+0.08i	-0.03+0.09i	-0.03+0.10i	-0.03+0.11i
		-0.01i	-0.01i	-0.01i	-0.01i	-0.01i	-0.01i	-0.01i	-0.02i
$B^- \rightarrow \omega \pi^-$	III	1	1	1	1	1	1	1	1
		-0.05+0.17i	-0.04+0.11i	-0.03+0.07i	-0.02+0.01i	-0.05+0.17i	-0.040.11i	-0.03+0.04i	0.02-0.21i
		0.01i	0.01i	0.01i	0.01i	0.01i	0.02i	0.03i	0.04i
$B^- \rightarrow \rho^- \eta$	III	1	1	1	1	1	1	1	1
		0.01i	-0.01i	-0.02i	0.01-0.03i	0.01i	0.01i	0.01i	0.01i
		0.001i	0.0004i	0.0004i	0.0004i	0.001i	-0.002i	-0.005i	-0.01i
$B^- \rightarrow \rho^- \eta'$	III	1	1	1	1	1	1	1	1
		-0.04+0.07i	-0.06+0.12i	-0.06+0.16i	-0.08+0.23i	-0.04+0.07i	-0.05+0.09i	-0.06+0.11i	-0.07+0.15i
		0.02i	0.02i	0.02i	0.02i	0.02i	0.02i	0.02i	0.02i
$B^- \rightarrow \rho^0 K^-$	III,VI	1	1	1	1	1	1	1	1
		0.16+0.49i	0.17+0.59i	0.18+0.67i	0.2+0.79i	0.16+0.49i	0.18+0.59i	0.2+0.71i	0.27+1.1i
		-0.38-0.9i	-0.38-0.89i	-0.38-0.9i	-0.38-0.9i	-0.38-0.9i	-0.48-1.1i	-0.62-1.4i	-1.1-2.5i
$\overline{B}_d^0 \rightarrow K^{*-} \pi^+$	IV	1	1	1	1	1	1	1	1
		-0.08+0.54i	-0.08+0.54i	-0.08+0.54i	-0.08+0.54i	-0.08+0.54i	-0.08+0.52i	-0.08+0.51i	-0.08+0.49i
		0.05-0.01i	0.05-0.01i	0.05-0.01i	0.05-0.01i	0.05-0.01i	0.01	-0.02+0.01i	-0.06+0.02i
$B^- \rightarrow \overline{K}^{*0} \pi^-$	IV	0	0	0	0	0	0	0	0
		1	1	1	1	1	1	1	1
		-0.03+0.01i	-0.03+0.01i	-0.03+0.01i	-0.03+0.01i	-0.03+0.01i	-0.004	0.01	0.03-0.01i
$B^- \rightarrow K^{*0} K^-$	IV	0	0	0	0	0	0	0	0
		1	1	1	1	1	1	1	1
		-0.03+0.01i	-0.03+0.01i	-0.03+0.01i	-0.03+0.01i	-0.03+0.01i	-0.004	0.012	0.03-0.01i
$B^- \rightarrow K^{*-} K^0$	IV	0	0	0	0	0	0	0	0
		1	1	1	1	1	1	1	1
		0.09	0.08	0.07	0.06	0.09	0.03	-0.03+0.01i	-0.15+0.03i

Table VI. (continued)

Decay	Class	$N_c^{\text{eff}}(LL) = 2$				$N_c^{\text{eff}}(LL) = N_c^{\text{eff}}(LR)$			
		2	3	5	∞	2	3	5	∞
$\overline{B}_d^0 \rightarrow \phi\pi^0$	V	0 1	0 1	0 1	0 1	0 1	0 1	0 1	0 1
		-0.35+0.12i	-0.97+0.62i	1.3+0.27i	0.34-0.04i	-0.35+0.12i	1.+0.06i	0.28-0.04i	0.14-0.03i
$\overline{B}_d^0 \rightarrow \phi\eta$	V	0 1	0 1	0 1	0 1	0 1	0 1	0 1	0 1
		-0.35+0.12i	-0.97+0.62i	1.3+0.27i	0.34-0.04i	-0.35+0.12i	1.+0.06i	0.28-0.04i	0.14-0.03i
$\overline{B}_d^0 \rightarrow \phi\eta'$	V	0 1	0 1	0 1	0 1	0 1	0 1	0 1	0 1
		-0.35+0.12i	-0.97+0.62i	1.3+0.27i	0.34-0.04i	-0.35+0.12i	1.+0.06i	0.28-0.04i	0.14-0.03i
$B^- \rightarrow \phi\pi^-$	V	0 1	0 1	0 1	0 1	0 1	0 1	0 1	0 1
		-0.35+0.12i	-0.97+0.62i	1.3+0.27i	0.34-0.04i	-0.35+0.12i	1.+0.06i	0.28-0.04i	0.14-0.03i
$\overline{B}_d^0 \rightarrow K^{*0}\overline{K}^0$	VI	0 1	0 1	0 1	0 1	0 1	0 1	0 1	0 1
		0.09	0.08	0.07	0.06	0.09	0.03	-0.03+0.01i	-0.15+0.03i
$\overline{B}_d^0 \rightarrow \overline{K}^{*0}K^0$	VI	0 1	0 1	0 1	0 1	0 1	0 1	0 1	0 1
		-0.03+0.01i	-0.03+0.01i	-0.03+0.01i	-0.03+0.01i	-0.03+0.01i	-0.004	0.012	0.03-0.01i
$\overline{B}_d^0 \rightarrow \overline{K}^{*0}\pi^0$	VI	0.01-0.07i 1	0.01-0.07i 1	0.01-0.07i 1	0.01-0.07i 1	0.01-0.07i 1	-0.01i 1	-0.01+0.03i 1	-0.01+0.08i 1
		-0.21+0.07i	-0.21+0.07i	-0.21+0.07i	-0.21+0.07i	-0.21+0.07i	-0.18+0.06i	-0.16+0.05i	-0.13+0.04i
$\overline{B}_d^0 \rightarrow \rho^0\overline{K}^0$	VI	-0.18+0.54i 1	-0.14+0.48i 1	-0.12+0.43i 1	-0.09+0.37i 1	-0.18+0.54i 1	-0.02+0.07i 1	0.12-0.41i 1	0.32-1.3i 1
		1.8-0.14i	1.6-0.18i	1.4-0.18i	1.2-0.18i	1.8-0.14i	2.1-0.22i	2.3-0.3i	2.7-0.46i
$\overline{B}_d^0 \rightarrow \omega\overline{K}^0$	VI	0.02+0.28i 1	0.92-0.39i 1	0.10-0.24i 1	0.03-0.11i 1	0.02+0.28i 1	0.01-0.03i 1	-0.02+0.06i 1	-0.02+0.09i 1
		0.21-0.1i	-0.6-0.6i	-0.22	-0.10+0.01i	0.21-0.1i	-0.27	-0.12+0.02i	-0.08+0.02i
$\overline{B}_d^0 \rightarrow \overline{K}^{*0}\eta$	VI	0.07+0.03i 1	0.06+0.03i 1	0.06+0.03i 1	0.05+0.02i 1	0.07+0.03i 1	0.01 1	-0.04-0.02i 1	-0.10-0.04i 1
		0.11-0.04i	0.10-0.03i	0.09-0.03i	0.08-0.03i	0.11-0.04i	0.13-0.04i	0.14-0.04i	0.16-0.05i
$\overline{B}_d^0 \rightarrow \overline{K}^{*0}\eta'$	VI	-0.58-0.67i 1	0.47-0.84i 1	0.46-0.27i 1	0.28-0.09i 1	-0.58-0.67i 1	-0.06-0.11i 1	0.01+0.82i 1	-1.3+1.5i 1
		0.43+0.32i	-0.17+0.56i	-0.24+0.22i	-0.16+0.09i	0.43+0.32i	0.28+0.35i	0.07+0.3i	0.02-0.03i
$\overline{B}_d^0 \rightarrow \phi\overline{K}^0$	VI	0 1	0 1	0 1	0 1	0 1	0 1	0 1	0 1
		-0.11+0.03i	-0.13+0.04i	-0.16+0.05i	-0.22+0.08i	-0.11+0.03i	-0.13+0.04i	-0.16+0.05i	-0.32+0.12i
$B^- \rightarrow K^{*-}\pi^0$	VI	-0.09+0.59i 1	-0.09+0.59i 1	-0.09+0.59i 1	-0.09+0.59i 1	-0.09+0.59i 1	-0.08+0.52i 1	-0.08+0.48i 1	-0.07+0.43i 1
		0.19-0.06i	0.18-0.06i	0.18-0.06i	0.18-0.06i	0.19-0.06i	0.13-0.04i	0.10-0.03i	0.05-0.02i
$B^- \rightarrow \rho^-\overline{K}^0$	VI	0 1	0 1	0 1	0 1	0 1	0 1	0 1	0 1
		0.09	0.07	0.06	0.06	0.09	0.03	-0.03+0.01i	-0.13+0.03i
$B^- \rightarrow \phi K^-$	VI	0 1	0 1	0 1	0 1	0 1	0 1	0 1	0 1
		-0.11+0.03i	-0.13+0.04i	-0.16+0.05i	-0.22+0.08i	-0.11+0.03i	-0.13+0.04i	-0.16+0.05i	-0.32+0.12i
$B^- \rightarrow K^{*-}\eta$	VI	0.44i 1	0.4i 1	0.37i 1	0.33i 1	0.44i 1	-0.06+0.41i 1	-0.11+0.39i 1	-0.17+0.36i 1
		0.19-0.05i	0.17-0.05i	0.16-0.04i	0.14-0.04i	0.19-0.05i	0.14-0.04i	0.10-0.03i	0.05-0.02i
$B^- \rightarrow K^{*-}\eta'$	VI,III	0.31-1.2i 1	1.8-0.18i 1	0.85+0.55i 1	0.34+0.4i 1	0.31-1.2i 1	1.4-0.82i 1	2.6+0.48i 1	1.1+3.8i 1
		0.17+0.07i	-0.01+0.26i	-0.10+0.11i	-0.07+0.04i	0.17+0.07i	0.25+0.18i	0.26+0.39i	-0.13+0.6i
$B^- \rightarrow \omega K^-$	VI,III	-0.06+1.0i 1	3.0-1.6i 1	0.34-0.84i 1	0.11-0.39i 1	-0.06+1.0i 1	0.29-0.71i 1	0.06-0.24i 1	0.02-0.08i 1
		0.33-0.17i	0.97-0.76i	-0.33-0.01i	-0.15+0.02i	0.33-0.17i	-0.30+0.01i	-0.11+0.02i	-0.05+0.01i

Table VII. Same as Table V except for charmless $B_{u,d} \rightarrow VV$ decays.

Decay	Class	$N_c^{\text{eff}}(LL) = 2$				$N_c^{\text{eff}}(LL) = N_c^{\text{eff}}(LR)$			
		2	3	5	∞	2	3	5	∞
$\overline{B}_d^0 \rightarrow \rho^- \rho^+$	I	1	1	1	1	1	1	1	1
		0.17+0.06i 0.01	0.17+0.06i 0.01	0.17+0.06i 0.01	0.17+0.06i 0.01	0.17+0.06i 0.01	0.18+0.06i 0.001	0.18+0.06i -0.01	0.19+0.06i -0.01
$\overline{B}_d^0 \rightarrow \rho^0 \rho^0$	II	1	1	1	1	1	1	1	1
		-0.77-0.25i 0.32+0.02i	-0.77-0.25i 0.32+0.02i	-0.77-0.25i 0.32+0.02i	-0.77-0.25i 0.32+0.02i	-0.77-0.25i 0.32+0.02i	-7.7-2.4i 2.9+0.17i	1.5+0.47i -0.53-0.03i	0.61+0.18i -0.19-0.01i
$\overline{B}_d^0 \rightarrow \omega \omega$	II	1	1	1	1	1	1	1	1
		1.3+0.46i 0.08+0.01i	0.91+0.35i 0.08+0.01i	0.63+0.27i 0.08+0.01i	0.2+0.15i 0.08+0.01i	1.3+0.46i 0.08+0.01i	5.9+2.4i 0.92+0.05i	-0.27-0.2i -0.2-0.01i	0.34+0.06i -0.09
$B^- \rightarrow \rho^- \rho^0$	III	1	1	1	1	1	1	1	1
		0 0.07	0 0.07	0 0.07	0 0.07	0 0.07	0 0.07	0 0.07	0 0.07
$B^- \rightarrow \rho^- \omega$	III	1	1	1	1	1	1	1	1
		0.36+0.12i 0.02	0.3+0.11i 0.02	0.25+0.09i 0.02	0.18+0.07i 0.02	0.36+0.12i 0.02	0.3+0.11i 0.02	0.24+0.09i 0.02	0.13+0.06i 0.02
$\overline{B}_d^0 \rightarrow K^{*-} \rho^+$	IV	-0.22+0.07i 1	-0.22+0.07i 1	-0.22+0.07i 1	-0.22+0.07i 1	-0.22+0.07i 1	-0.21+0.07i 1	-0.21+0.06i 1	-0.2+0.06i 1
		0.05-0.01i 0.05-0.02i	0.05-0.01i 0.05-0.02i	0.05-0.01i 0.05-0.02i	0.05-0.01i 0.05-0.02i	0.05-0.01i 0.05-0.02i	0.01 0.01	-0.02+0.01i -0.03+0.01i	-0.06+0.02i -0.06+0.02i
$\overline{B}_d^0 \rightarrow \overline{K}^{*0} \rho^0$	IV	1	1	1	1	1	1	1	1
		-0.38+0.1i 0	-0.38+0.1i 0	-0.38+0.1i 0	-0.38+0.1i 0	-0.38+0.1i 0	-0.34+0.09i 0	-0.32+0.08i 0	-0.29+0.07i 0
$\overline{B}_d^0 \rightarrow \overline{K}^{*0} K^{*0}$	IV	1	1	1	1	1	1	1	1
		-0.03+0.01i -0.27+0.09i	-0.03+0.01i -0.27+0.09i	-0.03+0.01i -0.27+0.09i	-0.03+0.01i -0.27+0.09i	-0.03+0.01i -0.27+0.09i	-0.004 -0.22+0.07i	0.01 -0.18+0.06i	0.03-0.01i -0.14+0.04i
$B^- \rightarrow K^{*-} \rho^0$	IV	1	1	1	1	1	1	1	1
		0.4-0.11i 0	0.4-0.11i 0	0.4-0.11i 0	0.41-0.11i 0	0.4-0.11i 0	0.34-0.09i 0	0.3-0.07i 0	0.26-0.06i 0
$B^- \rightarrow \overline{K}^{*0} \rho^-$	IV	1	1	1	1	1	1	1	1
		-0.03+0.01i 0	-0.03+0.01i 0	-0.03+0.01i 0	-0.03+0.01i 0	-0.03+0.01i 0	-0.004 0	0.01 0	0.03-0.01i 0
$B^- \rightarrow K^{*-} K^{*0}$	IV	1	1	1	1	1	1	1	1
		-0.03+0.01i 0	-0.03+0.01i 0	-0.03+0.01i 0	-0.03+0.01i 0	-0.03+0.01i 0	-0.004 0	0.01 0	0.03-0.01i 0
$\overline{B}_d^0 \rightarrow \rho^0 \phi$	V	1	1	1	1	1	1	1	1
		-0.35+0.12i 0	-0.97+0.62i 0	1.3+0.27i 0	0.34-0.04i 0	-0.35+0.12i 0	1.0+0.06i 0	0.28-0.04i 0	0.14-0.03i 0
$\overline{B}_d^0 \rightarrow \omega \phi$	V	1	1	1	1	1	1	1	1
		-0.35+0.12i 0	-0.97+0.62i 0	1.3+0.27i 0	0.34-0.04i 0	-0.35+0.12i 0	1.0+0.06i 0	0.28-0.04i 0	0.14-0.03i 0
$B^- \rightarrow \rho^- \phi$	V	1	1	1	1	1	1	1	1
		-0.35+0.12i 0	-0.97+0.62i 0	1.3+0.27i 0	0.34-0.04i 0	-0.35+0.12i 0	1.0+0.06i 0	0.28-0.04i 0	0.14-0.03i 0
$\overline{B}_d^0 \rightarrow \rho^0 \omega$	VI	1	1	1	1	1	1	1	1
		-0.12+0.03i -0.04+0.01i	-0.14+0.04i -0.05+0.02i	-0.17+0.05i -0.06+0.02i	-0.23+0.08i -0.08+0.03i	-0.12+0.03i -0.04+0.01i	-0.14+0.04i -0.01	-0.17-0.05i 0.04-0.02i	-0.31+0.11i 0.24-0.1i
$\overline{B}_d^0 \rightarrow \overline{K}^{*0} \omega$	VI	1	1	1	1	1	1	1	1
		-0.03+0.01i 0.05-0.02i	-0.04+0.01i 0.07-0.02i	-0.05+0.02i 0.09-0.03i	-0.11+0.07i 0.20-0.11i	-0.03+0.01i 0.05-0.02i	-0.01 0.12-0.04i	0.07-0.04i 0.36-0.19i	-0.15+0.02i -0.33+0.04i
$\overline{B}_d^0 \rightarrow \overline{K}^{*0} \phi$	VI	1	1	1	1	1	1	1	1
		-0.11+0.03i -0.17+0.06i	-0.13+0.04i -0.22+0.09i	-0.16+0.05i -0.3+0.13i	-0.22+0.08i -0.64+0.41i	-0.11+0.03i -0.17+0.06i	-0.13+0.04i -0.26+0.11i	-0.16+0.05i -0.6+0.35i	-0.32+0.12i 0.38-0.06i
$B^- \rightarrow K^{*-} \omega$	VI	1	1	1	1	1	1	1	1
		0.1-0.03i 0	0.13-0.04i 0	0.18-0.06i 0	0.39-0.22i 0	0.1-0.03i 0	0.13-0.04i 0	0.25-0.12i 0	-0.08 0
$B^- \rightarrow K^{*-} \phi$	VI	1	1	1	1	1	1	1	1
		-0.11+0.03i -0.17+0.06i	-0.13+0.04i -0.22+0.09i	-0.16+0.05i -0.3+0.13i	-0.22+0.08i -0.64+0.41i	-0.11+0.03i -0.17+0.06i	-0.13+0.04i -0.26+0.11i	-0.16+0.05i -0.6+0.35i	-0.32+0.12i 0.38-0.06i
$B^- \rightarrow K^{*-} \phi$	VI	1	1	1	1	1	1	1	1
		-0.11+0.03i -0.17+0.06i	-0.13+0.04i -0.22+0.09i	-0.16+0.05i -0.3+0.13i	-0.22+0.08i -0.64+0.41i	-0.11+0.03i -0.17+0.06i	-0.13+0.04i -0.26+0.11i	-0.16+0.05i -0.6+0.35i	-0.32+0.12i 0.38-0.06i

Table VIII. Branching ratios (in units of 10^{-6}) averaged over CP-conjugate modes for charmless $B_{u,d} \rightarrow PP$ decays. Predictions are made for $k^2 = m_b^2/2$, $\eta = 0.370$, $\rho = 0.175$, and $N_c^{\text{eff}}(LR) = 2, 3, 5, \infty$ with $N_c^{\text{eff}}(LL)$ being fixed to be 2 in the first case and treated to be the same as $N_c^{\text{eff}}(LR)$ in the second case. Results using the BSW model and the light-cone sum rule for heavy-to-light form factors are shown in the upper and lower entries, respectively. Experimental values (in units of 10^{-6}) are taken from [1,38–40,44,49,55]. Our preferred predictions are those for $N_c^{\text{eff}}(LL) = 2$ and $N_c^{\text{eff}}(LR) = 5$.

Decay	Class	$N_c^{\text{eff}}(LL) = 2$				$N_c^{\text{eff}}(LL) = N_c^{\text{eff}}(LR)$				Expt.
		2	3	5	∞	2	3	5	∞	
$\overline{B}_d^0 \rightarrow \pi^+ \pi^-$	I	11.3	11.3	11.4	11.4	11.3	12.8	14.0	15.9	< 8.4
		9.49	9.51	9.53	9.55	9.49	10.7	11.7	13.3	
$\overline{B}_d^0 \rightarrow \pi^0 \pi^0$	II,VI	0.33	0.33	0.34	0.34	0.33	0.09	0.21	0.90	< 9.3
		0.28	0.28	0.28	0.29	0.28	0.08	0.18	0.75	
$\overline{B}_d^0 \rightarrow \eta \eta$	II,VI	0.24	0.26	0.27	0.30	0.24	0.13	0.16	0.43	< 18
		0.20	0.21	0.22	0.24	0.20	0.10	0.13	0.35	
$\overline{B}_d^0 \rightarrow \eta \eta'$	II,VI	0.27	0.33	0.40	0.51	0.27	0.10	0.14	0.50	< 27
		0.22	0.27	0.32	0.41	0.22	0.08	0.11	0.40	
$\overline{B}_d^0 \rightarrow \eta' \eta'$	II,VI	0.08	0.11	0.14	0.21	0.08	0.02	0.03	0.16	< 47
		0.06	0.09	0.11	0.17	0.06	0.01	0.02	0.13	
$B^- \rightarrow \pi^- \pi^0$	III	8.63	8.63	8.63	8.63	8.63	6.82	5.52	3.83	< 16
		7.23	7.23	7.23	7.23	7.23	5.71	4.63	3.21	
$B^- \rightarrow \pi^- \eta$	III	5.92	6.00	6.06	6.16	5.92	4.70	3.85	2.79	< 15
		4.89	4.96	5.01	5.09	4.89	3.88	3.18	2.30	
$B^- \rightarrow \pi^- \eta'$	III	3.70	3.88	4.07	4.39	3.70	2.74	2.09	1.29	< 12
		3.03	3.19	3.34	3.60	3.03	2.26	1.73	1.07	
$\overline{B}_d^0 \rightarrow K^- \pi^+$	IV	14.0	14.9	15.7	16.8	14.0	15.6	16.9	18.9	$14 \pm 3 \pm 2$
		14.0	12.4	13.0	14.0	14.0	12.9	14.0	15.7	
$B^- \rightarrow \overline{K}^0 \pi^-$	IV	16.0	17.1	17.9	19.3	16.0	18.9	21.4	25.4	$14 \pm 5 \pm 2$
		13.3	14.2	14.9	16.0	13.3	15.7	17.8	21.1	
$B^- \rightarrow K^- K^0$	IV	0.85	0.91	0.95	1.03	0.85	1.00	1.14	1.35	< 9.3
		0.68	0.73	0.77	0.82	0.68	0.81	0.91	1.08	
$\overline{B}_d^0 \rightarrow \overline{K}^0 \pi^0$	VI	5.92	6.37	6.74	7.32	5.92	6.75	7.47	8.64	< 41
		4.93	5.30	5.61	6.10	4.93	5.62	6.23	7.21	
$\overline{B}_d^0 \rightarrow K^0 \overline{K}^0$	VI	0.80	0.85	0.90	0.96	0.80	0.94	1.07	1.27	< 17
		0.64	0.69	0.72	0.77	0.64	0.76	0.86	1.02	
$\overline{B}_d^0 \rightarrow \pi^0 \eta$	VI	0.22	0.25	0.27	0.30	0.22	0.24	0.26	0.29	< 8
		0.18	0.20	0.22	0.25	0.18	0.20	0.21	0.24	
$\overline{B}_d^0 \rightarrow \pi^0 \eta'$	VI	0.08	0.15	0.22	0.34	0.08	0.07	0.07	0.07	< 11
		0.06	0.12	0.18	0.28	0.06	0.06	0.06	0.06	
$\overline{B}_d^0 \rightarrow \overline{K}^0 \eta$	VI	0.95	0.84	0.75	0.63	0.95	1.32	1.67	2.30	< 33
		0.73	0.64	0.57	0.48	0.73	1.02	1.29	1.78	
$\overline{B}_d^0 \rightarrow \overline{K}^0 \eta'$	VI	25.5	35.1	43.8	58.8	25.5	27.2	28.6	30.7	$59_{-16}^{+18} \pm 9$
		20.4	28.0	34.9	46.8	20.4	21.7	22.8	24.6	
$B^- \rightarrow K^- \pi^0$	VI	9.45	9.98	10.4	11.1	9.45	10.7	11.8	13.5	$15 \pm 4 \pm 3$
		7.83	8.26	8.62	9.18	7.83	8.85	9.73	11.1	
$B^- \rightarrow K^- \eta$	VI	1.57	1.44	1.33	1.19	1.57	2.17	2.75	3.81	< 14
		1.23	1.12	1.04	0.92	1.23	1.70	2.15	2.99	
$B^- \rightarrow K^- \eta'$	VI	26.3	36.3	45.5	61.1	26.3	27.4	28.3	29.7	$74_{-13}^{+8} \pm 10$
		21.0	28.9	36.2	48.7	21.0	21.9	22.6	23.7	

Table IX. Same as Table VIII except for charmless $B_{u,d} \rightarrow VP$ decays.

Decay	Class	$N_c^{\text{eff}}(LL) = 2$				$N_c^{\text{eff}}(LL) = N_c^{\text{eff}}(LR)$				Expt.
		2	3	5	∞	2	3	5	∞	
$\overline{B}_d^0 \rightarrow \rho^- \pi^+$	I	29.6	29.6	29.6	29.6	29.6	33.4	36.5	41.6	} $35_{-10}^{+11} \pm 5$
$\overline{B}_d^0 \rightarrow \rho^+ \pi^-$	I	7.39	7.15	7.14	7.14	7.39	8.06	8.83	10.0	
$\overline{B}_d^0 \rightarrow \rho^+ K^-$	I,IV	1.04	1.20	1.34	1.58	1.04	1.16	1.26	1.42	
$\overline{B}_d^0 \rightarrow \rho^0 \pi^0$	II	0.82	0.81	0.81	0.81	0.81	0.03	0.33	2.31	< 18
$\overline{B}_d^0 \rightarrow \omega \pi^0$	II	0.24	0.17	0.12	0.08	0.24	0.08	0.05	0.17	< 14
$\overline{B}_d^0 \rightarrow \omega \eta$	II	0.51	0.48	0.46	0.45	0.51	0.02	0.16	1.25	< 12
$\overline{B}_d^0 \rightarrow \omega \eta'$	II	0.33	0.35	0.36	0.37	0.33	0.01	0.15	1.04	< 60
$\overline{B}_d^0 \rightarrow \rho^0 \eta$	II	0.05	0.05	0.05	0.05	0.05	0.01	0.03	0.12	< 13
$\overline{B}_d^0 \rightarrow \rho^0 \eta'$	II,VI	0.02	0.02	0.03	0.05	0.02	0.003	0.01	0.06	< 23
$B^- \rightarrow \rho^- \pi^0$	III	18.5	18.5	18.5	18.5	18.5	18.3	18.1	17.8	< 77
$B^- \rightarrow \rho^0 \pi^-$	III	8.09	8.08	8.09	8.09	8.09	4.78	2.77	0.81	$15 \pm 5 \pm 4$
$B^- \rightarrow \omega \pi^-$	III	7.97	7.82	7.72	7.62	7.97	4.84	2.92	1.01	< 23
$B^- \rightarrow \rho^- \eta$	III	11.6	11.3	11.3	11.3	11.6	10.3	9.59	8.51	< 32
$B^- \rightarrow \rho^- \eta'$	III	7.41	7.56	7.71	7.99	7.41	6.63	6.04	5.20	< 47
$B^- \rightarrow \rho^0 K^-$	III,VI	0.48	0.47	0.48	0.51	0.48	0.30	0.21	0.15	< 22
$\overline{B}_d^0 \rightarrow K^{*-} \pi^+$	IV	4.83	4.83	4.83	4.83	4.83	5.38	5.85	6.59	22_{-6-5}^{+8+4}
$B^- \rightarrow \overline{K}^{*0} \pi^-$	IV	5.35	5.35	5.35	5.35	5.35	6.84	8.17	10.4	< 27
$B^- \rightarrow K^{*0} K^-$	IV	0.27	0.28	0.28	0.28	0.27	0.35	0.42	0.54	< 12
$B^- \rightarrow K^{*-} K^0$	IV	0.03	0.02	0.03	0.04	0.03	0.01	0.01	0.01	–

Table IX. (Continued)

Decay	Class	$N_c^{\text{eff}}(LL) = 2$				$N_c^{\text{eff}}(LL) = N_c^{\text{eff}}(LR)$				Expt.
		2	3	5	∞	2	3	5	∞	
$\overline{B}_d^0 \rightarrow \phi\pi^0$	V	0.01	0.001	0.01	0.03	0.01	0.01	0.05	0.17	< 5.4
		0.01	0.0004	0.004	0.02	0.01	0.01	0.04	0.13	
$\overline{B}_d^0 \rightarrow \phi\eta$	V	0.003	0.0003	0.003	0.02	0.003	0.01	0.03	0.09	< 9
		0.002	0.0002	0.002	0.01	0.002	0.003	0.02	0.07	
$\overline{B}_d^0 \rightarrow \phi\eta'$	V	0.002	0.0002	0.002	0.01	0.002	0.003	0.02	0.06	< 31
		0.002	0.0001	0.001	0.01	0.002	0.002	0.01	0.04	
$B^- \rightarrow \phi\pi^-$	V	0.01	0.001	0.01	0.06	0.01	0.02	0.10	0.36	< 4
		0.01	0.001	0.01	0.05	0.01	0.01	0.08	0.29	
$\overline{B}_d^0 \rightarrow K^{*0}\overline{K}^0$	VI	0.01	0.02	0.02	0.03	0.01	0.01	0.01	0.004	-
		0.03	0.04	0.05	0.07	0.03	0.02	0.02	0.01	
$\overline{B}_d^0 \rightarrow \overline{K}^{*0}K^0$	VI	0.26	0.26	0.26	0.26	0.26	0.33	0.39	0.50	-
		0.21	0.21	0.21	0.21	0.21	0.27	0.32	0.41	
$\overline{B}_d^0 \rightarrow \overline{K}^{*0}\pi^0$	VI	1.76	1.76	1.77	1.77	1.76	2.16	2.53	3.15	< 28
		1.11	1.12	1.13	1.14	1.1	1.32	1.52	1.88	
$\overline{B}_d^0 \rightarrow \rho^0\overline{K}^0$	VI	0.95	1.05	1.18	1.38	0.95	1.02	1.16	1.45	< 27
		0.95	1.25	1.43	1.72	0.95	1.12	1.21	1.42	
$\overline{B}_d^0 \rightarrow \omega\overline{K}^0$	VI	0.62	0.05	0.50	2.70	0.62	0.28	2.44	9.73	< 57
		0.34	0.10	0.72	3.03	0.34	0.39	2.38	8.66	
$\overline{B}_d^0 \rightarrow \overline{K}^{*0}\eta$	VI	3.57	4.26	4.85	5.81	3.57	3.83	4.05	4.40	< 30
		4.32	5.44	6.42	8.04	4.32	4.27	4.23	4.22	
$\overline{B}_d^0 \rightarrow \overline{K}^{*0}\eta'$	VI	0.08	0.16	0.52	1.55	0.08	0.13	0.16	0.24	< 20
		0.61	0.14	0.32	1.64	0.61	0.99	1.28	1.80	
$\overline{B}_d^0 \rightarrow \phi\overline{K}^0$	VI	10.7	7.01	4.60	1.96	10.7	5.63	2.73	0.34	< 28
		8.81	5.75	3.78	1.61	8.81	4.62	2.24	0.28	
$B^- \rightarrow K^{*-}\pi^0$	VI	3.27	3.27	3.26	3.26	3.27	3.63	3.93	4.42	< 99
		3.01	3.01	3.00	2.99	3.01	3.34	3.63	4.11	
$B^- \rightarrow \rho^-\overline{K}^0$	VI	0.32	0.45	0.57	0.77	0.32	0.24	0.19	0.12	< 48
		0.56	0.78	0.99	1.34	0.56	0.42	0.32	0.20	
$B^- \rightarrow \phi K^-$	VI	10.9	7.55	4.96	2.11	10.9	6.07	2.94	0.36	< 5.9
		9.08	6.20	4.07	1.73	9.08	4.98	2.42	0.30	
$B^- \rightarrow K^{*-}\eta$	VI	3.74	4.41	5.00	5.95	3.74	3.45	3.24	2.94	< 30
		4.48	5.60	6.59	8.24	4.48	3.89	3.44	2.84	
$B^- \rightarrow K^{*-}\eta'$	VI,III	0.54	0.43	0.65	1.53	0.54	0.69	0.85	1.16	< 87
		1.41	0.53	0.49	1.54	1.41	2.00	2.58	3.65	
$B^- \rightarrow \omega K^-$	VI,III	0.88	0.52	1.21	3.90	0.88	0.93	3.91	13.2	$15_{-6}^{+7} \pm 2$
		0.82	0.88	1.81	4.70	0.82	1.44	4.43	13.1	

Table X. Same as Table VIII except for charmless $B_{u,d} \rightarrow VV$ decays.

Decay	Class	$N_c^{\text{eff}}(LL) = 2$				$N_c^{\text{eff}}(LL) = N_c^{\text{eff}}(LR)$				Expt.
		2	3	5	∞	2	3	5	∞	
$\overline{B}_d^0 \rightarrow \rho^- \rho^+$	I	21.9	21.9	21.9	21.9	21.9	24.7	27.0	30.7	< 2200
		35.8	35.8	35.8	35.8	35.8	40.3	44.2	50.3	
$\overline{B}_d^0 \rightarrow \rho^0 \rho^0$	II	0.55	0.55	0.55	0.55	0.55	0.05	0.25	1.57	< 40
		0.90	0.90	0.90	0.90	0.90	0.07	0.41	2.57	
$\overline{B}_d^0 \rightarrow \omega \omega$	II	0.65	0.55	0.50	0.45	0.65	0.07	0.16	1.24	< 19
		1.04	0.89	0.81	0.72	1.04	0.11	0.26	2.00	
$B^- \rightarrow \rho^- \rho^0$	III	17.2	17.2	17.2	17.2	17.2	13.6	11.0	7.64	< 120
		28.1	28.1	28.1	28.1	28.1	22.2	18.0	12.5	
$B^- \rightarrow \rho^- \omega$	III	17.2	17.1	17.0	16.8	17.2	13.9	11.5	8.37	< 61
		27.9	27.7	27.5	27.2	27.9	22.6	18.6	13.5	
$\overline{B}_d^0 \rightarrow K^{*-} \rho^+$	IV	3.65	3.65	3.65	3.65	3.65	4.08	4.43	4.99	-
		5.86	5.86	5.86	5.86	5.86	6.54	7.11	8.01	
$\overline{B}_d^0 \rightarrow \overline{K}^{*0} \rho^0$	IV	0.88	0.87	0.86	0.86	0.88	0.99	1.12	1.38	< 460
		1.26	1.25	1.24	1.22	1.26	1.38	1.55	1.92	
$\overline{B}_d^0 \rightarrow \overline{K}^{*0} K^{*0}$	IV	0.20	0.20	0.20	0.20	0.20	0.25	0.30	0.38	-
		0.40	0.40	0.40	0.40	0.40	0.51	0.60	0.77	
$B^- \rightarrow K^{*-} \rho^0$	IV	3.53	3.58	3.59	3.61	3.53	4.00	4.40	5.11	< 900
		6.10	6.14	6.16	6.19	6.10	6.87	7.60	8.89	
$B^- \rightarrow \overline{K}^{*0} \rho^-$	IV	4.00	4.00	4.00	4.00	4.00	5.11	6.11	7.76	-
		6.42	6.42	6.42	6.42	6.42	8.21	9.80	12.5	
$B^- \rightarrow K^{*-} K^{*0}$	IV	0.21	0.21	0.21	0.21	0.21	0.27	0.32	0.41	-
		0.42	0.42	0.42	0.42	0.42	0.54	0.64	0.82	
$\overline{B}_d^0 \rightarrow \rho^0 \phi$	V	0.005	0.0004	0.004	0.02	0.005	0.006	0.04	0.13	< 13
		0.01	0.0006	0.007	0.04	0.01	0.01	0.06	0.20	
$\overline{B}_d^0 \rightarrow \omega \phi$	V	0.005	0.0004	0.004	0.02	0.005	0.006	0.04	0.13	< 21
		0.01	0.0006	0.007	0.04	0.01	0.01	0.06	0.20	
$B^- \rightarrow \rho^- \phi$	V	0.01	0.001	0.01	0.05	0.01	0.01	0.08	0.28	< 16
		0.02	0.0014	0.015	0.08	0.02	0.02	0.12	0.43	
$\overline{B}_d^0 \rightarrow \rho^0 \omega$	VI	0.18	0.12	0.08	0.04	0.18	0.10	0.05	0.02	< 11
		0.30	0.20	0.13	0.06	0.30	0.16	0.08	0.02	
$\overline{B}_d^0 \rightarrow \overline{K}^{*0} \omega$	VI	5.57	3.06	1.56	0.27	5.57	1.93	0.37	0.41	< 23
		9.97	5.14	2.43	0.29	9.97	2.97	0.35	1.44	
$\overline{B}_d^0 \rightarrow \overline{K}^{*0} \phi$	VI	8.75	5.58	3.66	1.56	8.75	4.48	2.17	0.27	< 21
		16.8	11.0	7.20	3.06	16.8	8.81	4.27	0.53	
$B^- \rightarrow K^{*-} \omega$	VI	5.65	3.26	1.90	0.88	5.65	1.82	0.56	1.78	< 87
		10.1	5.50	3.03	1.38	10.1	2.82	0.81	4.21	
$B^- \rightarrow K^{*-} \phi$	VI	9.31	5.93	3.90	1.66	9.31	4.77	2.31	0.29	< 41
		17.9	11.7	7.66	3.25	17.9	9.37	4.54	0.56	